ERDC/GSL TR-08-26

Geotechnical and Structures Laboratory

US Army Corps
of Engineers®
Engineer Research and
Development Center

Evaluation of Minimum Asphalt Concrete Thickness Criteria

Haley P. Bell and L. Webb Mason

October 2008

ERDC/GSL TR-08-26
October 2008

Evaluation of Minimum Asphalt Concrete Thickness Criteria

Haley P. Bell and L. Webb Mason

Geotechnical and Structures Laboratory
U.S. Army Engineer Research and Development Center
3909 Halls Ferry Road
Vicksburg, MS 39180-6199

Final report

Prepared for Headquarters, Air Combat Command
129 Andrews Street, Suite 102
Langley AFB, VA 23666

Abstract: Personnel of the U.S. Army Engineer Research and Development Center (ERDC) were tasked by Headquarters, Air Combat Command to evaluate the Department of Defense's (DoD) minimum asphalt concrete thickness criteria outlined in Unified Facilities Criteria 3-260-02. Recent improvements to the DoD's flexible pavement design procedure and a renewed emphasis on the design and construction of contingency pavements has prompted concerns regarding the design and evaluation of thin asphalt concrete pavements. An evaluation of the DoD's minimum asphalt concrete thickness criteria was conducted during February 2007 to April 2008 under the ERDC's Hangar 4 test facility. The project consisted of constructing a full-scale test section with six varying test items that represented three airfield types encountered in both peacetime and contingency scenarios. Four of the items met the DoD's minimum asphalt concrete thickness criteria, and two items did not meet the criteria. Each item was instrumented and trafficked with either a C-17 wheel or an F-15E wheel using a Heavy Vehicle Simulator. Traffic test results concluded that the DoD's current minimum asphalt concrete thickness criteria are acceptable. Further results from the evaluation are presented and include material characterization tests and data, rut depth measurements, centerline and cross section profiles, falling weight deflectometer data, instrumentation response data, and forensic investigation assessments.

Contents

Figures and Tables

Figures

Tables

Preface

The project described in this report was sponsored by Headquarters, Air Combat Command, Langley Air Force Base, VA.

Personnel of the U.S. Army Engineer Research and Development Center (ERDC), Geotechnical and Structures Laboratory (GSL), Vicksburg, MS, prepared this publication. The findings and recommendations presented in this report are based upon the results of a full-scale asphalt concrete test section constructed under the ERDC's Hangar 4 test facility to evaluate the Department of Defense's minimum asphalt concrete thickness criteria outlined in Unified Facilities Criteria 3-260-02. The test section was constructed during February to May 2007, and trafficking of the test section was conducted during June 2007 to March 2008. Forensic investigations took place during April 2008. The ERDC evaluation team consisted of Webb Mason, Haley Bell, Quint Mason, and Rhoda Moreno, Airfields and Pavements Branch (APB), GSL; Tommy Carr and Tony Brogdon, Information Technology Laboratory; and Dennis Beausoliel, Charles Wilson, Randy Bufkin, Leroy Hardin, Jessie Gaskin, and Carl Gaston, Directorate of Public Works. Bell and Mason prepared this publication under the supervision of Dr. Gary L. Anderton, Chief, APB; Dr. Larry N. Lynch, Chief, Engineering Systems and Materials Division; Dr. William P. Grogan, Deputy Director, GSL; and Dr. David W. Pittman, Director, GSL.

COL Gary E. Johnston was Commander and Executive Director of ERDC. Dr. James R. Houston was Director.

Recommended changes for improving this publication in content and/or format should be submitted on DA Form 2028 (Recommended Changes to Publications and Blank Forms) and forwarded to Headquarters, U.S. Army Corps of Engineers, ATTN: CECW-EW, 441 G Street NW, Washington, DC 20314.

Unit Conversion Factors

Multiply	By	To Obtain
degrees Fahrenheit	(F-32)/1.8	degrees Celsius
feet	0.3048	meters
inches	0.0254	meters
kips (force) per square inch	6.894757	megapascals
pounds (force) per square inch	6.894757	kilopascals
pounds (mass)	0.45359237	kilograms

1 Introduction

Background

Recent improvements have occurred to the Department of Defense's (DoD) flexible pavement design procedure. There has also been a renewed emphasis on the design and construction of contingency pavements. Both developments have prompted concerns regarding the design and evaluation of pavements with thin asphalt concrete. In design, minimum asphalt concrete thickness requirements ensure that an adequate wearing surface is provided to the pavement to distribute the high surface stresses to the base material and to ensure a watertight paved surface. The DoD's asphalt concrete pavement design procedures are even more rigorous than commercial airfield pavement design due to the extremely high tire pressures from fighter aircraft and the heavy loads from cargo aircraft. However, the military's shrinking budget for infrastructure is forcing pavement engineers to design at minimum limits within the current criteria. In addition, contingency operations frequently require that maneuvers be conducted from austere airfields, often not meeting peacetime layer thickness or material requirements. Thus, there is a need to validate current minimum asphalt concrete thickness requirements (Tables 1 and 2) outlined in Unified Facilities Criteria (UFC) 3-260-02 and to quantify the effects of operating cargo and fighter aircraft on thin asphalt concrete pavements within the theater of operations.

Table 1. Air Force flexible airfield pavement minimum surface and aggregate base course thickness requirements (UFC 3-260-02).

	Traffic Area	100-CBR Base		80-CBR Base	
		Surface (in.)	Base (in.)	Surface (in.)	Base (in.)
Light Load	A	4	6	5	6
Shortfield	A	4	6	5	6

Objective and scope

The purpose of this project was to determine if improvements are needed to the DoD's minimum asphalt concrete thickness criteria and observe the consequences of operating military aircraft on representative thin asphalt concrete pavements. To accomplish this, a full-scale test section was constructed of six different test items representing three pavement

Table 2. Air Force aggregate base course gradation requirements (UFC 3-260-02).

Sieve Designation	Percentage by Weight Passing Square-Mesh Sieve		
	No. 1	No. 2	No. 3
50-mm (2-in.)	100	-----	-----
37.5-mm (1-1/2-in.)	70-100	100	-----
25-mm (1-in.)	45-80	60-100	100
12.5-mm (1/2-in.)	30-60	30-65	40-70
4.75-mm (No. 4)	20-50	20-50	20-50
2.0-mm (No. 10)	15-40	15-40	15-40
0.425-mm (No. 40)	5-25	5-25	5-25
0.075-mm (No. 200)	0-8	0-8	0-8

scenarios. Each item was instrumented and trafficked in a normally distributed traffic pattern with either a C-17 or F-15E wheel using a Heavy Vehicle Simulator (HVS-A). At selected traffic intervals, the surface was inspected for distresses, permanent deformation was measured, and falling weight deflectometer (FWD) tests were performed. This report addresses the following objectives:

- Verify the structural adequacy for the minimum thickness requirements used in current asphalt concrete pavement design.
- Identify the principle failure mechanisms for premature deterioration of thin asphalt concrete pavements in the theater of operations.
- Quantify the service life of thin asphalt concrete pavements encountered in the theater of operations.

This report presents laboratory tests and results of foundation materials, field testing procedures, traffic evaluation results, data analyses, conclusions, and recommendations for future work regarding the test and evaluation of thin flexible airfield pavements.

2 Test Plan

The following paragraphs present the approach for evaluating the DoD's minimum asphalt concrete thickness criteria. Figure 1 presents a flow chart of the evaluation process. Chapters 3, 4, and 5 provide further details regarding the materials testing, test section construction, and evaluation procedures, respectively.

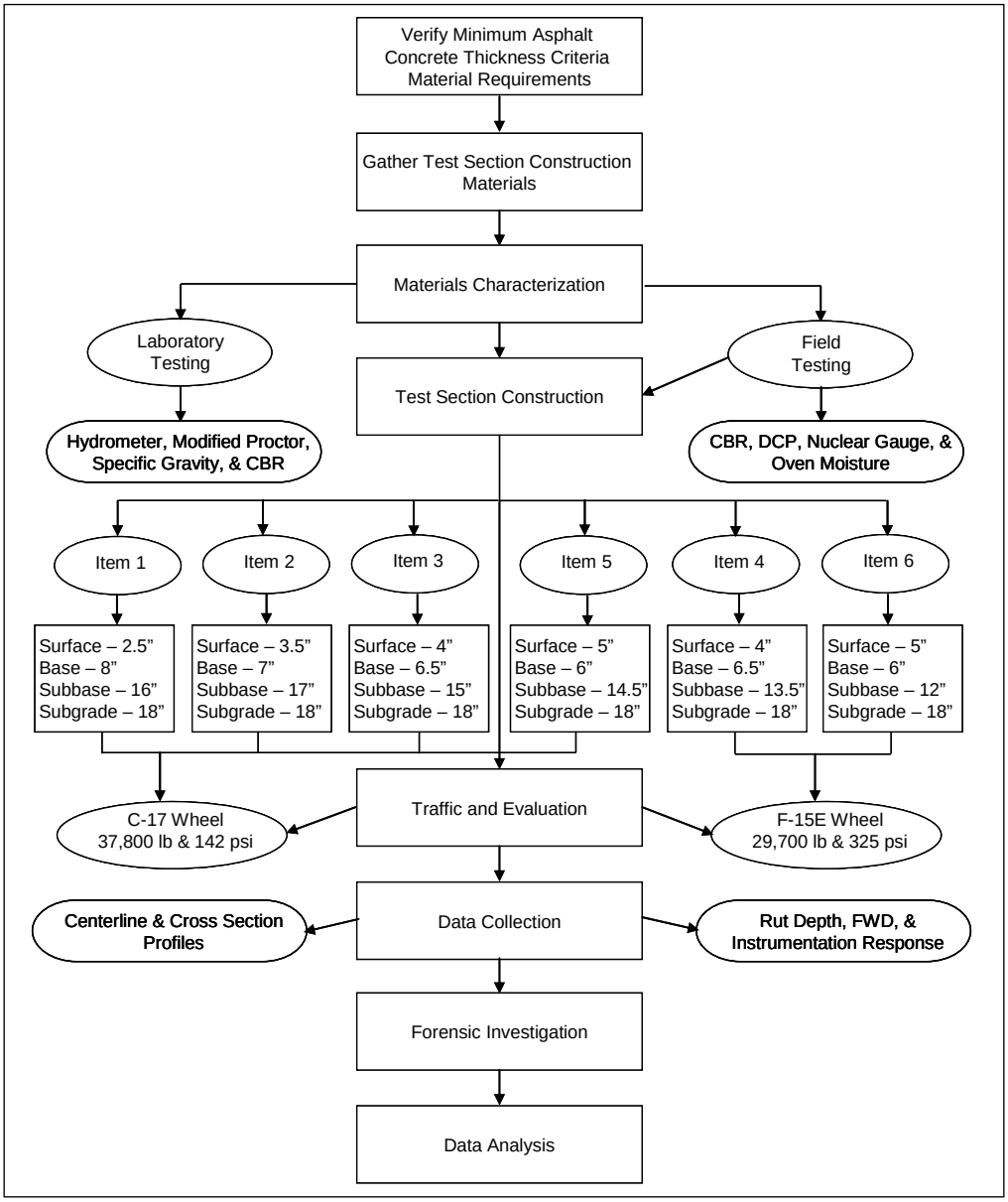

Figure 1. Test plan flow chart.

The general approach to this project was to evaluate the structural performance of representative thin asphalt concrete pavements using full-scale field testing. The test section, divided into six items, consisted of three different airfield types (contingency cargo, shortfield cargo, and light load) that address both peacetime and contingency pavement scenarios.

Two items (Items 1 and 2) were constructed under the minimum asphalt concrete thickness requirements (2.5 and 3.5 in. of asphalt concrete, respectively). The base course for Items 1 and 2 consisted of crushed gravel. Items 3, 4, 5, and 6 were constructed within the limits of the minimum asphalt concrete thickness criteria. Items 3 and 4 were constructed of 4 in. of asphalt concrete with a crushed limestone base course. Items 5 and 6 were constructed of 5 in. of asphalt concrete with the crushed gravel base course. All items consisted of a 3:1 blend of crushed gravel and sand for the subbase and high-plasticity clay for the subgrade. Figure 2 shows a plan view of the test section.

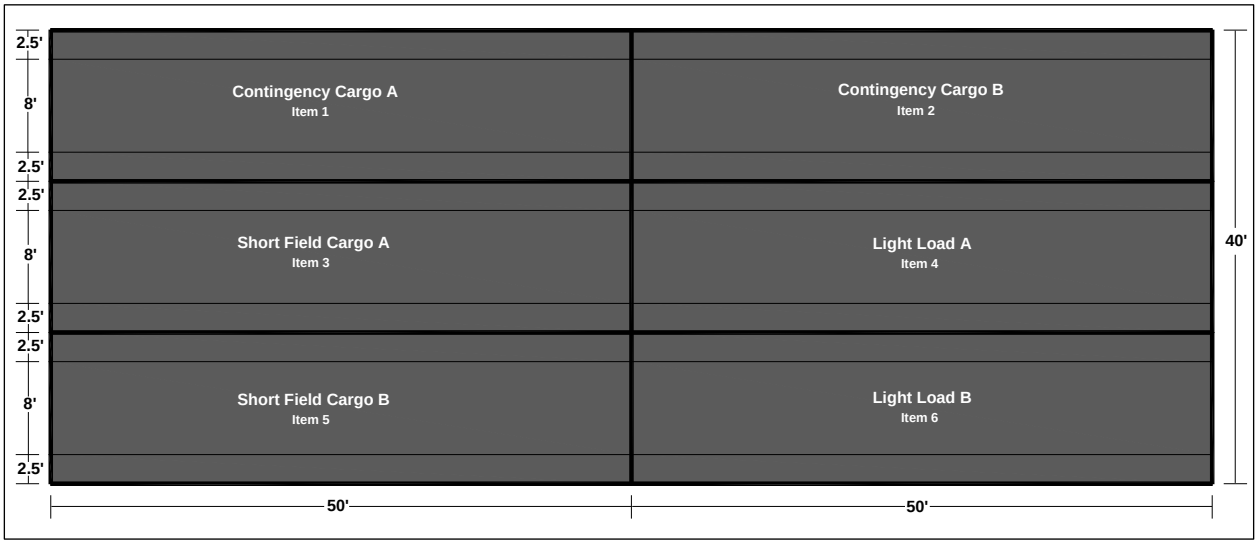

Figure 2. Plan view of test section.

The base courses under the asphalt concrete surface were required to meet certain gradation and fractured faces requirements to obtain a California Bearing Ratio (CBR) of 80 or 100% (Table 1). CBR is an index of strength measured by a shear test. Well-graded crushed gravel was chosen for the 80-CBR material, and well-graded crushed limestone was chosen for the 100-CBR base course material. Material samples (asphalt concrete, base courses, subbase, and subgrade) were characterized in the laboratory before construction of the test section so that the desired density and moisture measurements could be determined. The density and moisture

measurements determined from the laboratory testing were used to ensure that the desired in situ CBR would be achieved.

Various instrumentation gauges were installed within the pavement structure along the centerline of the traffic lanes. The instrumentation consisted of asphalt strain gauges placed at the bottom of the asphalt concrete to measure the tensile strain. Earth pressure cells (EPC) were placed in the base course, subbase, and subgrade to measure the stress distribution through the pavement system, and single-depth deflectometers (SDD) were installed near the top of the subgrade to measure the deflection at the top of the subgrade. Figure 3 shows a schematic of the instrumentation layout for each item.

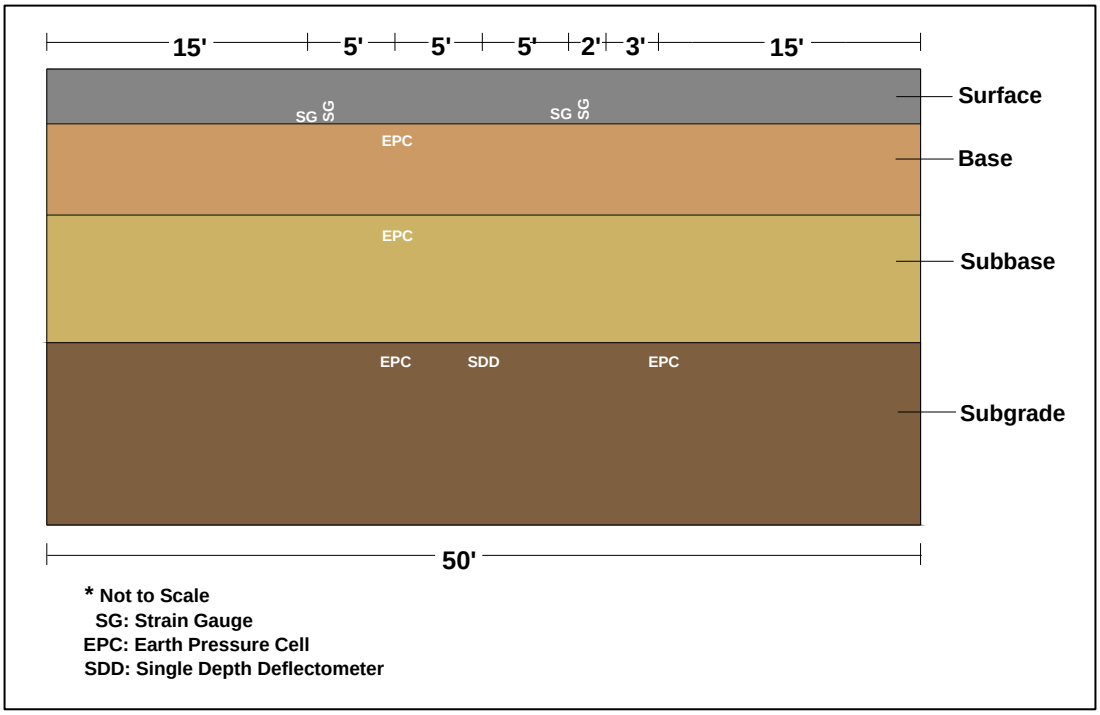

Figure 3. Instrumentation layout.

The contingency cargo and shortfield test items (Items 1, 2, 3, and 5) were trafficked with a C-17 wheel loaded to approximately 37,800 lb with 142-psi tire pressure. The light load test items (Items 4 and 6) were trafficked with an F-15E wheel loaded to approximately 29,700 lb with 325-psi tire pressure. The traffic was applied using the Engineer Research and Development Center's (ERDC) HVS-A in a simulated normal distribution pattern.

At selected traffic intervals, the surface was inspected for distress, permanent deformation was measured, instrumentation response data was collected, and FWD tests were performed. The failure criterion for asphalt concrete pavements is typically based upon 1 in. of permanent deformation or rutting. However, each item was trafficked beyond failure (approximately 1.5 to 2 in. of rutting). A forensic investigation was conducted upon the completion of the traffic tests to determine the failure mechanisms and influence on overall pavement performance.

3 Materials Characterization

Laboratory testing

The foundation materials were characterized before construction of the full-scale test section began so that they could be constructed to provide the desired in-place properties. Soil strength is typically represented using CBR. The CBR is an index of strength measured by a shear test. The resistance to penetration in the test is expressed as a percentage of the resistance for a standard crushed stone. Typical values for compacted, fair to good subgrades are between 10 and 20% of standard. A good subbase is between 30 and 50% of standard, and a good gravel base is between 50% and 80% of standard (American Society of Civil Engineers 1950).

The subgrade for all items consisted of a high-plasticity clay locally referred to as buckshot clay with a target CBR of 10%, and the subbase material consisted of a 3:1 blend of crushed gravel and sand, respectively, with a target CBR of approximately 30%. The base course material for four of the items (Items 1, 2, 5, and 6) was crushed gravel with a target CBR of 80%. The base courses of the other two items (Items 3 and 4) were constructed of crushed limestone with a target CBR of 100%. The asphalt concrete consisted of a high-quality airfield mix. Each material was sampled from their respective stockpiles and transported to the ERDC's soils laboratory for a series of testing including hydrometer analysis (grain-size analysis-ASTM D 422-63 (2007)), modified Proctor test (ASTM D 1557-02), specific gravity (ASTM D 854-06), and unsoaked CBR (ASTM D 1883-07).

The following paragraphs describe the laboratory test results of the materials used for constructing the test section.

Subgrade

High-plasticity clay material, classified by the Unified Soil Classification System (USCS) (ASTM D 2487-06) as CH, has been used as subgrade material for numerous test sections at the ERDC over previous years. This material is used because of the uniform conditions the clay provides over time. The CH material has been characterized in the ERDC's soils laboratory several times, so the specific subgrade material for this test section

was not characterized. The results of previous laboratory tests were used for this project, and they are summarized in Figures 4 through 6. These data were used to determine the target moisture content and dry density needed to obtain the 10-CBR soil strength. According to the previous laboratory test results, the subgrade soil should have a moisture content of about 32% (Figure 5) and a dry density of approximately 88 lb/ft^3 (Figure 6) to obtain the desired CBR of 10%.

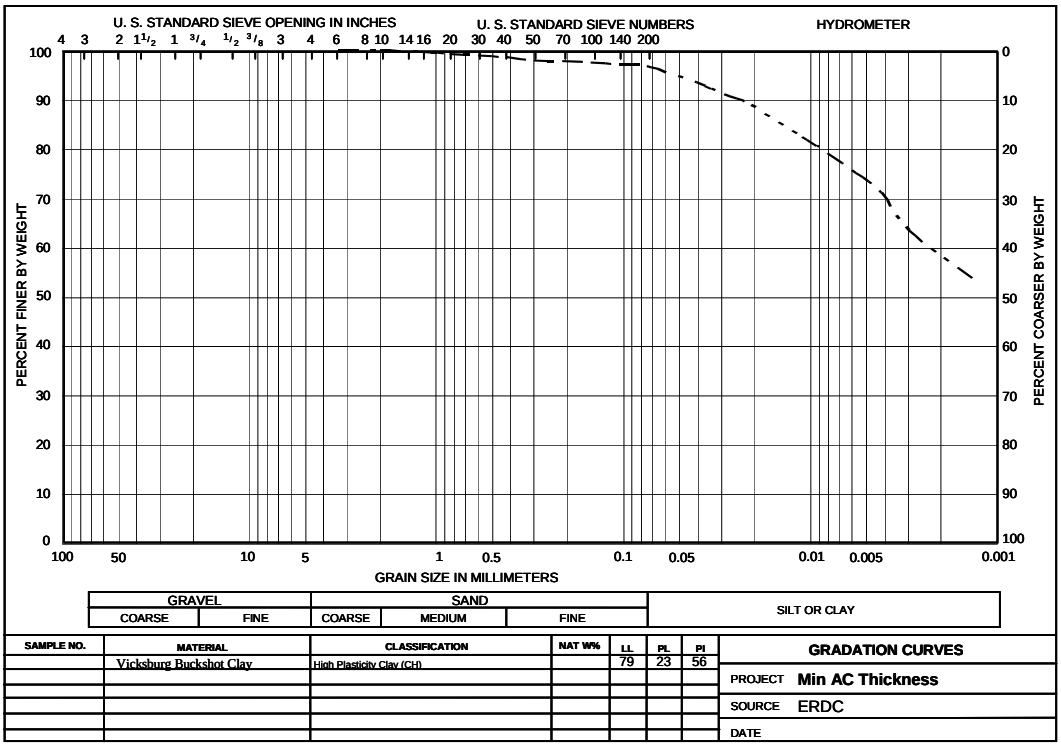

Figure 4. Grain-size distribution curve for the subgrade material.

Subbase

Samples of the 3:1 blend of crushed gravel and sand used for the subbase were tested in the ERDC's soils laboratory before placement in the test pit. This material was chosen because it was locally and readily available. The USCS classified the blend as poorly-graded sand or SP. The laboratory test data were used to determine the moisture content and dry density needed to obtain the approximate soil strength of 30 CBR. According to the laboratory test results (Table 3), the subbase should have a moisture content of 7.8% and a dry density of approximately 130.8 lb/ft^3 to obtain the desired 30 CBR. Figure 7 presents the gradation curve of the subbase material.

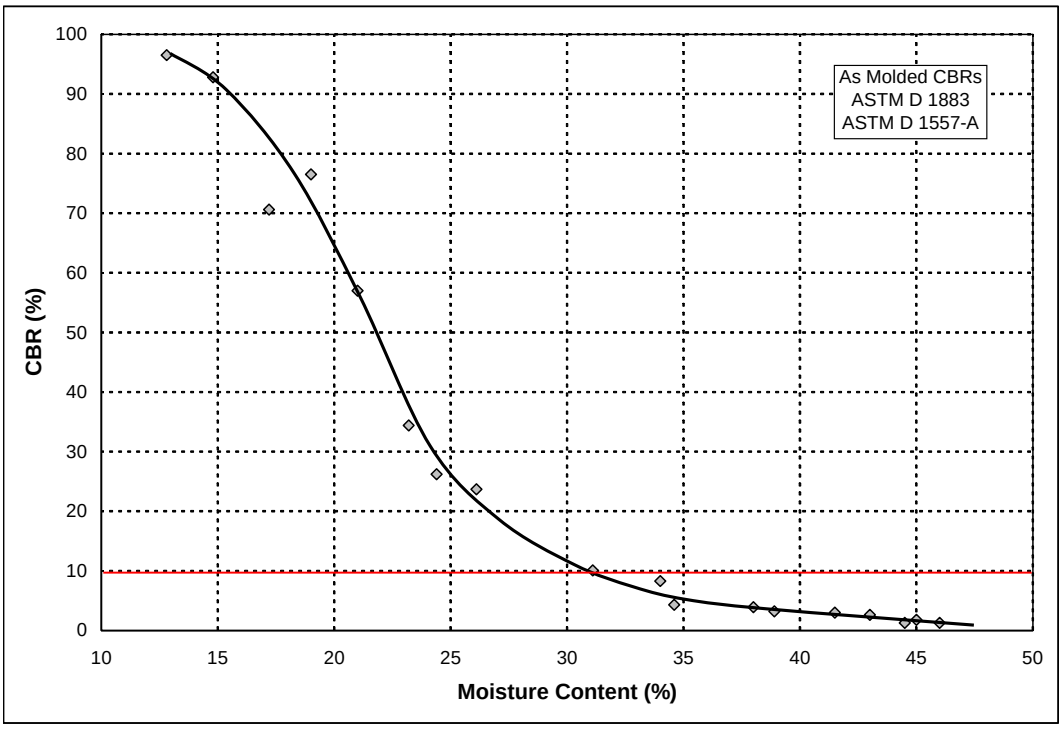

Figure 5. CBR versus moisture content for CH material.

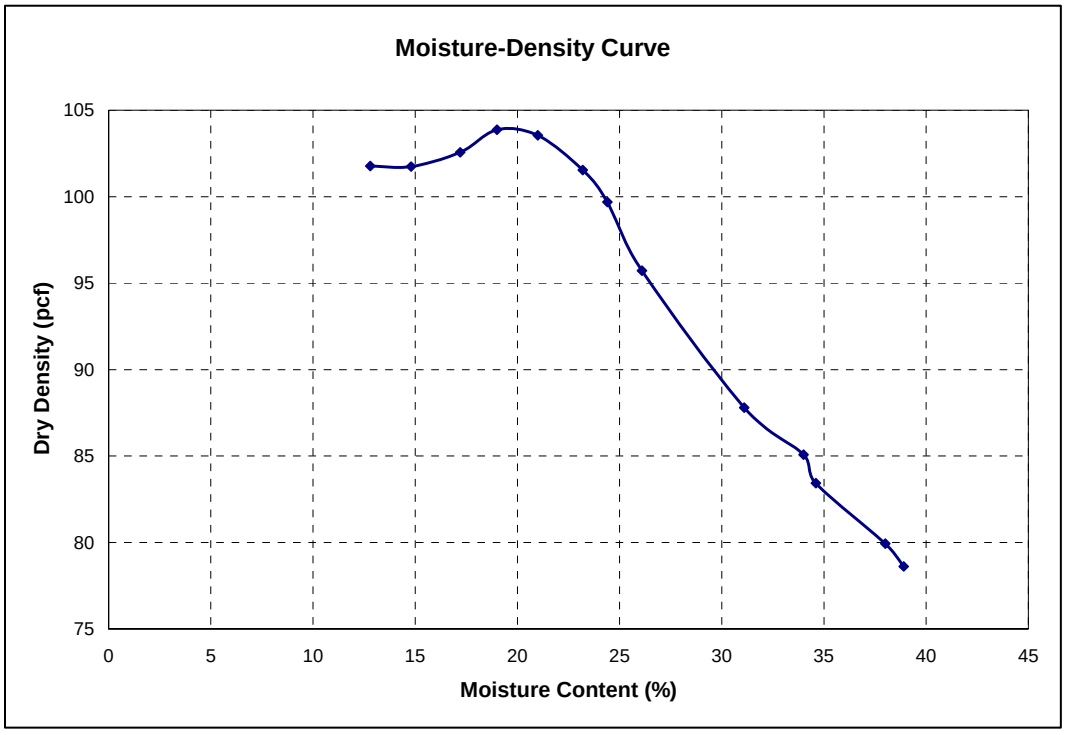

Figure 6. Dry density versus moisture content for CH material.

Table 3. Materials laboratory characterization summary.

Foundation Layer	USCS	Maximum Dry Density (lb/ft^3)	Optimum Moisture Content (%)	Specific Gravity
Subgrade	CH	88.0	32.0	2.74
Subbase	SP	130.8	7.8	2.66
Base (gravel)	GW	117.6	5.7	2.67
Base (limestone)	GW	143.8	6.7	2.74

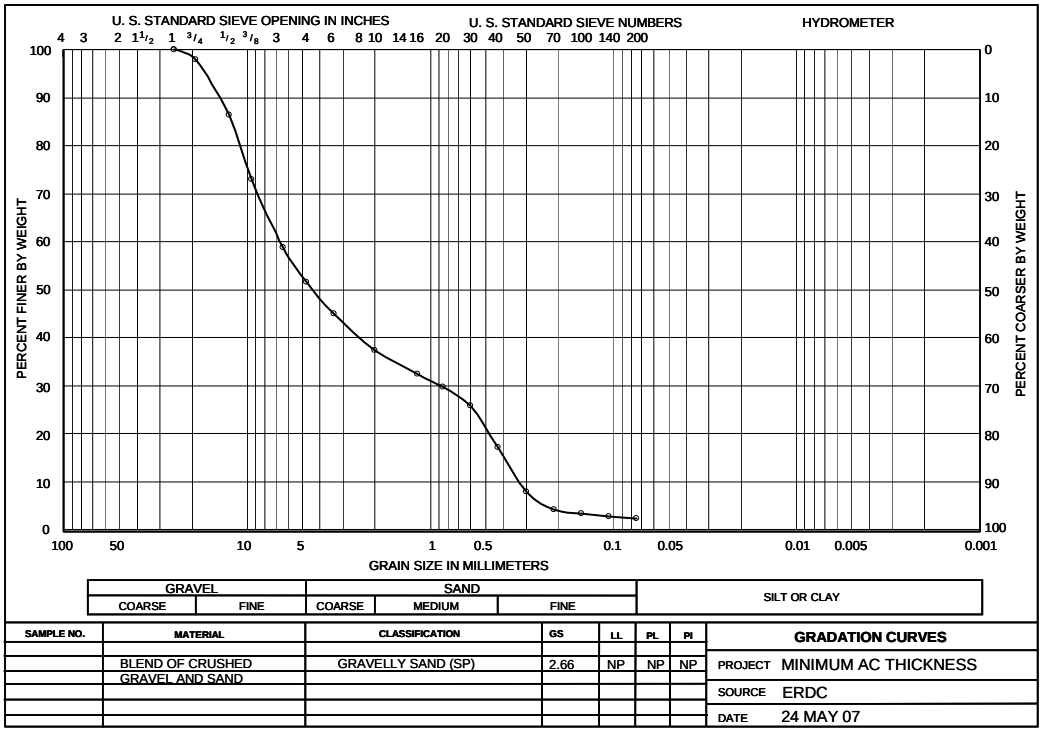

Figure 7. Grain-size distribution curve for the subbase material.

Base

Crushed gravel and crushed limestone base course material samples were also characterized in the ERDC's soils laboratory. The USCS classified the crushed gravel and crushed limestone materials as well-graded gravel or GW. As with the subgrade and subbase test results, these data were used to determine the moisture content and dry density needed to obtain the 80-CBR soil strength for the crushed gravel and 100-CBR soil strength for the crushed limestone. Figures 8 and 9 show grain-size distribution curves for the two base course materials.

According to the laboratory test results (Table 3), the crushed limestone should have a moisture content of 6.7% and a dry density of approximately 143.8 lb/ft^3 to obtain 100 CBR. The crushed gravel should have a moisture

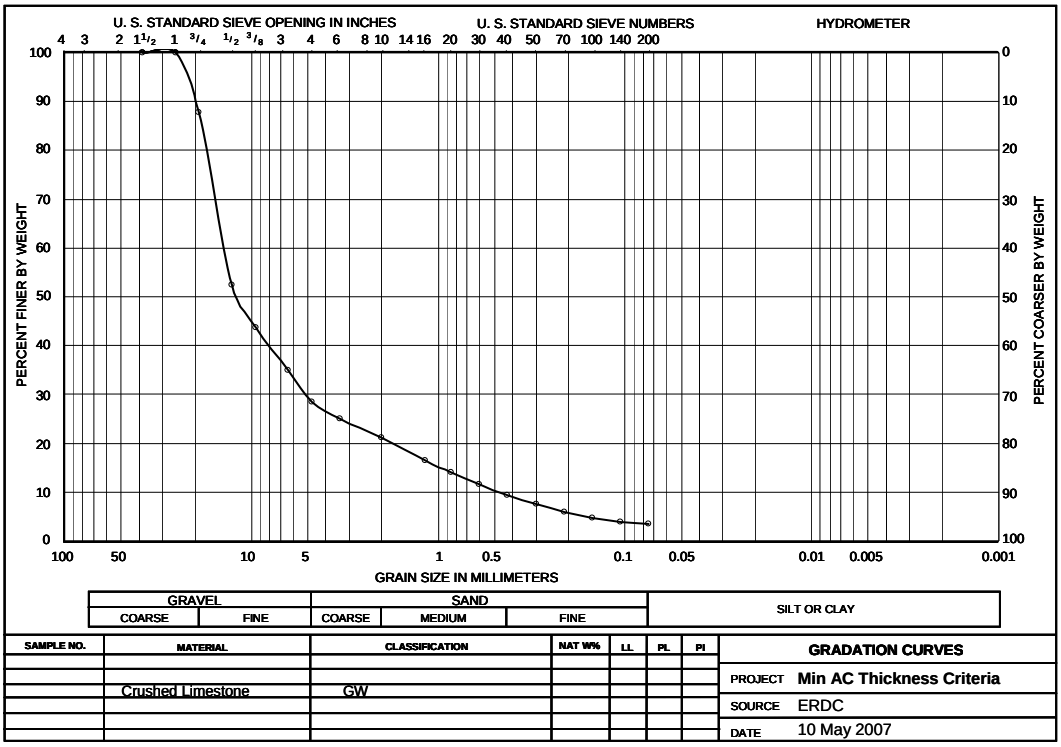

Figure 8. Grain-size distribution curve for the crushed limestone base course material.

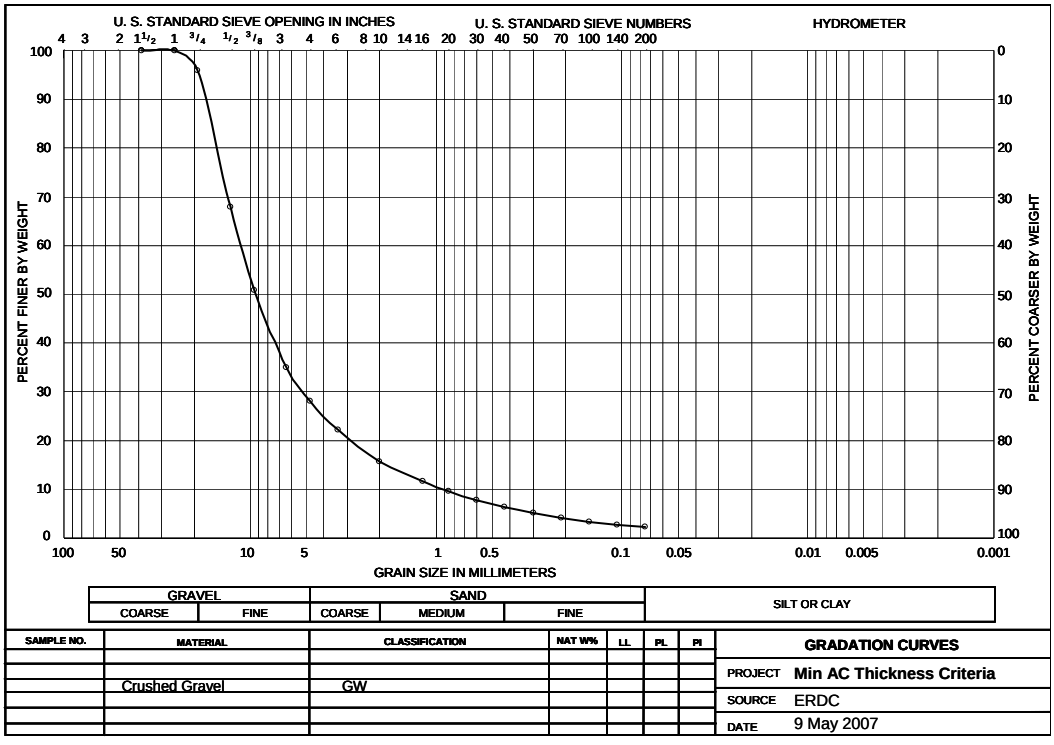

Figure 9. Grain-size distribution curve for the crushed gravel base course material.

content of 5.7% and a dry density of approximately 117.6 lb/ft^3 to obtain the desired 80 CBR. Table 3 presents a summary of the laboratory results of the base, subbase, and subgrade materials.

Asphalt concrete

The asphalt concrete used for the test section was classified as a performance grade (PG) 67-22. The classification was verified by evaluating binder samples in the asphalt laboratory. The binder samples underwent and passed the Superpave Performance Grading test performed in accordance with AASHTO M 320. The asphalt concrete was chosen because it is locally available and appropriate for the southeastern climate.

The average density of the asphalt concrete obtained in the laboratory was 145.5 lb/ft^3. Table 4 shows the blend percentages for the bituminous mixture, and Table 5 shows the aggregate blend for the asphalt concrete mixture. Table 6 presents the results of the Superpave Performance Grading received from the asphalt laboratory.

Table 4. Bituminous mixture blend.

Aggregate Size	Percent
3/4 in. Crushed Gravel	34
½-in. Crushed Gravel	10
#8 Limestone	15
Coarse Sand	15
C-2 Sand	25
Hydrated Lime	1
Total	100

Table 5. Asphalt concrete aggregate blend.

Sieve Size	Percent Finer
1 in.	100
¾ in.	100
½ in.	98
3/8 in.	93
No. 4	66
No. 8	46
No. 16	35
No. 30	28
No. 50	18
No. 100	11
No. 200	6

Table 6. Superpave Performance Grading results.

	Temperature (°C)	Result	Pass/Fail
Original Binder			
Rotational Viscosity AASHTO T316 3 Pa-s, max	135	0.485 Pa-s	Pass
Dynamic Shear Rheometer AASHTO T315 1.00 kPa, min	67	1.065 kPa	Pass
Rolling Thin Film Over Aged (AASHTO T240)			
Mass Change AASHTO T240 1.00%, max	-----	0.13%	Pass
Dynamic Shear Rheometer AASHTO T315 2.20 kPa, min	67	2.419 kPa	Pass
Pressure Aging Vessel (AASHTO R28)			
Dynamic Shear Rheometer AASHTO T315 5000 kPa, max	25	4898 kPa	Pass
Bending Beam Rheometer AASHTO T313 Stiffness, 300 MPa, max m-value, 0.30, min	-12	200.5 MPa 0.309	Pass Pass
Performance Grade: PG 67-22			

Field testing

Each layer of foundation materials underwent a series of in situ tests that characterized the actual material used for the pavement structure. The tests included CBR, dynamic cone penetrometer (DCP), nuclear density, nuclear moisture, and oven moisture. CBR and DCP tests are two methods for characterizing the strength of each layer in the test section. Both tests were conducted to ensure consistency throughout the test section. The field test results (dry density and moisture content) for all foundation materials were comparable with the laboratory test results. The following paragraphs give a description of each in situ test used on the test section.

California Bearing Ratio

In situ CBR tests were conducted at three transverse locations on each quarter point (Stations 12.5, 25, and 37.5) of each underlying layer to determine the condition of the soil at the time of testing. The transverse locations included tests on the centerline, west of the centerline

(approximately 1 ft from the centerline), and east of the centerline (approximately 1 ft from the centerline). The station numbers correspond to the distance from the beginning of the item (Station 0) in linear feet. Each item was 50 ft long.

CBR tests were mainly designed for subgrade and subbase material but can be completed on base course materials (American Society for Testing and Materials 2004). Also, it is important to note that CBR tests indicate the strength of the soil at the time of testing. If, for example, the moisture content changes after a CBR test, the strength of the soil (CBR) will also most likely change. The procedure used for completing the in situ CBR tests can be found in ASTM D 4429-04. Figure 10 shows a CBR test being conducted on the subgrade material.

Figure 10. Performing an in situ CBR test on the subgrade.

Dynamic cone penetrometer

A dual mass DCP soil test device was used to obtain subsurface soil data at representative locations. The DCP has a steel cone attached to one end of a metal rod with a 10.1- or 17.6-lb sliding drop hammer located on the other end. The 10.1-lb hammer was used for the subgrade and subbase materials, and the 17.6-lb hammer was used for the base materials. For each subsurface material, the cone of the DCP was placed on top of the soil, and the

hammer was dropped repeatedly to drive the cone through the underlying pavement layers. The material's resistance to penetration was recorded in terms of millimeters penetrated per hammer blow. The CBR was then determined based on a correlation procedure recommended in ASTM D 6951-03. DCP tests were performed at three transverse locations (on the centerline and west and east of the centerline) on each quarter point of each item. The results were illustrated on a plot of CBR versus depth for each test. Figure 11 shows an example of a DCP plot for the subgrade on Station 25 of Item 4.

It is important to note that the lack of confinement at the top of the testing layer affects DCP measurements. Therefore, certain penetration depths are required to measure the actual strength of the surface soil layer with the DCP. The DCP can accurately measure strengths of thin surface layers of fine-grained plastic materials but requires thicker surface layers for accurate results of nonplastic coarse-grained materials (Webster et al. 1994). This was considered when analyzing the results of the DCP tests on the test section.

Nuclear gauge

The Troxler nuclear moisture-density gauge (Figure 12), calibrated using a certified Primary Calibration Standard Block, was used throughout the pavement structure to rapidly measure each layer's respective density and moisture content. Using the density gauge replaces the traditional density test methods described in ASTM D 6938, ASTM D 2950, and ASTM C 1040. The nuclear gauge reports the dry density, wet density, and percent moisture. To use the nuclear gauge, the surface to be tested is smoothed, and sand is spread out over the area to fill any voids. A steel rod (about 1-in. diam) is driven into the surface and removed so that the rod attached to the nuclear gauge, which is used to measure the properties, can easily be inserted. The nuclear gauge device sits on top of the surface until the test is complete. The measurements are presented on the screen of the instrument. The detailed procedure can be found in ASTM D 6938-08a.

Oven moisture

Oven moisture tests are conducted to determine the moisture content of the soil. This test method is conducted by sampling small portions of the in situ material and drying them in an oven. For this project, samples were obtained immediately after CBR tests were completed. The basic

DCP TEST DATA

Project: *Eval of Min AC Thickness* Date: 5-Apr-07
Location: Item 4, STA 25 Soil Type(s): CH - Top of Subgrade

Hammer: (●) 10.1 lbs. ( ) 17.6 lbs. ( ) Both hammers used
Soil Type: (●) CH ( ) CL ( ) All other soils

No. of Blows	Accumulative Penetration (mm)	Type of Hammer
0	5	2
1	20	2
1	30	2
1	45	2
1	60	2
1	80	2
1	95	2
1	105	2
1	120	2
1	135	2
2	155	2
2	175	2
2	200	2
2	220	2
2	240	2
2	255	2
2	280	2
2	300	2
2	320	2
2	345	2
2	365	2
2	385	2
2	400	2
2	415	2
3	435	2
3	460	2
3	480	2
3	505	2
3	530	2
4	550	2
4	565	2
5	580	2
5	600	2
		2
		2
		2
		2
		2
		2
		2
		2
		2
		2
		2

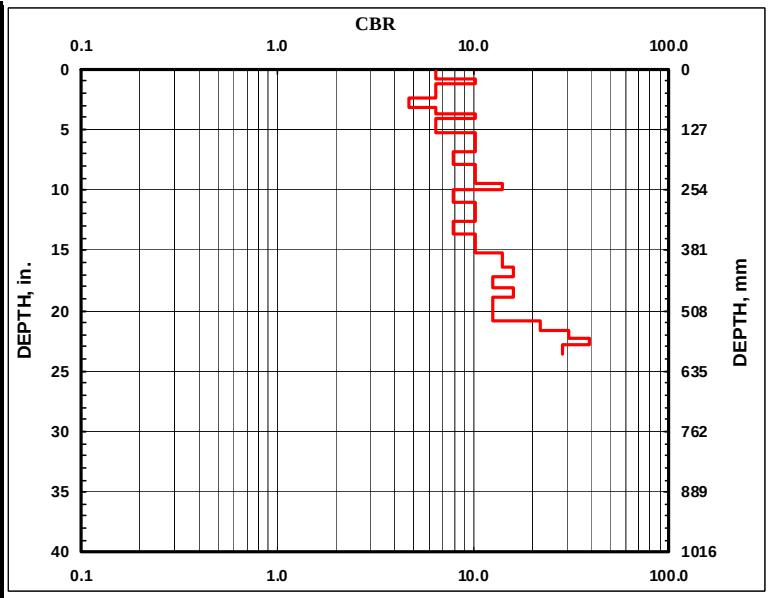

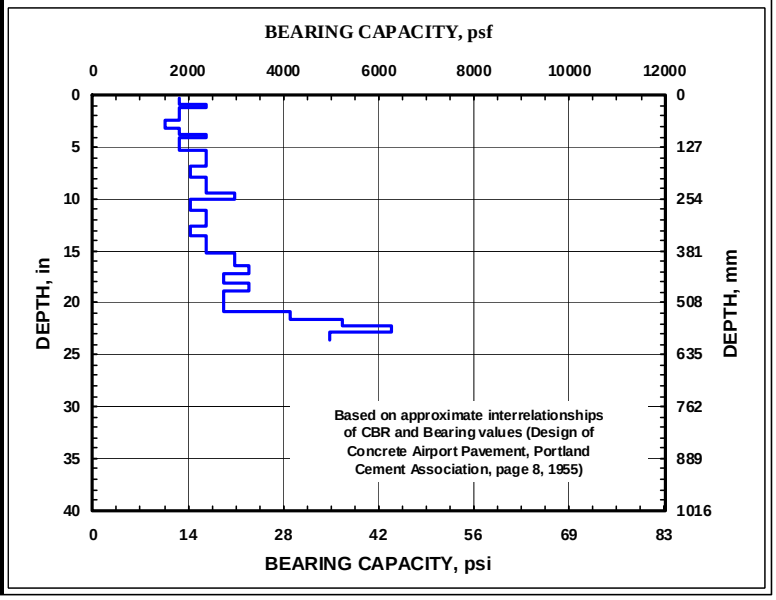

Figure 11. DCP test result on top of the subgrade of Item 4.

Figure 12. Nuclear gauge testing on the subbase material.

procedure is to weigh a dry, empty container. Then, add a representative sample removed from the test section, and place it in the empty container. Next, the container with the sample is weighed and placed in a drying oven until dry. Once the sample has dried in the oven, the container is removed and weighed, and the moisture content is calculated. The detailed procedure can be found in ASTM D 4643-00.

4 Test Section Construction

General

The full-scale test section, 100 ft long and 39 ft wide, was constructed under the ERDC's Hangar 4 test facility to evaluate the structural performance of representative thin asphalt concrete pavements. The test section was divided into six items which represented three different airfield types (contingency cargo, shortfield cargo, and light load) that address both peacetime and contingency pavement scenarios. The contingency cargo pavements represent thin asphalt concrete pavements likely to be encountered at austere airfields. The shortfield cargo pavements represent better quality contingency pavements and/or peacetime training airfields where problems with slippage cracking in thin asphalt concrete pavements have been reported, and the light load pavements represent thin asphalt concrete pavements subjected to high tire pressure fighter aircraft. Figure 2 (Chapter 2) shows the plan view of the test section.

Items 1 and 2 were constructed outside the limits of the DoD's minimum asphalt concrete thickness criteria. These items represent contingency cargo pavements that are under the 4-in. minimum asphalt concrete requirement. Item 1 was constructed of 2.5 in. of asphalt concrete, and Item 2 was constructed of 3.5 in. of asphalt concrete. Both items were constructed with the crushed gravel base course material (target CBR of 80%).

Items 3, 4, 5, and 6 were constructed within the limits of the DoD's minimum asphalt concrete thickness criteria. Items 3 and 4 were constructed of 4 in. of asphalt concrete with the crushed limestone base course (target CBR of 100%). Items 5 and 6 were constructed of 5 in. of asphalt concrete with the crushed gravel base course (target CBR of 80%). The DoD's minimum asphalt concrete thickness criteria requires at least 4 in. of asphalt concrete over a 100-CBR base course and 5 in. of asphalt concrete over an 80-CBR base course.

Table 7 presents the test variable matrix measured for the test section. The base, subbase, and subgrade thicknesses are average thicknesses determined from centerline and cross section profile readings. The paragraphs

Table 7. Test variable matrix.

Item	Surface Thickness (in.)	Base Thickness (in.)	Subbase Thickness (in.)	Subgrade Thickness (in.)
1	2.5	8.0	16.0	18.0
2	3.5	7.0	17.0	18.0
3	4.0	6.5	15.0	18.0
4	4.0	6.5	13.5	18.0
5	5.0	6.0	14.5	18.0
6	5.0	6.0	12.0	18.0

under the following heading describe the procedures used for placing each underlying material in the test.

Construction procedures

Construction began by excavating a 39-ft wide by 100-ft long by an approximate 3.5-ft deep test pit. The existing subgrade was leveled and compacted. The test pit was then lined with an impermeable 6-mil polyethylene tarp to help retain the moisture in the underlying layers.

Subgrade

The subgrade material consisted of approximately 18 in. of high-plasticity clay (CH). This material was used because it is locally available and has a relatively good affinity for retaining moisture. The material was processed outside of the test pit so that the moisture content could be adjusted to the desired percentage. The repeated processing procedure included spreading the material to a uniform 12-in. depth at a nearby preparatory site, pulverizing the material with a rotary mixer, adjusting the moisture content of the material, pulverizing the CH again, and stockpiling the soil. Once the optimum moisture content was achieved, the CH was placed in the test pit in three uncompacted 8-in. lifts.

Each lift was compacted using a rubber tire roller to approximately 6 in. for a total thickness of about 18 in. The subgrade was then finished using a steel wheel roller in order to achieve a smooth surface. Each compacted lift was subjected to nuclear density, nuclear moisture, oven moisture, DCP, and CBR testing following the methods described in Chapter 3 to ensure the desired values were reached. The CH material easily achieved the target CBR of approximately 10% (Table 8). Figure 13 shows a lift of the CH material in the test pit before compaction.

Table 8. Pre-test field measurements.

Item	Foundation Layer	Dry Density (lb/ft³)	Moisture Content (%)	CBR (%)
1	Base	120.6	2.7	37.6
	Subbase	126.8	3.4	46.0
	Subgrade	91.5	30.1	9.8
2	Base	119.1	2.7	54.2
	Subbase	126.0	3.3	45.2
	Subgrade	92.7	30.0	9.9
3	Base	140.4	1.7	95.6
	Subbase	125.8	3.3	47.3
	Subgrade	94.5	30.5	9.3
4	Base	141.8	2.1	100.0
	Subbase	125.1	3.5	55.0
	Subgrade	94.8	30.6	9.1
5	Base	120.7	2.4	51.5
	Subbase	125.4	3.4	56.0
	Subgrade	93.3	28.2	9.4
6	Base	118.6	2.4	40.0
	Subbase	126.4	3.5	42.0
	Subgrade	94.6	28.0	9.5

Figure 13. One lift of CH material before compaction.

Subbase

The three parts crushed gravel to one part sand blend of subbase material (SP) was processed by spreading concrete sand and crushed gravel at a nearby preparatory site. An endloader with a 1-3/4-yd^3 bucket was used for determining quantities of each material for the mix ratio of the blend. The material was stirred and flipped by the endloader several times. Then, the material was spread and blended with a rotary mixer again until the mixture was of uniform consistency. Once the desired moisture content was achieved, the material was placed in 7- or 8-in. uncompacted lifts and compacted to 6 in. for a total depth of approximately 16, 17, 15, 13.5, 14.5, and 12 in. for Items 1, 2, 3, 4, 5, and 6, respectively.

The final compacted subbase (Figure 14) was subjected to nuclear density, nuclear moisture, oven moisture, and DCP testing to ensure the desired measurements were reached. CBR tests were not conducted on the subbase because the material was too loose; accurate measurements could not be achieved. The strength of the subbase material, determined using the DCP, was a CBR of approximately 42 to 55% (Table 6). Target CBR was 30%; however, there were no minimum or maximum strength requirements for the subbase. The material was constructed of a suitable strength

Figure 14. Compacting the subbase material.

for this study. The subbase thicknesses were verified by conducting centerline and cross section profiles using a rod and level. This also ensured that the surface was level.

Base

The base course material for Items 1, 2, 5, and 6 consisted of crushed gravel received from a quarry in Crystal Springs, MS. For Item 1, the material was placed in two 6-in. uncompacted lifts and compacted to approximately 4 in. for a total depth of about 8 in. For Item 2, the material was placed in 5- and 6-in. uncompacted lifts and compacted to about 3 and 4 in., respectively, for a total depth of about 7 in. For Items 5 and 6, the crushed gravel material was placed in one 8-in. uncompacted lift and compacted to approximately 6 in.

The crushed gravel used in Items 1, 2, 5, and 6 met the gradation (Table 2) and fractured faces count requirements outlined in the DoD's airfield pavement design manual (UFC 3-260-02) for an 80-CBR material. The fractured faces requirements are:

- At least 45% of the material must have two or more fractured faces.
- At least 50% of the material must have one or more fractured faces.

The fractured faces count results indicated that approximately 67.8% of the material had two or more fractured faces, and approximately 91% of the material had one or more fractured faces. Density measurements were also met, and compaction efforts were maximized; however, the in situ material was only able to achieve CBR strengths between 37.6 and 54.2% (Table 8); the target CBR was 80%. The CBR measurements for the base course material were determined using the DCP on a 1-in.-diam hole drilled through the asphalt concrete. The DCP tests were conducted on the covered, compacted material.

The minimum CBR strength required for the crushed gravel base course was 80%. Laboratory results indicated the CBR would be 80 to 100%. The CBR measured from the laboratory tests was from a tightly compacted cylinder, and the CBR test conducted in the field was on in situ material that could not be as tightly compacted. Therefore, it was difficult to achieve the same strength level in the field.

The base course material for Items 3 and 4 consisted of crushed limestone. For these items, the crushed limestone material was placed in one 8-in. uncompacted lift and compacted to about 6.5 in. Density and moisture measurements were comparable with the laboratory results, and the material reached a CBR of approximately 95.6 to 100% (Table 8). The elevation and levelness of all base material was verified by centerline and cross section profile readings. Figure 15 shows the limestone being placed between the two crushed gravel base course lanes.

Figure 15. Placing crushed limestone between the crushed gravel base courses.

Asphalt concrete

A prime coat was applied to the top of the base course 2 days prior to paving (Figure 16). The prime coat was used to increase the bond between the base course and the surface. The asphalt concrete was placed in single lifts for Items 1 and 2 (2.5 in. for Item 1 and 3.5 in. for Item 2). The asphalt concrete was placed in two 2-in. lifts for Items 3 and 4 and two 2.5-in. lifts for Items 5 and 6. After paving, the surface was compacted using a steel wheel roller. Density was measured throughout the paving and compacting process to ensure that the pavement was receiving 95% compaction with a density of at least 135 lb/ft^3 and not more than 142 lb/ft^3 (Figure 17).

Figure 16. Applying the prime coat.

Figure 17. Compacting the asphalt concrete and taking density measurements.

Instrumentation

Each item was instrumented with four 9-in.-diam EPC, one SDD, and four asphalt concrete strain gauges (two gauges perpendicular to each other) to measure the in situ pavement response to the aircraft loading. EPCs were placed 2 in. into the base, 4 in. into the subbase, and 4 in. into the subgrade to measure the vertical stress distribution through the pavement system caused by the wheel load and tire pressure. Two EPCs were placed in the subgrade to ensure that an accurate measurement was recorded. SDDs were installed 4 in. into the subgrade to measure the deflection and permanent deformation received from the loads. Strain gauges were placed at the bottom of the asphalt concrete (top of the base) to measure the tensile strain received at the bottom of the pavement. The strain gauges were placed parallel and perpendicular to traffic. Each gauge was installed directly on the centerline within the pavement structure. Figure 3 (Chapter 2) presents a schematic of the instrumentation layout for the items, and Figure 18 shows an EPC being installed in a base course layer.

Figure 18. EPC installation in a crushed gravel base course layer.

5 Traffic and Evaluation Procedures

Trafficking

Each item was trafficked in a normally distributed traffic pattern using the ERDC's HVS-A. The HVS-A is a fully automated machine that simulates accelerated aircraft traffic on airfield pavement test sections. The machine traffics forward and backward at a speed of approximately 5 mph over a 40-ft traffic span and a 4-ft wander width. The ERDC's HVS-A (Figure 19), one of eight in the world, is the largest because of its ability to traffic airfield pavements with high aircraft loads and tire pressures. Items 1, 2, 3, and 5 were trafficked with a single C-17 wheel loaded to approximately 37,800 lb with 142-psi tire pressure. Items 4 and 6 were trafficked with a single F-15E wheel loaded to approximately 29,700 lb with 325-psi tire pressure. The wheel loads and tire pressures used in this study were within the normal range of loads to be expected in the field. The maximum take-off weights for a C-17 and F-15E wheel are 44,930 and 35,235 lb, respectively.

The pass to coverage ratios for the single wheel C-17 and F-15E for the traffic patterns used in this study are 2.41 and 4.17, respectively. A pass is defined as one movement of the aircraft wheel down the length of the test section, and coverage is defined as one application of the aircraft wheel over every single point in the central portion of the 4-ft traffic lane. Figures 20 and 21 simulate the traffic patterns used on the test section. The offset index represents 1-in. distances between the loaded wheel for each pass. Each bar represents a precision of a wheel path. For example, if the HVS-A is set to start at index position 3, then the center of the tire will be over index position 3.

Although the DoD's failure criterion for asphalt concrete pavements is typically based upon 1 in. of permanent deformation, Items 1, 2, 3, and 5 were trafficked until approximately 2 in. of rutting occurred. Items 4 and 6 were trafficked until about 1.5 in. of rutting occurred. Figure 22 shows the loaded C-17 wheel trafficking on Item 2, and Figure 23 shows the loaded F-15E wheel trafficking on Item 4.

Figure 19. ERDC's HVS-A on the asphalt concrete test section.

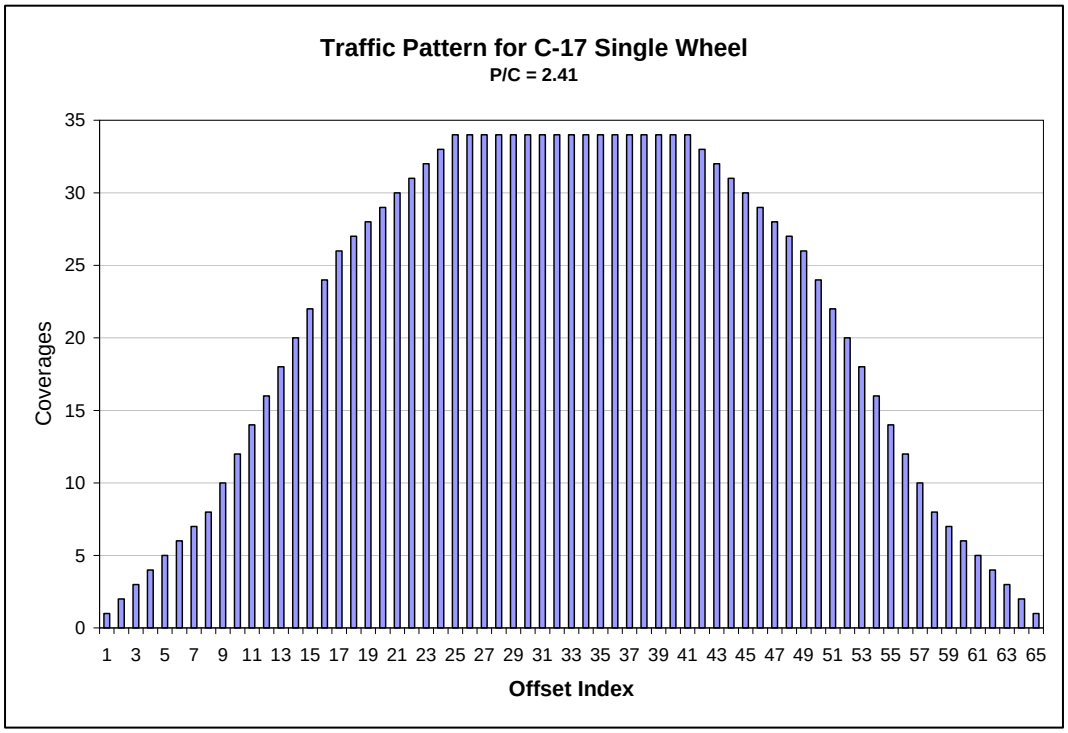

Figure 20. HVS-A traffic pattern for the single wheel C-17.

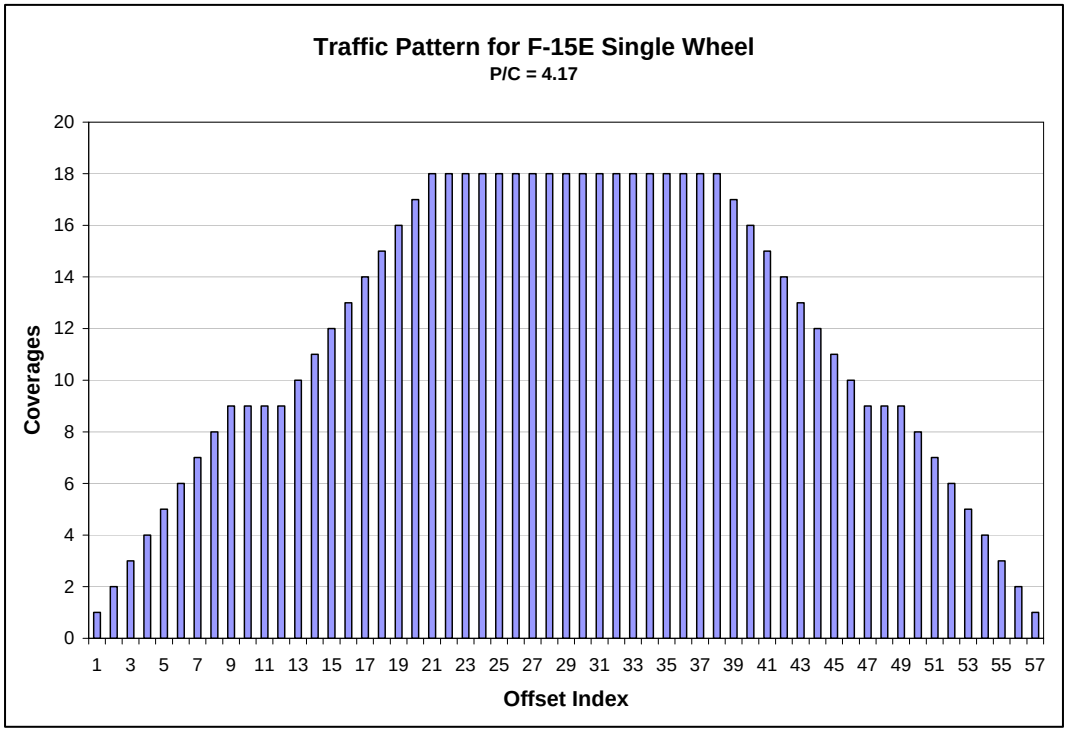

Figure 21. HVS-A traffic pattern for the single wheel F-15E.

Figure 22. C-17 wheel trafficking on Item 2.

Figure 23. F-15E wheel trafficking on Item 4.

Data collection

Data collection of the test section included surface permanent deformation measurements, surface centerline and cross section profile measurements, FWD tests, and instrumentation response measurements. With the exception of the instrumentation and FWD measurements, all data was collected at the same three-quarter points (Stations 12.5, 25, and 37.5) each time. The instrumentation and FWD data were collected at Stations 15, 20, 25, 30, and 35. Again, the station numbers correspond to the distance from the beginning of the item (Station 0) in linear feet.

At selected traffic intervals, the traffic was stopped, and the asphalt concrete pavements were inspected for distresses such as cracking and rutting. Rut depth measurements were recorded on the centerline, west of the centerline, and east of the centerline at each quarter point (Figure 24). If the average permanent deformation of the surface increased 1/8 in. or more, a full data set of measurements (FWD, centerline profile, cross section profiles, and instrumentation response) was collected. Otherwise, trafficking continued until the desired number of passes was achieved. This procedure was repeated until the permanent deformation reached approximately 1.5 to 2 in. The following paragraphs further explain the data collection procedures.

Figure 24. Taking rut depth measurements.

Centerline and cross section profiles

Rod and level centerline and cross section profiles (1-ft increments) were conducted to aid in the calculation of the surface elevation change after selected passes of the single wheel C-17 or F-15E. The results were used to illustrate the permanent surface deformation of the centerline and across the quarter points with the increase in pass level. Figure 25 shows cross section profiles being read on a quarter point of Item 1.

Falling weight deflectometer

The FWD is a nondestructive, impact load device that applies a single-impulse transient load of approximately 25- to 30-ms duration. With this trailer-mounted device, a dynamic force is applied to the pavement surface by dropping a weight onto a set of rubber cushions. This results in an impulse loading on an underlying circular plate 11.8 in. in diameter in contact with the pavement. The applied force and the pavement deflections, respectively, are measured with load cells and velocity transducers. The drop height of the weights can be varied from 0 to 15.7 in. to produce a force from 1,500 to 27,000 lb. The system is controlled with a laptop computer that also records the output data. Velocities were measured and deflections computed at the center of the load plate (D1) and at distances

Figure 25. Cross section profile readings on Item 1.

of 12, 24, 36, 48, 60, and 72 in. (D2 through D7) from the center of the load plate.[1]

For this project, pavement deflection measurements were recorded at force levels of approximately 25,000 lb. A linear elastic analysis backcalculation program, LEEP, was used to backcalculate the moduli of each pavement structure. Representative basins were used to determine modulus values of the various layers within the pavement structure in each item. The pavement structures were modeled in a three-layer system, an asphalt concrete layer, a combined base and subbase layer, and a subgrade layer. The program determined a set of modulus values that provided the best fit between a measured deflection basin and a computed deflection basin.

The FWD is normally trailer-mounted on a vehicle; however, for this project, the FWD was manually moved under the HVS-A and tested at Stations 15, 20, 25, 30, and 35 during the selected traffic intervals. Figure 26 shows FWD testing on Item 5.

[1] Bell, H. P. 2007. Airfield pavement evaluation, Illesheim Army Airfield, Storck Barracks, Federal Republic of Germany. Unpublished report, APB AAF-07-08. Vicksburg, MS: U.S. Army Engineer Research and Development Center.

Figure 26. FWD testing on Item 5.

Instrumentation

The instrumentation data was collected using static and dynamic readings over the center of each device or stack of devices. For static testing, the loaded C-17 or F-15E wheel was rolled over the device and briefly paused. For dynamic testing, the loaded C-17 or F-15E wheel was slowly rolled down the center of each instrument location without pausing. Also, at the start of most traffic intervals, the instrumentation data was recorded for approximately 10 min. (approximately 50 passes) to show the response as the wheel moved toward and away from each device.

Forensic investigation

After trafficking of the test section was complete, a 3-ft-wide trench was excavated across the center (Station 25) of each item for forensic investigation (Figure 27). Items 1, 2, 3, and 5 were trenched 9 to 10 months after trafficking was complete, and Items 4 and 6 were trenched 1 to 2 months after trafficking was complete. Each layer of the pavement structure was removed individually and assessed at the center of the rut and outside the traffic lane. DCP tests, CBR tests, nuclear density and moisture measurements, and oven moisture tests were completed at each location on each foundation layer. Furthermore, visual inspection and manual profile

measurements (3-in. increments) were performed to aid in determining where failure occurred.

Figure 27. Trench across the center of Items 1, 3, and 5 of the test section.

6 Pavement Performance Results

General

One purpose of a pavement structure is to protect the subgrade by distributing surface stresses to the foundation materials. Typically, higher stresses occur near the top of a pavement structure for a high tire pressure aircraft, while more damage occurs throughout the entire pavement structure for a higher load aircraft with a lower tire pressure. The difference in the location of damage is a result of the footprint of the aircraft. The large footprint of the C-17 aircraft causes the vertical stresses to be distributed out further and deeper into the pavement structure. The small footprint of the F-15E aircraft concentrates the stresses in a tighter location. The small concentration of stresses allows for more damage near the top of the pavement structure.

Failure of asphalt concrete airfield pavements with military aircraft traffic is typically defined as 1 in. of permanent deformation. Items 1, 2, 3, and 5 were trafficked until the average rut depth of the pavement reached about 2 in. Items 4 and 6 were trafficked until the average rut depth of the pavement reached about 1.5 in. The items were trafficked beyond the limits to evaluate what occurs after failure. The definition of failure at 1 in. of rutting is based on pavement serviceability. The aircraft needs a smooth riding surface for safety. Also, rut depths typically increase exponentially once a pavement receives a permanent deformation of about 1 in.

Several factors were considered when analyzing the traffic results of each item. Items 1, 2, 3, and 5 were trafficked with the C-17 wheel during the warm summer months of June, July, and August 2007. Items 4 and 6 were trafficked with the F-15E wheel during the cool winter months of January, February, and part of March 2008. Average asphalt concrete surface temperatures between the two seasons were 81 and 57°F, respectively. Also, the surface pavements of Items 4 and 6 were allowed to cure for about 7 to 8 months prior to the application of traffic, whereas the surface pavements of Items 1, 2, 3, and 5 cured between 2 weeks and 3 months. Furthermore, the test section was constructed and trafficked in a sheltered environment without the harsh environmental effects of rain, sun, etc. Table 9 presents the average results of the post-test in situ measurements. Test locations

Table 9. Post-test field measurements.

Item	Foundation Layer	Test Location	Dry Density (lb/ft^3)	Moisture Content (%)	CBR (%)
1	Base	Center	118.2	2.0	38.6
		Outside	118.2	2.0	58.6
	Subbase	Center	126.0	2.5	73.5
		Outside	121.2	2.7	70.4
	Subgrade	Center	86.2	29.4	10.0
		Outside	88.0	28.9	10.3
2	Base	Center	118.1	2.1	43.2
		Outside	112.9	2.1	36.7
	Subbase	Center	121.5	3.3	55.0
		Outside	125.0	2.9	57.1
	Subgrade	Center	92.3	27.8	9.2
		Outside	88.5	28.5	10.3
3	Base	Center	139.0	1.5	100.0
		Outside	132.1	1.4	100.0
	Subbase	Center	127.6	2.6	95.0
		Outside	127.1	2.2	90.0
	Subgrade	Center	84.9	28.8	9.4
		Outside	89.5	29.4	9.0
4	Base	Center	143.4	1.3	100.0
		Outside	134.2	1.5	100.0
	Subbase	Center	124.4	2.9	100.0
		Outside	123.7	3.2	97.0
	Subgrade	Center	90.5	29.9	9.5
		Outside	92.1	27.8	9.2
5	Base	Center	119.0	2.1	56.1
		Outside	121.5	2.1	58.8
	Subbase	Center	119.2	2.9	75.8
		Outside	117.1	2.7	79.9
	Subgrade	Center	88.8	29.2	9.0
		Outside	90.1	28.0	8.9
6	Base	Center	118.4	2.6	54.5
		Outside	114.9	2.6	56.8
	Subbase	Center	121.9	3.6	90.5
		Outside	123.9	3.3	90.0
	Subgrade	Center	92.8	27.8	10.0
		Outside	92.3	28.4	9.4

included the center of the rut and outside of the rut. The following paragraphs give the evaluation results of each item.

Item 1

Surface distresses

The only surface distress noted from Item 1 was rutting (Figure 28). Item 1 was trafficked with the C-17 wheel until 776 passes when about 2 in. of rutting had occurred. Failure with an average of 1 in. of rutting occurred around 234 passes. Rutting is a load related distress caused by an accumulation of vertical compressions (Collop et al. 1995). The presence of rutting indicated that a permanent deformation occurred in one or more of the layers of the pavement structure. The vertical stresses that occurred under the loaded wheel caused compression of the pavement materials. Figure 29 shows an overall view of Item 1 after trafficking was complete.

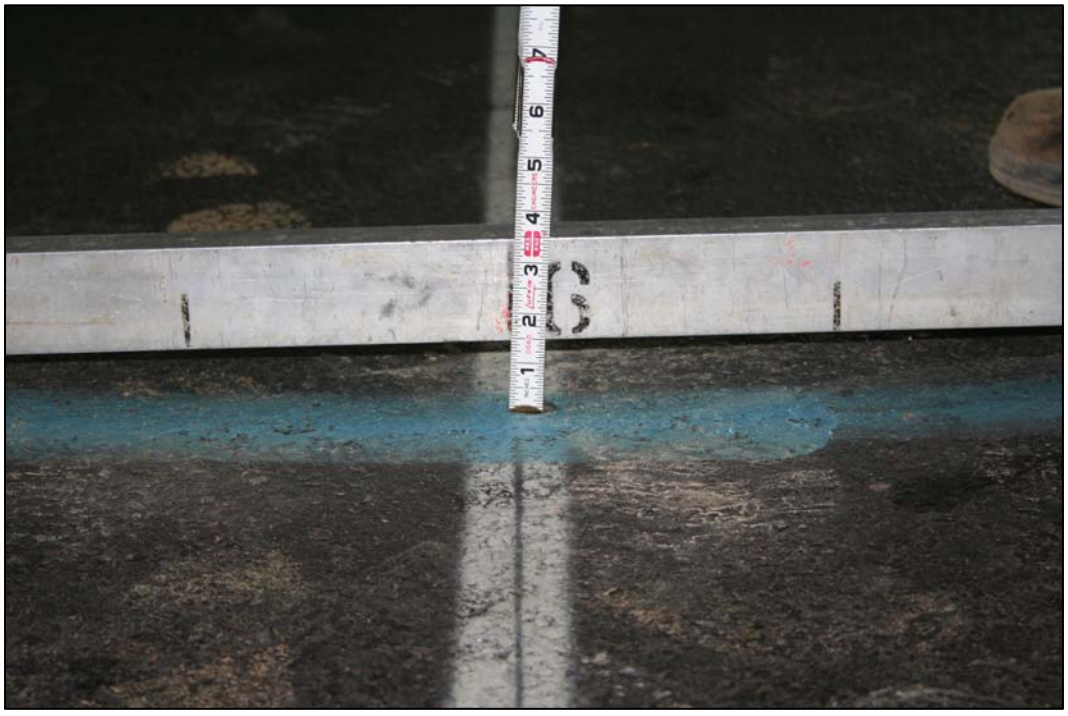

Figure 28. Item 1 centerline rutting after 302 passes.

Falling weight deflectometer

The backcalculated modulus values shown in Figure 30 were computed using WESDEF. WESDEF is a common backcalculation tool used by the ERDC within PCASE software. Literature states that WESDEF may yield unrealistic values when the surface is less than 3 in. thick (Headquarters,

Figure 29. Overall view of Item 1 after traffic completion.

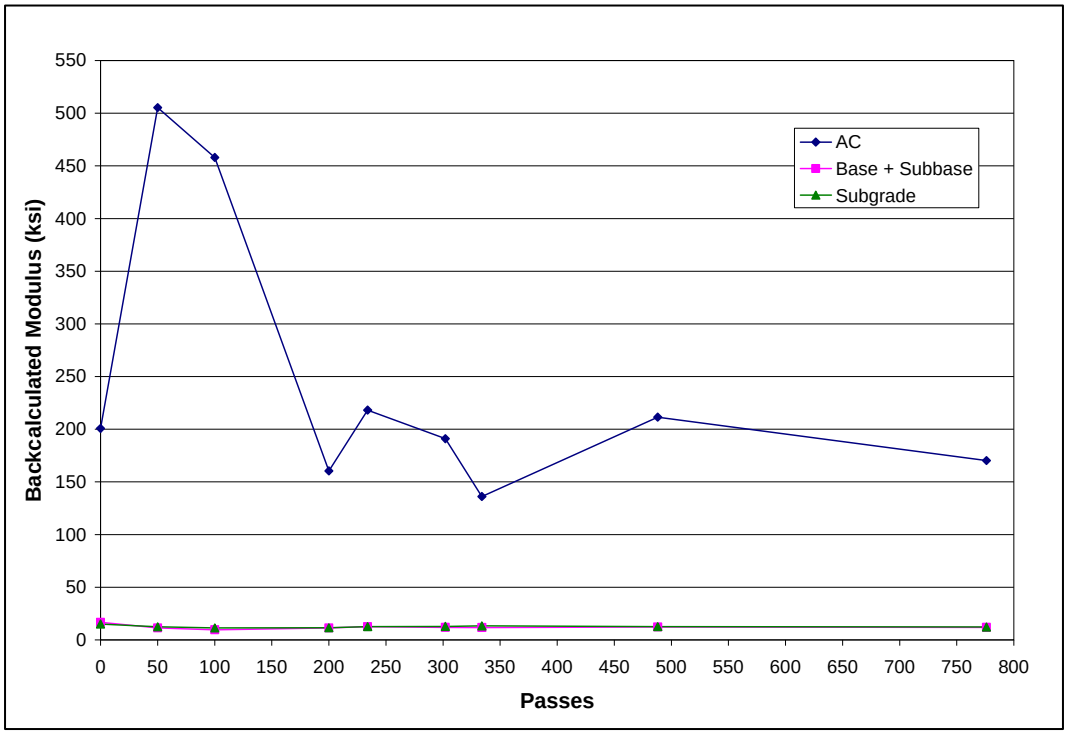

Figure 30. Item 1 backcalculated moduli results.

Departments of the Army, the Navy, and the Air Force 2001). The asphalt concrete modulus values do vary, but they do not seem unrealistic based on typical FWD data. The surface was only 2.5 in. thick, the pavement temperature was in the upper 80°F range, and the pavement was new (2 weeks old). Figure 4-6 in UFC 3-260-03 recommends, at 20 Hz and an average pavement temperature of 85°F, an asphalt concrete modulus value of 350,000 psi; the average asphalt concrete backcalculated modulus for Item 1 was 250,000 psi.

The subgrade modulus values shown in Figure 30 average about 12,000 psi, which is typical for high-plasticity clay (Huang 2004). Figure 31 shows the average stiffness values of the pavement structure with increasing pass level. The stiffness values were determined by dividing the load by the measured deflection at the center of the load plate (D1). The stiffness values did not change much with increasing passes, averaging about 250 kips/in.

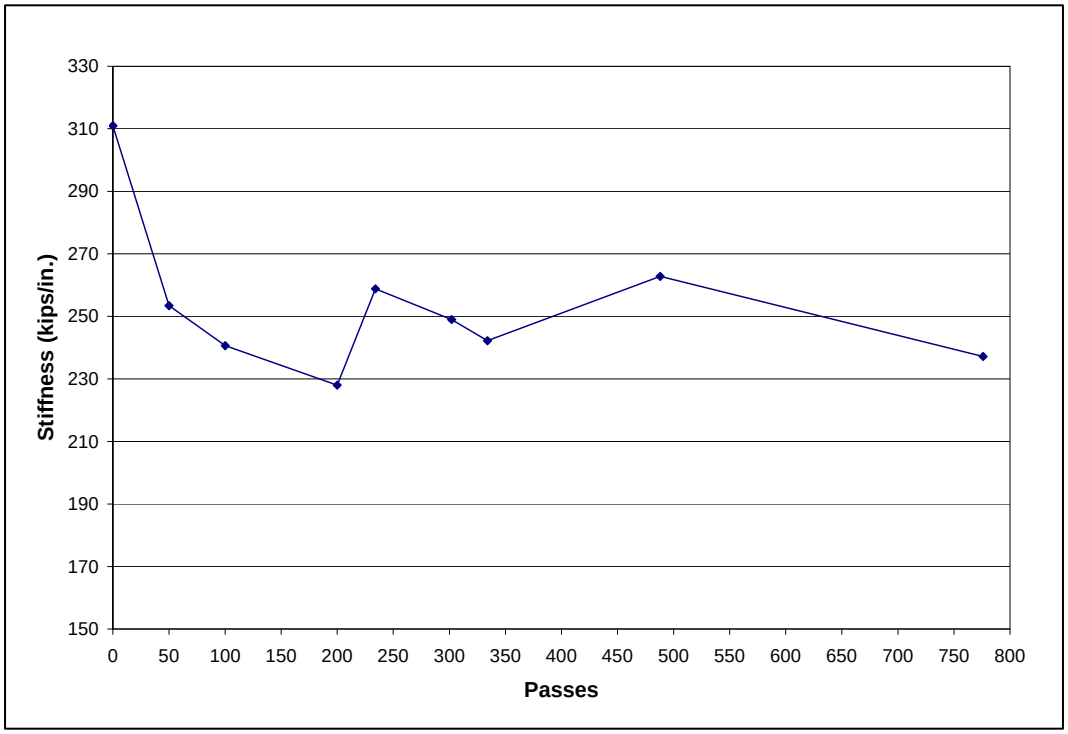

Figure 31. Item 1 stiffness results.

Centerline and cross section profiles

The centerline and cross section profiles of Item 1 showed upheaval on the sides and ends of the traffic lane. Item 1 received a maximum of about 0.50 in. of upheaval at failure (234 passes) and about 0.80 in. of upheaval

after 776 passes. Upheaval typically indicates that there is shear, or an outward movement of material, somewhere within the pavement structure. Figure 32 shows the cross section profiles at Station 37.5, and Figure 33 presents the centerline profiles down the traffic lane. The data for the cross section and centerline profile plots for all items were normalized to zero starting at 0 passes.

Rut depths

Figure 34 shows the rut depth measurements versus increasing pass level for Item 1. Item 1 failed around 234 passes. Failure was determined by averaging the rut depths across the traffic lanes at Stations 12.5, 25, and 37.5. The rut depth measurements in Figure 34 show that the rut depths did not consistently increase with pass level. The occasional decrease in rut depth was dependent upon the side of the lane the wheel was on when trafficking stopped. If the wheel stopped trafficking on the east side of the traffic lane, then the west side of the traffic lane may have had a decrease in rut depth from the previous measurement. This was due to the loaded wheel shoving the asphalt concrete (and/or possibly underlying material) from side to side.

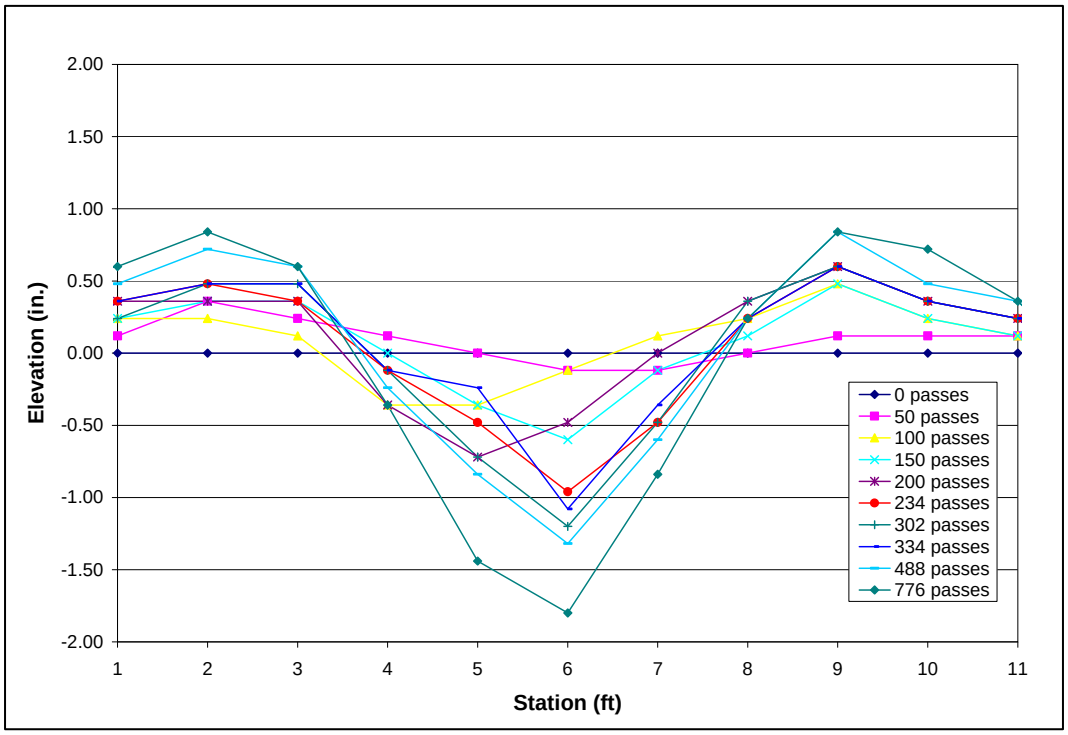

Figure 32. Item 1 cross section profiles at Station 37.5.

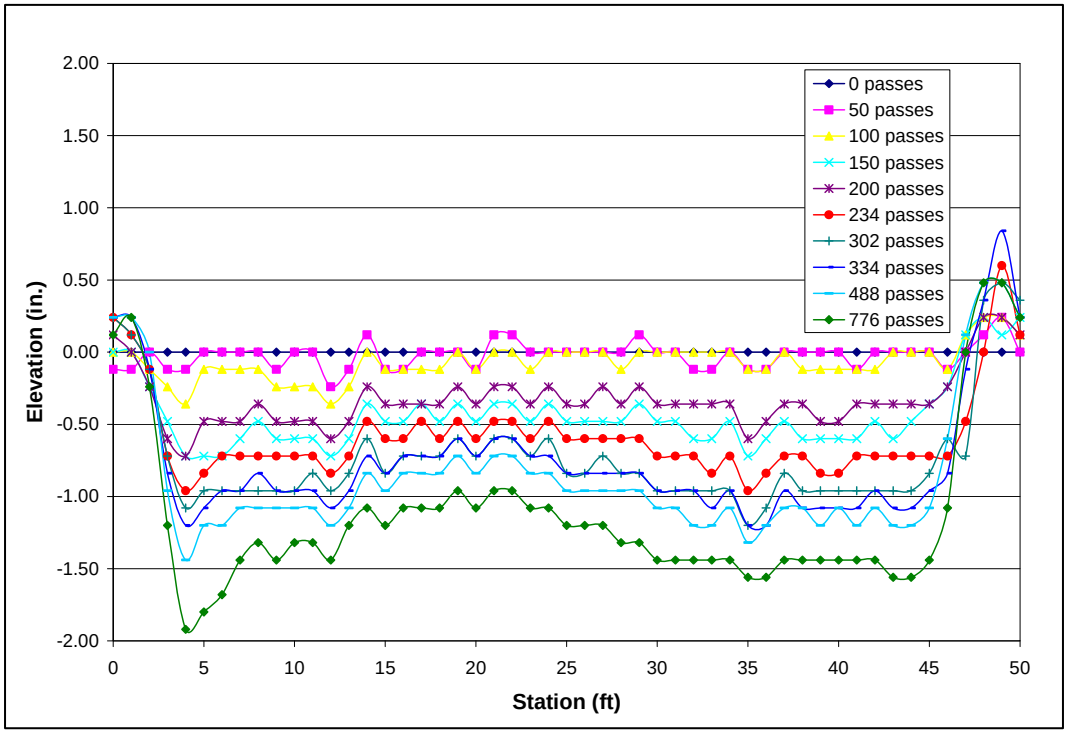

Figure 33. Item 1 centerline profiles.

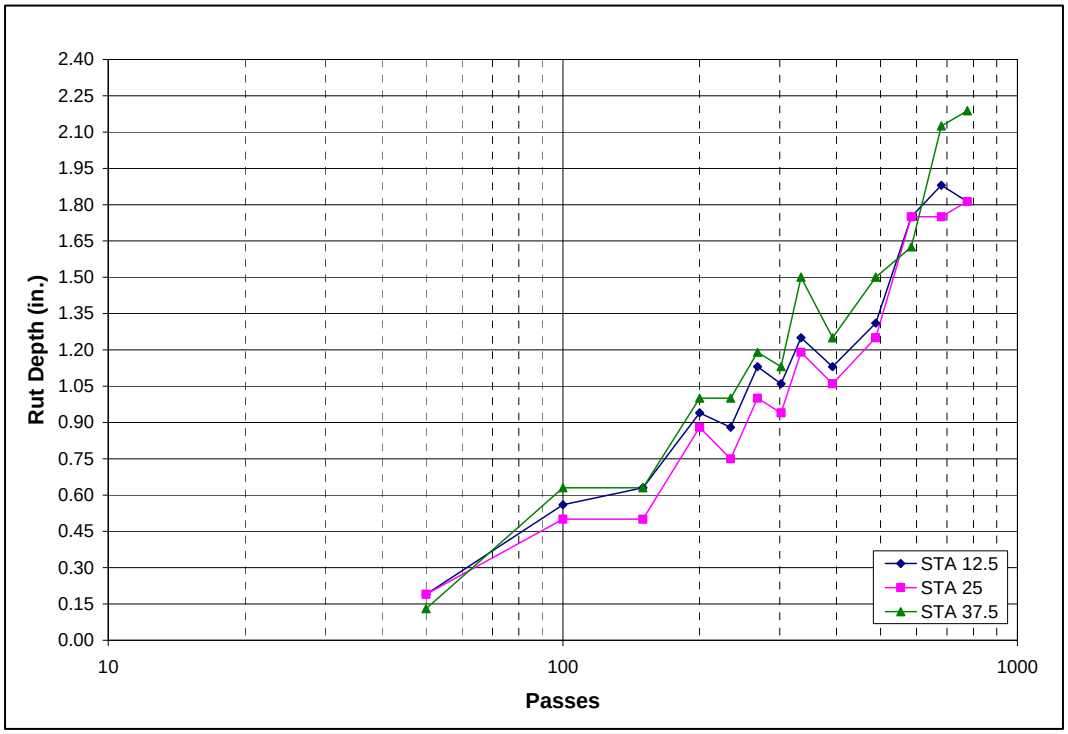

Figure 34. Item 1 rut depth measurements west of the centerline.

Instrumented pavement response

Earth pressure cells

Static and dynamic pressure measurements from the in situ instrumentation were collected at selected traffic intervals. Figure 35 shows a plot of Item 1's maximum dynamic pressure measurements recorded throughout the pavement structure. The EPC measurements within the pavement structure showed, as expected, that there was minimal change in pressure with increasing pass level. The stress measurements in the base course of Item 1 seemed rather high for the C-17 wheel. The tire pressure from the loaded wheel was 142 psi; however, the EPC recorded stress measurements 4.5 in. into the pavement structure between 175 and 200 psi. Reasons for the unexpected high stress measurements in the base course could be a possible calibration error with the EPC installed in the base course of Item 1, or there could have been individual aggregates pressing on the gauge.

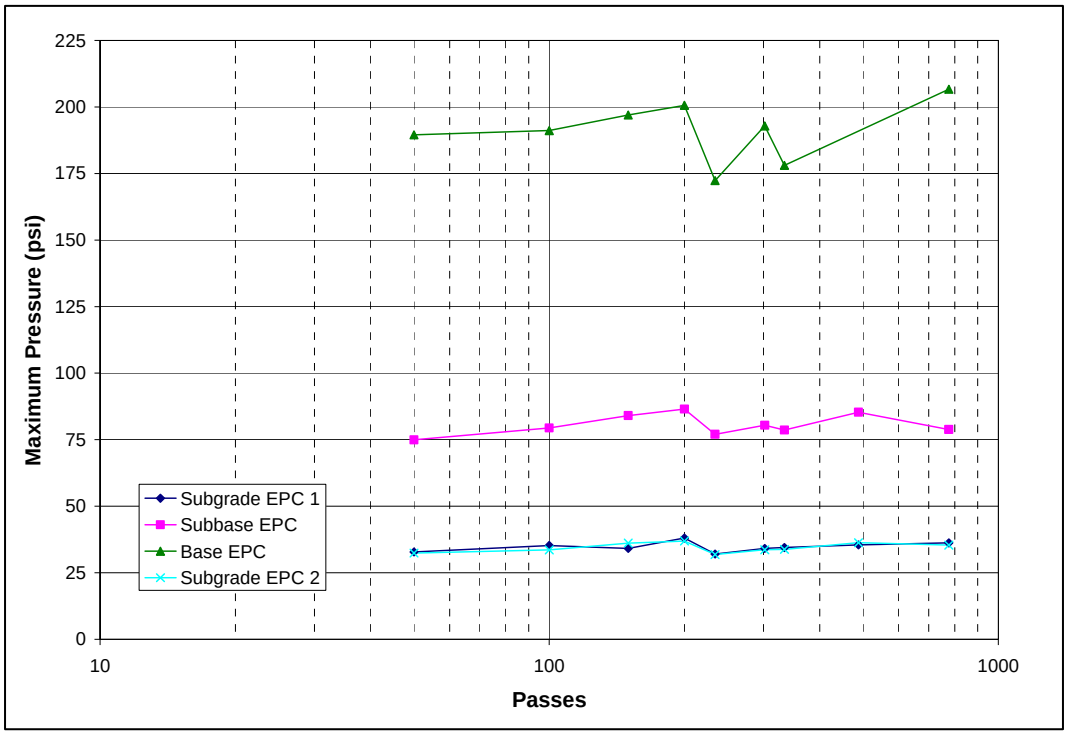

Figure 35. Item 1 maximum pressure measurements.

Linear elastic analysis of the pavement structure predicted the stresses to be approximately 130, 80, and 30 psi in the base, subbase, and subgrade, respectively. The in situ vertical stress measurements in the subbase and subgrade were comparable with the linear elastic analysis results.

Asphalt concrete strain gauges

Figure 36 presents the maximum dynamic strain gauge measurements at the bottom of the asphalt concrete. Strain gauges 1 and 3 were placed parallel to traffic, and strain gauges 2 and 4 were placed perpendicular to traffic. The asphalt concrete strain gauges placed underneath the surface layer parallel and perpendicular to traffic showed that the maximum horizontal strains were much higher than expected. This seemed to be the case for every item. Linear elastic analysis (WinJULEA) using the backcalculated modulus values from the FWD data predicted the strain measurements for Item 1 to be between 700 and 1,200 microstrain. The gauges under the asphalt concrete pavement measured average maximum strains of 2,400 to 2,800 microstrain. There was no trend associated with the tensile strain and increasing pass; the measurements were somewhat consistent throughout trafficking.

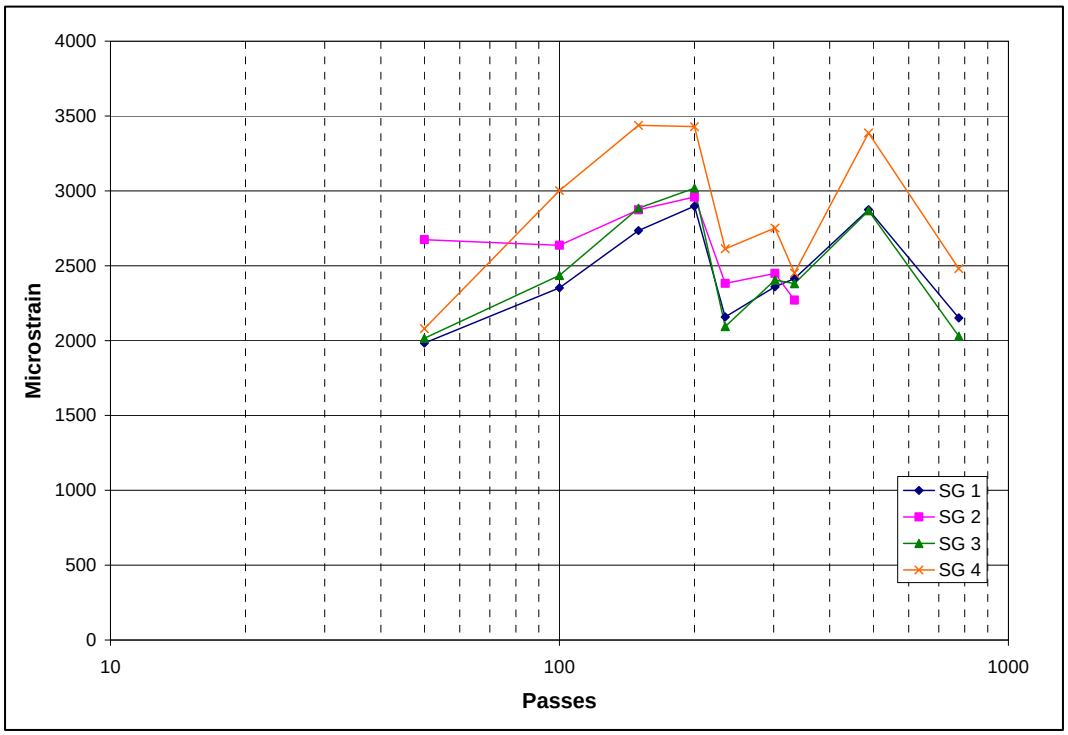

Figure 36. Item 1 maximum strain gauge measurements at the bottom of the asphalt concrete.

Reasons for these higher strain measurements are unclear. However, linear elastic analysis models are not always effective, and they do simplify the problem. On the other hand, another probable reason for the questionable strain gauge measurements could have been a calibration

error, or the manufacturer could have a fault in their production of the strain gauges.

Single depth deflectometers

Figure 37 shows the SDD measurements recorded in the subgrade of Item 1. The results show that the permanent deformation increased at a slightly faster rate once the C-17 wheel reached around 175 passes. The elastic deformation essentially remained the same with each pass. Total deformation includes the elastic deformation and permanent deformation.

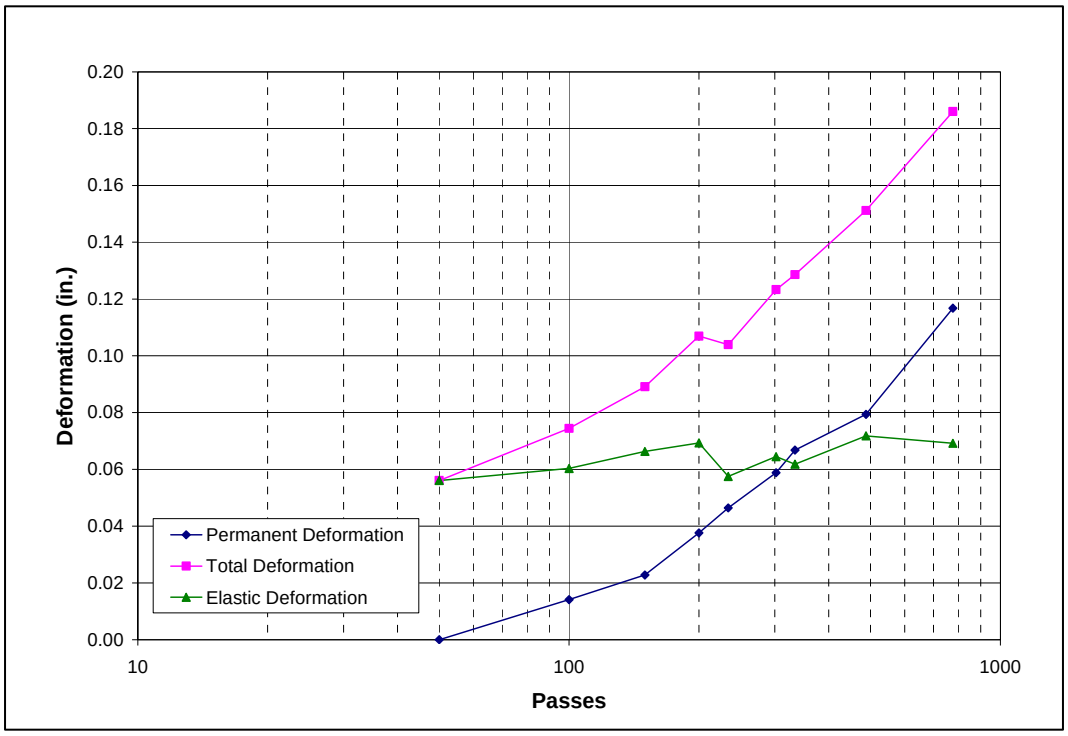

Figure 37. Item 1 subgrade SDD measurements.

Forensics

Item 1 was trenched across Station 25 for forensic investigation. DCP and CBR tests were conducted in the middle of the rut and outside of the rut for each underlying layer. The post-analysis DCP tests indicated that the base and subgrade sustained their strength during trafficking (at the center of the rut); there was no increase in strength over time. The subbase CBR, however, increased about 27% inside the rut. This is a rather large increase in strength. However, Item 1 was trafficked 2 weeks after construction was complete, and the forensics was not conducted until about 9 months after trafficking was complete. There was a 20% increase

in strength outside of the rut in the base course. This is likely due to movement of the base course as a result of shear flow. There was essentially no difference in post-test strength in the middle of the rut and outside the rut for the subbase and subgrade.

Post-test moisture measurements showed approximately 0.8% moisture was lost in the base and subbase. This small amount of moisture loss could be attributed to the expected small margin of error associated with testing. The subgrade did not lose moisture. This shows the great affinity for CH material to hold water over time. Comparing pre-test and post-test nuclear density gauge measurements concluded that there was no measured densification in any of the underlying layers.

Failure location in the pavement structure of any of the items was not clear based on visual inspection alone. The items were not trafficked to catastrophic failure, so it was difficult to visually pinpoint which layer or layers may have had movement. Visual inspection did show that there was no evidence of subgrade pumping in Item 1 because the subbase was not contaminated with clay. Figure 38 shows a profile view of Item 1 after trenching. The picture is of the center of the rut. From the picture, it is difficult to distinguish between the base and subbase material, so red lines were drawn to show each layer.

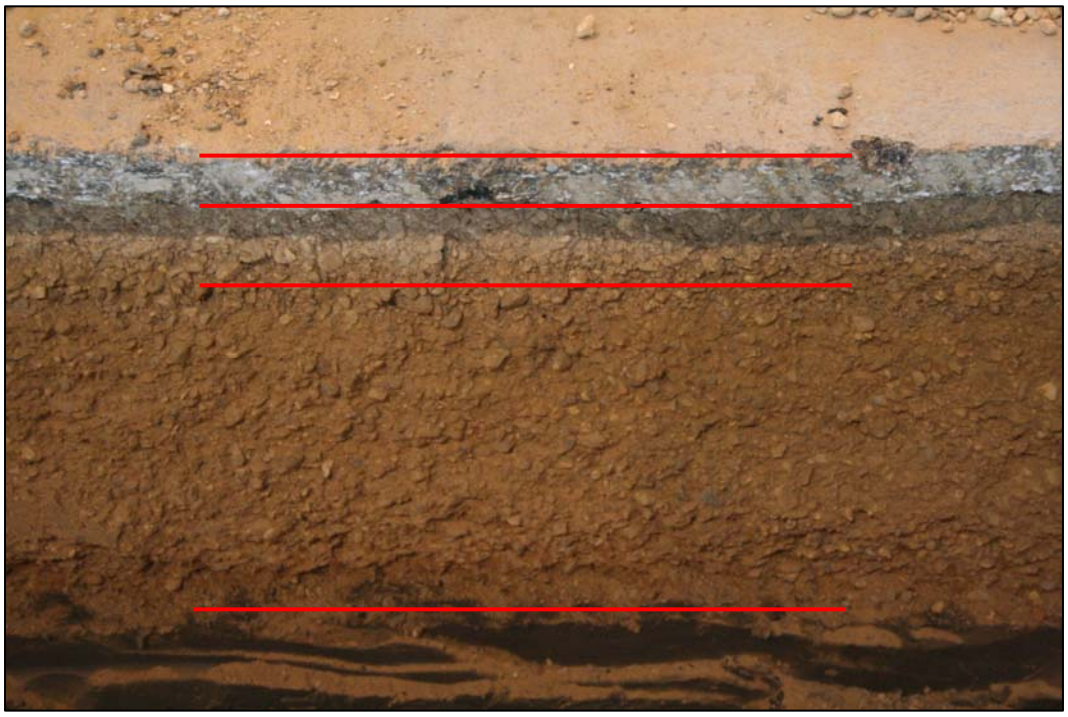

Figure 38. Item 1 trenched profile view.

Manual profile measurements were conducted in 3-in. increments to show the deformation or shape of each layer. The results showed that the asphalt concrete thickness remained constant at 2.5 in., so the surface was not the cause of the failure. The underlying layers were more difficult to assess. The further down a pavement structure, the harder it is to identify what may have occurred as a result of aircraft traffic. The base course thickness for Item 1 was relatively constant at about 7 in. except for inside the rut and directly outside the rut. The base material thicknesses inside the rut and outside the rut were about 6.5 and 7.25 in., respectively. Based on the profile measurements, there seemed to be some movement in the base course as a result of shear flow. There also appeared to be movement in the subbase and subgrade, most likely as a result of shear flow.

Item 2

Surface distresses

Rutting and a small amount of polished aggregate were the two surface distresses noted from Item 2. Polished aggregate is a flexible pavement distress caused by repeated traffic loadings when using aggregate with polish potential. The aggregate begins to appear above the asphalt concrete, and the surface of the aggregate becomes smooth and slick as a result of repeated traffic. This distress is significant because it causes a pavement to lose its friction (Shahin et al. 1976-1977).

Item 2 was trafficked with the C-17 wheel until 3,600 passes, achieving an average of just over 2 in. of rutting. Pavement failure with an average of 1 in. of rutting occurred around 623 passes. Figure 39 shows a rut on Item 2 after 295 passes. Figure 40 shows polished aggregate on the surface after traffic completion, and Figure 41 shows an overall view of Item 2 after traffic completion.

Falling weight deflectometer

Figure 42 presents the backcalculated modulus values of the pavement structure with increasing pass levels. The modulus values of the base plus subbase and subgrade are consistent with each pass, and the surface modulus does not show any type of trend. Figure 43 shows the stiffness values of the pavement structure with pass increase. The stiffness values are higher than those measured from the FWD testing of Item 1. This is

Figure 39. Item 2 centerline rutting at Station 12.5 after 295 passes.

Figure 40. Item 2 polished aggregate after traffic completion (3,600 passes).

Figure 41. Overall view of Item 2 after traffic completion (3,600 passes).

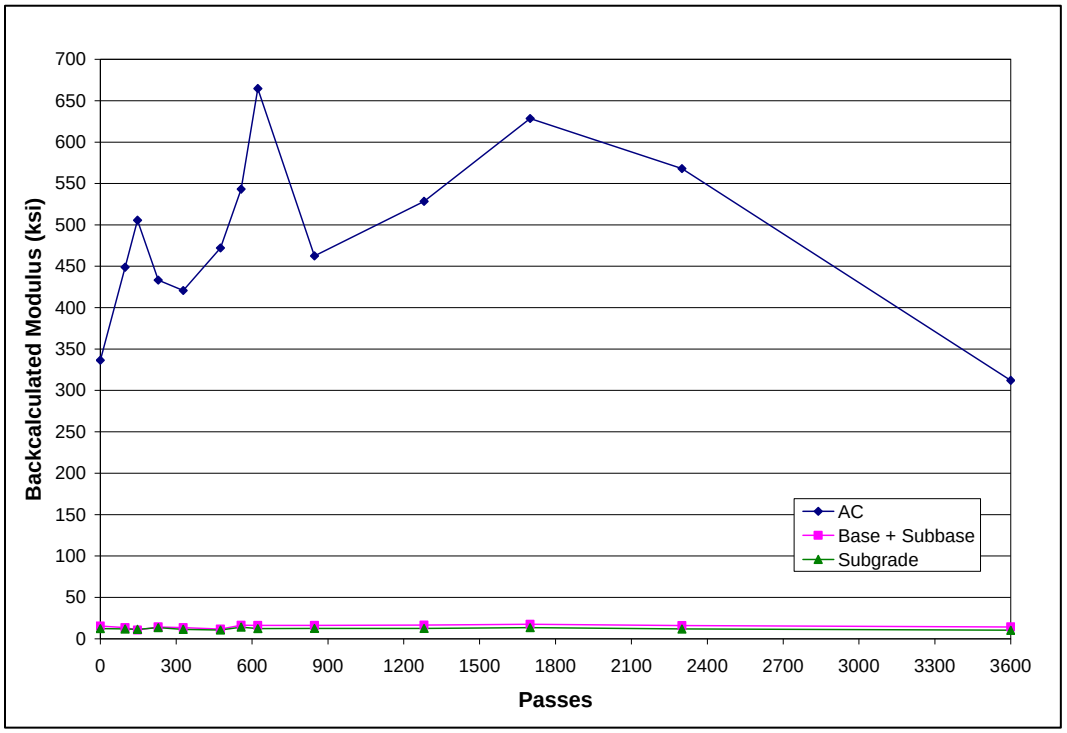

Figure 42. Item 2 backcalculated moduli results.

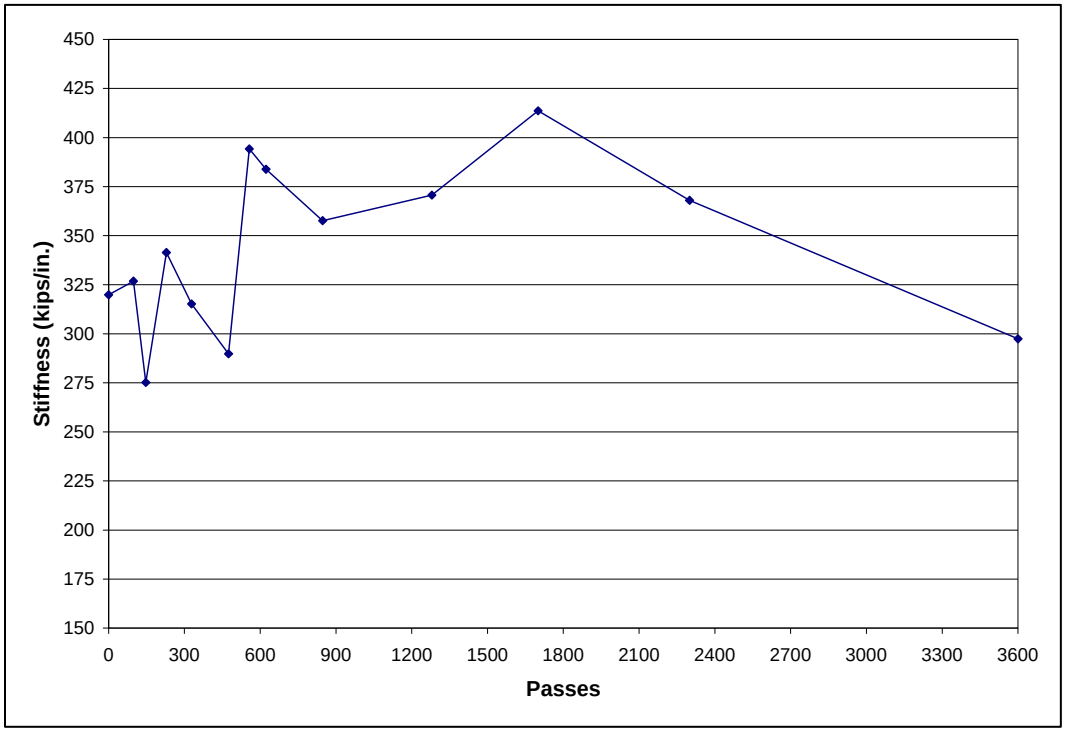

Figure 43. Item 2 stiffness results.

not surprising because the surface of Item 2 was 1 in. thicker than the surface of Item 1. There is no trend associated with stiffness and pass level.

Centerline and cross section profiles

Figures 44 and 45 show the centerline and cross section profiles of Item 2. The plots show pavement upheaval on the sides and ends of the traffic lane. Item 2 received a maximum of about 0.35 in. of upheaval on the sides of the traffic lane at failure (623 passes) and about 0.80 in. of upheaval after 3,600 passes.

Rut depths

Figure 46 shows the rut depth measurements on the centerline of Item 2. Station 37.5 rutted at a slower rate compared to Stations 12.5 and 25. The pre-test DCP data for Item 2 indicated that the pavement structure at Station 37.5 was slightly stronger (approximately 8 CBR) than the pavement structure at Stations 12.5 and 25. This is most likely due to better compaction at Station 37.5. Figure 46 also shows the rut depth beginning to increase at a greater rate at about 3,000 passes.

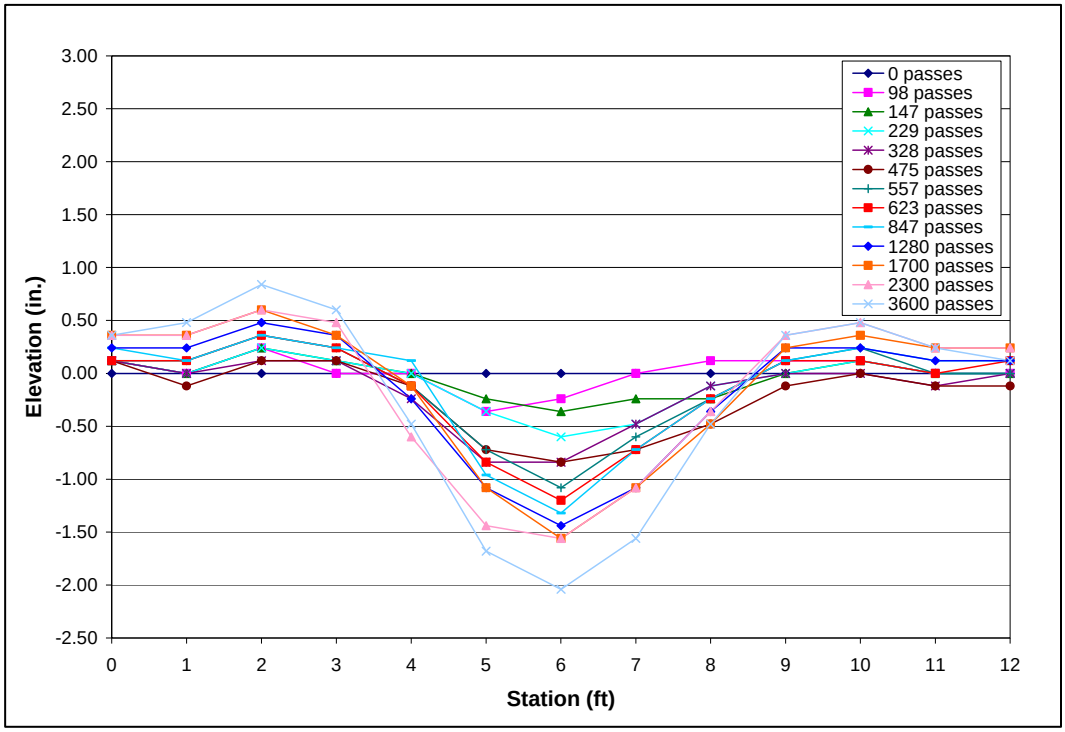

Figure 44. Item 2 cross section profiles at Station 25.

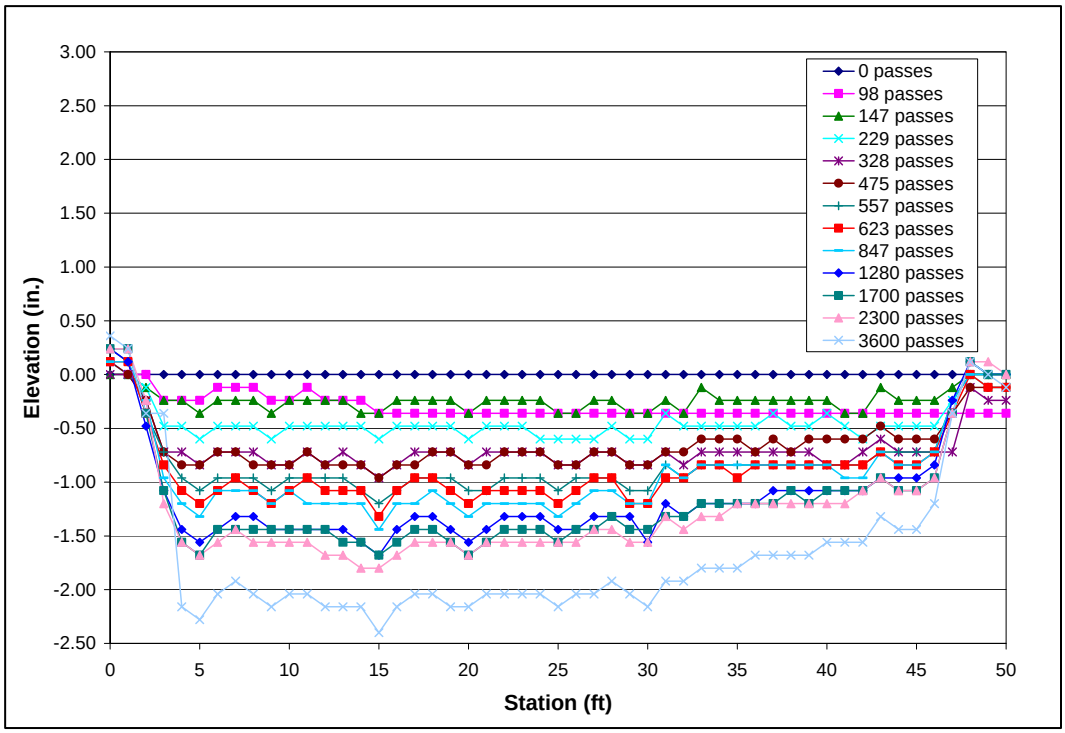

Figure 45. Item 2 centerline profiles.

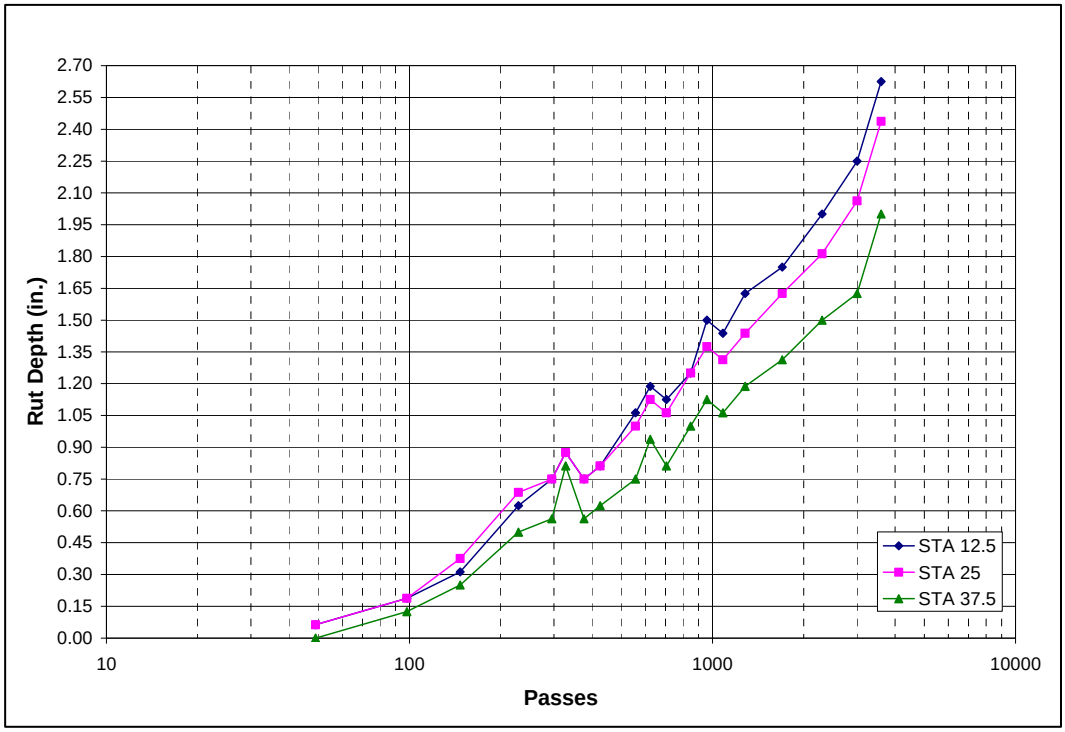

Figure 46. Item 2 centerline rut depth measurements.

Instrumented pavement response

Earth pressure cells

Figure 47 presents the results of the dynamic maximum pressure measurements recorded in the pavement structure of Item 2. The vertical stresses measured in the base were, overall, slightly lower than the predicted stresses (approximately 115 psi). The stresses in the subbase and subgrade were comparable with the linear elastic analysis predictions (approximately 75 and 30 psi, respectively). The plot shows that the subgrade and subbase measurements were relatively constant throughout trafficking, although the subbase EPC shows a small pressure increase around 600 passes. The subbase began receiving higher stresses once failure became apparent; failure of 1 in. of rutting occurred around 623 passes. The maximum pressures in the base course were not consistent; however, there was a slight decreasing trend in pressure with an increase in passes.

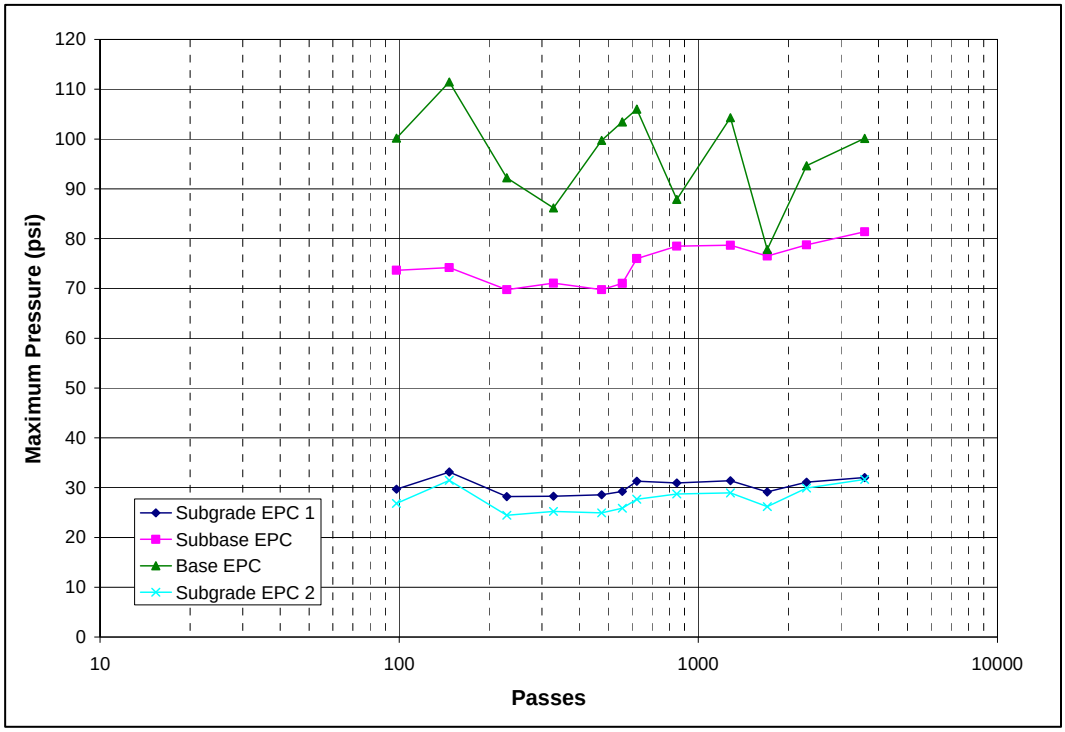

Figure 47. Item 2 maximum pressure measurements.

Asphalt concrete strain gauges

Figure 48 presents the maximum tensile strain measurements at the bottom of the asphalt concrete. Again, strain gauges 1 and 3 were placed parallel to traffic, while strain gauges 2 and 4 were placed perpendicular to traffic. The maximum horizontal strains for Item 2 were much higher than expected. Linear elastic analysis using the backcalculated modulus values from the FWD data predicted the strain measurements for Item 2 to be between 800 and 1,100 microstrain. The gauges under the asphalt concrete pavement measured average maximum strains of 2,200 to 3,100 microstrain. There was a slight increasing trend associated with the tensile strain and increasing pass. The measurements were consistent throughout trafficking; however, there was a noticeable strain increase (approximately 400 to 800 microstrain) at 623 passes (failure) for each of Item 2's strain gauges.

Single depth deflectometers

Figure 49 shows the SDD dynamic measurements recorded in the subgrade. The plot shows that there was a steady increase in permanent deformation with increasing pass level. The permanent deformation recorded in the subgrade was around 0.35 in.

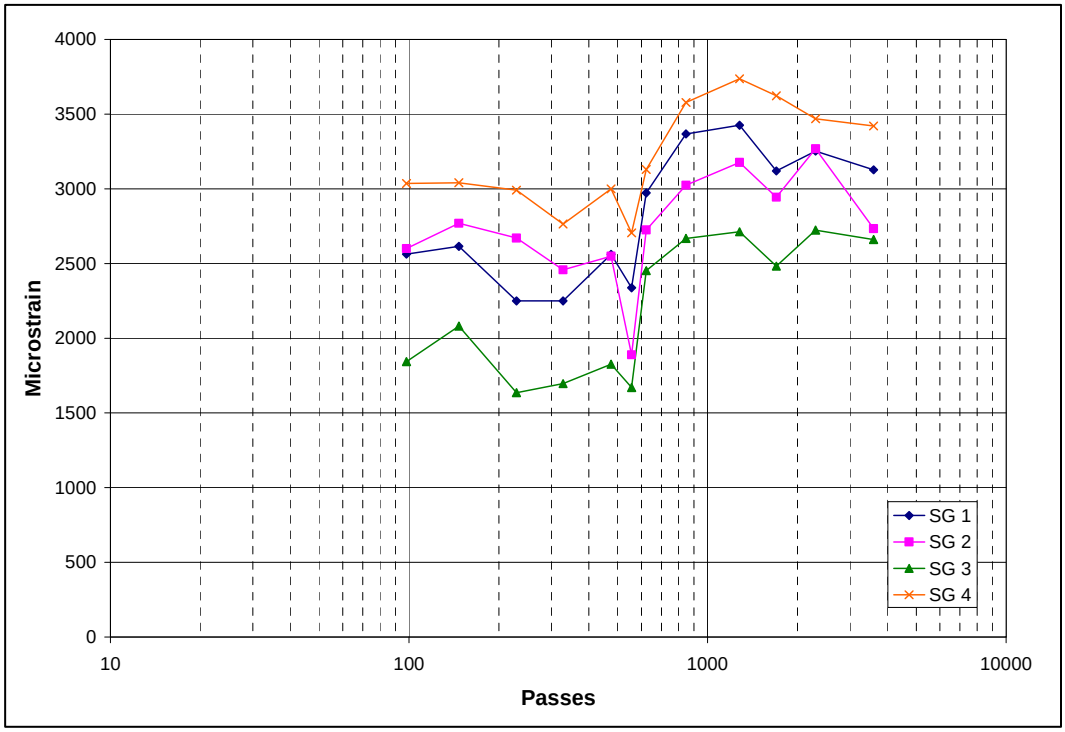

Figure 48. Item 2 maximum strain gauge measurements at the bottom of the asphalt concrete.

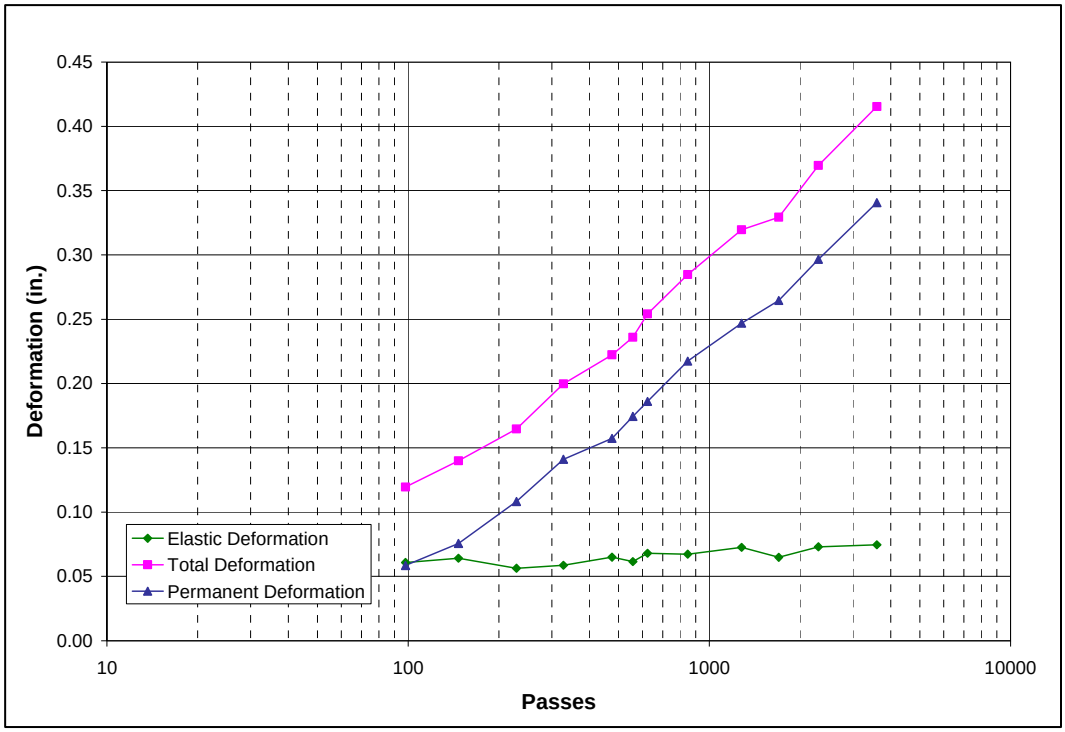

Figure 49. Item 2 subgrade SDD measurements.

Forensics

Item 2 was trenched across Station 25 for forensic investigation. The post-analysis DCP tests results showed that there was no increase in strength over time in the base or subgrade. However, there was an approximate 10% increase in CBR for the subbase and a 10% decrease in CBR for the base. For Item 2, there was a minimal difference in post-test strength in the middle of the rut and outside the traffic lane. The base layer in the middle of the rut had a CBR of approximately 7% more than what was measured directly outside of the rut.

Post-test moisture measurements showed minimal loss in moisture with the base, subbase, and subgrade. Comparing pre-test and post-test nuclear density gauge measurements concluded that there was no densification of the base, subbase, or subgrade. The densities did, however, decrease slightly outside of the rut for the base and subgrade. The density increased slightly outside of the rut for the subbase. Again, this small change in density could possibly be a result of the margin of error associated with the nuclear gauge.

Visual inspection did not reveal any evidence of subgrade pumping in Item 2. Figure 50 shows a profile view of Item 2 after trenching. The picture was taken from the right side (east side) of the traffic lane. The red line depicts the interface between the base and subbase. The subgrade, barely shown at the bottom of the picture, had not been removed when the photo was taken.

The manual profile results showed that the asphalt concrete thickness remained constant at 3.5 in., so the pavement did not fail as a result of the asphalt concrete. As expected, the underlying layers were more difficult to assess. The base course thickness for Item 2 was relatively constant, although it seemed a little low compared to the pre-test data (approximately 0.20 in. lower). This was somewhat unexpected because the density measurements indicated that there was no densification of the base course layer. Based on the profile measurements, movement seemed to be in the base, subbase, and subgrade. Nonetheless, it appeared as though most of the movement occurred in the subgrade, most likely as a result of shear flow.

Figure 50. Item 2 trenched profile view.

Item 3

Surface distresses

Rutting and polished aggregate were the surface distresses noted from Item 3 (Figures 51, 52, and 53) after trafficking. Polished aggregate was noticeable shortly before 1,000 passes. Item 3 was trafficked with the C-17 wheel until about 14,000 passes. Failure arose around 2,850 passes. Although the item sustained a high number of passes, cracking never occurred. The absence of cracking is an indicator that the surface pavement was performing well. The asphalt concrete was able to flex with the load because the pavement was not too stiff. Of course, the items were trafficked in a sheltered environment without the harsh environmental effects of rain, sun, etc.

Falling weight deflectometer

Figure 54 shows the backcalculated moduli of the pavement structure from the FWD testing. The results show that the subbase and subgrade moduli remained consistent throughout trafficking. The base course moduli showed a slight decreasing trend with increasing passes. The stiffness values were opposite. Figure 55 shows a slight increasing trend with stiffness as the pass level increased.

Figure 51. Item 3 rutting after 147 passes.

Figure 52. Item 3 rutting after 1,544 passes.

Figure 53. Item 3 polished aggregate after 7,000 passes.

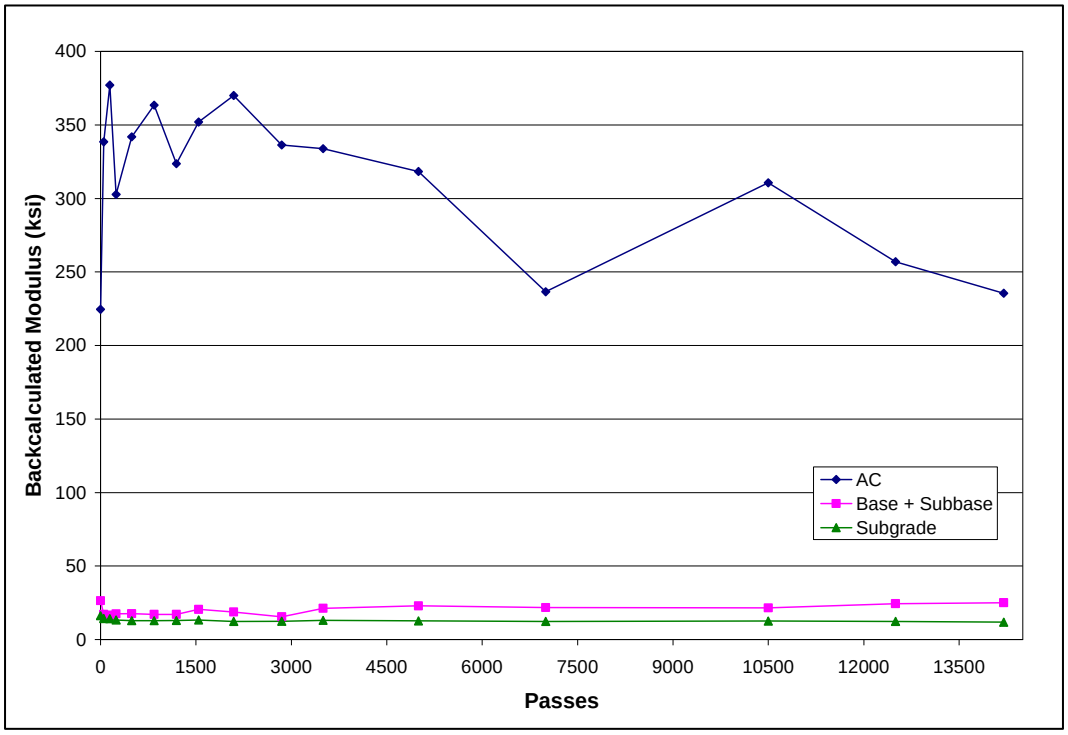

Figure 54. Item 3 backcalculated moduli results.

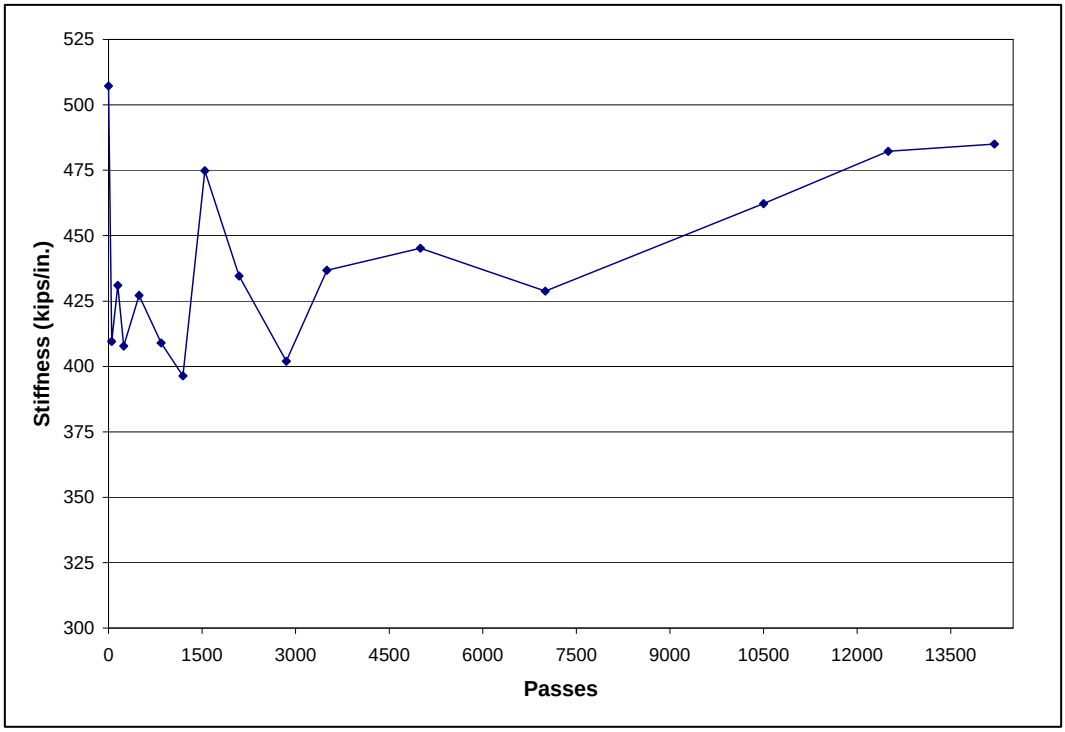

Figure 55. Item 3 stiffness results.

Centerline and cross section profiles

The centerline and cross section profiles of Item 3 showed slight upheaval on the sides and at the beginning and end of the traffic lanes (Figures 56 and 57). Item 3 received a maximum upheaval of 0.50 in. on the sides of the traffic lane after trafficking. At failure (2,850 passes), the maximum upheaval measured on the sides of the traffic lane was about 0.24 in.

Rut depths

Figure 58 shows the rut depth measurements versus increasing pass level for Item 3. Item 3 failed around 2,850 passes. Again, failure was determined by averaging the rut depths across the traffic lane at Stations 12.5, 25, and 37.5. Figure 58 also shows that the pavement structure at Station 12.5 was slightly weaker than the other stations. This is most likely due to an inconsistent compaction effort across the item. The pre-traffic DCP data at Station 12.5 for Item 3 showed that the base course material was slightly weaker than at Stations 25 and 37.5. This inadequate compaction effort possibly resulted in a more rapid failure rate at Station 12.5. However, this greater rate of rutting was also seen at Station 12.5 for Items 4 and 6. During trafficking, the HVS-A wheel appeared as though it may have been “pushing off” at Station 5 every time the machine started a

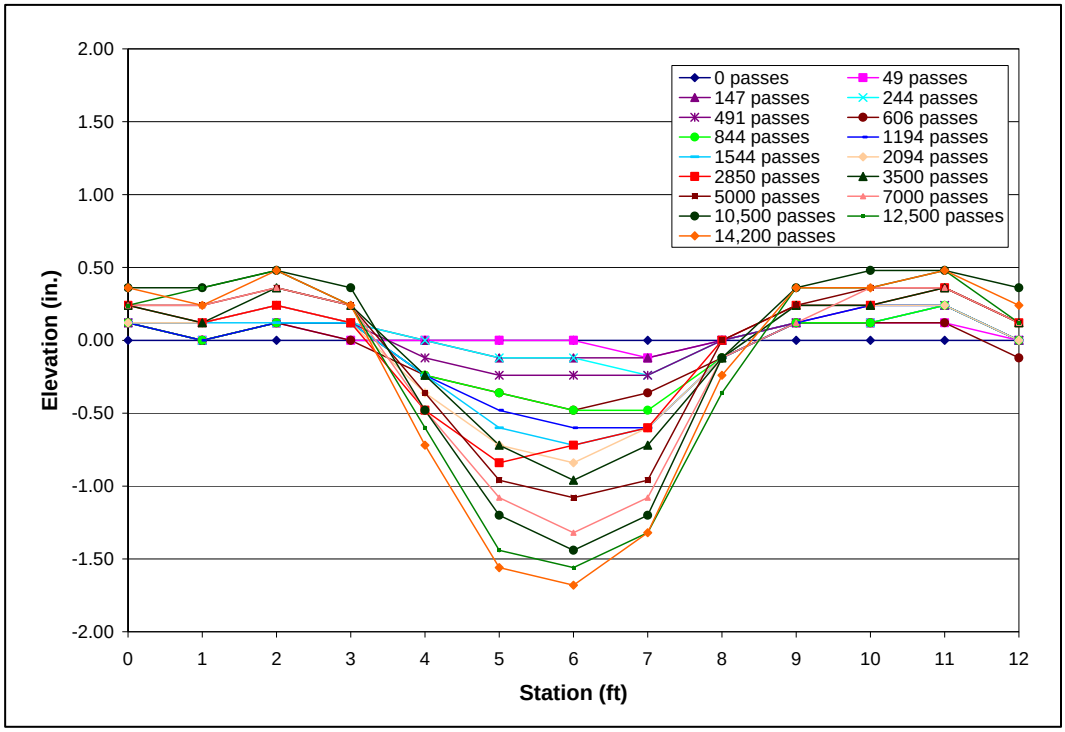

Figure 56. Item 3 cross section profiles at Station 37.5.

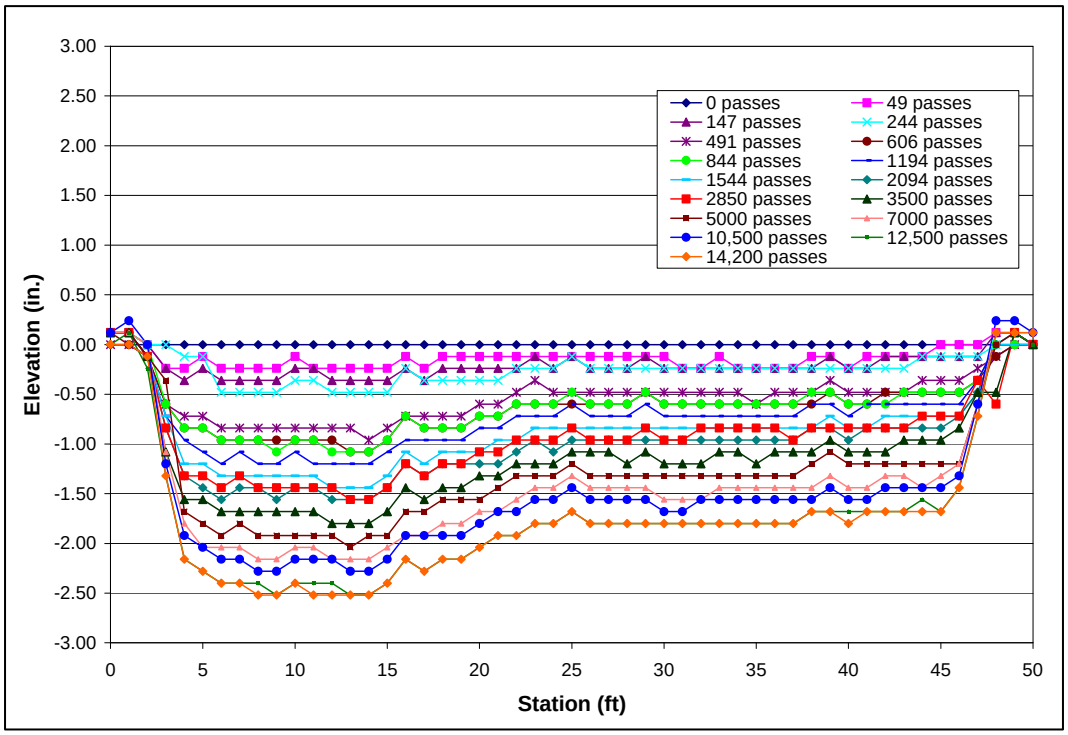

Figure 57. Item 3 centerline profiles.

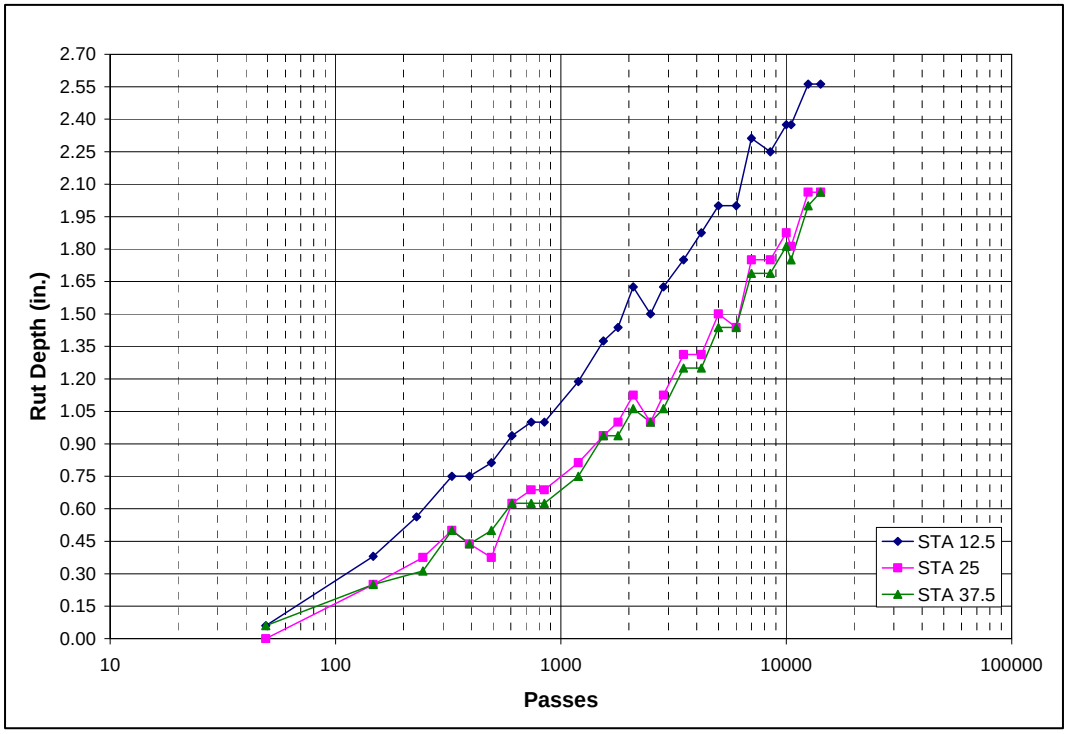

Figure 58. Item 3 centerline rut depth measurements.

pass. So, this is another possible reason as to why rutting at Station 12.5 was increasing at a faster rate than at Stations 25 and 37.5.

Instrumented pavement response

Earth pressure cells

Figure 59 shows a plot of Item 3's maximum dynamic pressure measurements recorded throughout the pavement structure. The EPC installed in the base course layer malfunctioned, so no pressure measurements were recorded. Linear elastic analysis predicted the stress measurements in the base course to be approximately 90 psi. The in situ EPC measurements in the subbase and subgrade showed that there was essentially no change in the vertical stresses with increasing pass level. Linear elastic analysis predicted the stresses in the subbase and subgrade to be approximately 65 and 30 psi, respectively. The predicted values were comparable with the actual measurements.

Asphalt concrete strain gauges

Figure 60 presents Item 3's maximum dynamic strain gauge measurements under the asphalt concrete. The maximum horizontal strains for

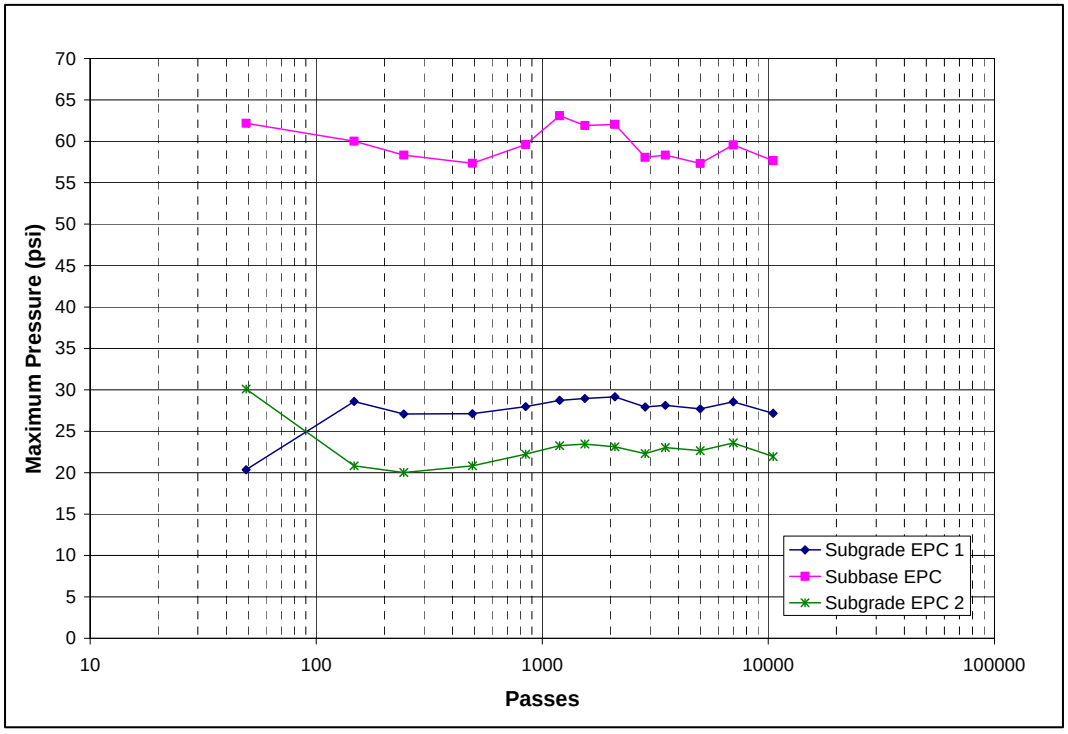

Figure 59. Item 3 maximum pressure measurements.

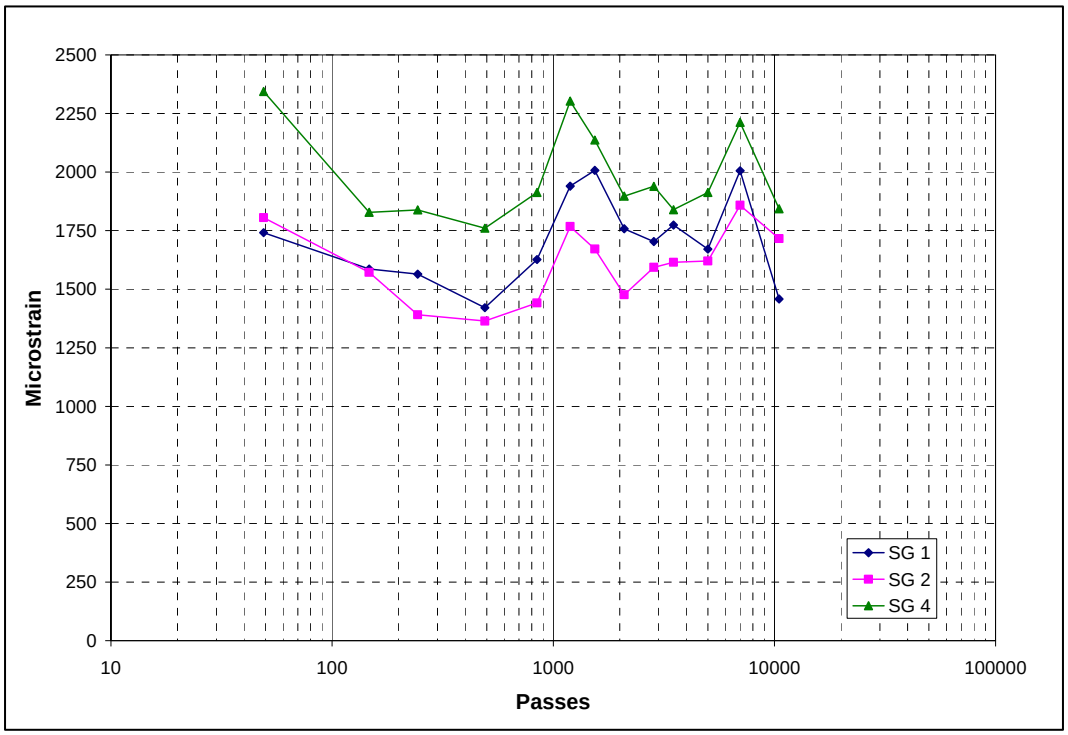

Figure 60. Item 3 maximum strain gauge measurements at the bottom of the asphalt concrete.

Item 3 were also higher than expected. Linear elastic analysis using the backcalculated modulus values from the FWD data predicted that the strain measurements for Item 3 should have been between 750 and 850 microstrain. The gauges under the asphalt concrete pavement measured average maximum strains of 1,500 to 1,900 microstrain. There was no trend associated with the tensile strain for increasing passes for any of Item 3's strain gauges. The measurements remained relatively constant throughout trafficking.

Single depth deflectometers

Figure 61 shows the SDD measurements recorded from the subgrade of Item 3. The results show that the permanent deformation increased at a slightly faster rate once the traffic count reached around 500 passes. The permanent deformation recorded in the subgrade after trafficking was about 0.23 in. The elastic deformation essentially remained the same with each pass.

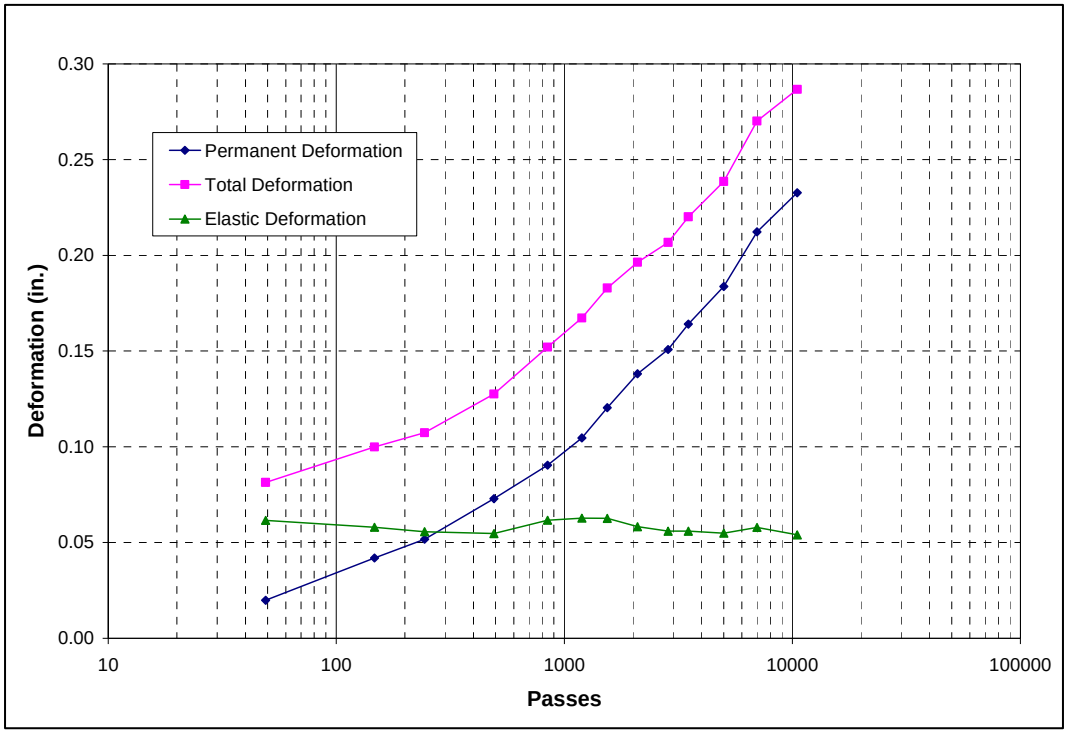

Figure 61. Item 3 subgrade SDD measurements.

Forensics

Item 3 was trenched across Station 25 for forensic investigation. The post-analysis DCP and CBR test results showed that the pavement structure

maintained or improved its strength with time. At the center of the rut and outside of the traffic lane, the base course for Item 3 was still approximately 100 CBR, and the subbase improved to approximately 93 CBR. This is a rather large gain in strength. The subbase in Items 1 and 2 gained in strength, but the gain was not as significant. The subgrade strength remained around 10 CBR both inside and outside of the rut.

Post-test moisture measurements showed an insignificant amount of moisture was lost in the base, subbase, and subgrade. According to the pre-test and post-test density measurements, there was no densification in the base or subgrade layers; however, there was a minimal increase in the dry density of the subbase. This could mean that there was some possible densification of the subbase.

Visual inspection did not reveal any evidence of subgrade pumping in Item 3. Figure 61 shows a profile view of Item 3 after trenching. The picture shows part of the base and subgrade and all of the subbase. Figure 62 clearly shows how difficult it was to assess each item. The interfaces of each layer within each item visually appeared to be level across the traffic lane.

Figure 62. Item 3 trenched profile view.

The manual profiles showed that the asphalt concrete thickness remained constant at 4 in., so the pavement did not fail as a result of the asphalt concrete. The base course thickness was relatively constant at 6.5 in. across the traffic lane. The profile measurements of Item 3 indicated that there was movement in the subbase and subgrade. It was not obvious as to which of these two layers received more failure. However, the SDD measurements showed that the subgrade received about 0.21 in. of permanent deformation.

Item 4

Surface distresses

The surface distresses from Item 4 included rutting, polished aggregate, and cracking. Micro-cracking began to occur on the pavement around 23,000 passes of the F-15E wheel. With time, the cracking began to take the shape of fatigue cracking. Cracking can occur in asphalt concrete pavements that are too stiff. Cracking likely occurred on Item 4 because the pavement temperature was about 26°F cooler than the surface temperature of Items 1, 2, 3, and 5. Also, Item 4 was trafficked with the F-15E wheel, which is a smaller tire with a lighter load and much higher tire pressure when compared to the C-17 wheel. The stresses were concentrated in a smaller area and higher in the pavement structure for Item 4, so the asphalt concrete received more damage. Figure 63 shows the pavement after failure of 1 in. of rutting.

Falling weight deflectometer

Figures 64 and 65 present the results of Item 4's FWD testing. Item 4 had an average asphalt concrete backcalculated modulus value of 1,278,000 psi. This is higher than what was seen with the FWD test results of Items 1, 2, 3, and 5. The stiffness values of the pavement structure were also higher. These results were expected because Item 4 was trafficked during the winter, and Items 1, 2, 3, and 5 were trafficked during the summer. Also, the asphalt concrete of Item 4 cured for about 5 to 6 months longer than the other items (not Item 6; curing of Item 6 was 1 month longer than Item 4). The asphalt concrete modulus values had a slight decreasing trend with the increase in pass level. This is most likely a result of fatigue damage. The subbase and subgrade backcalculated modulus values were consistent throughout trafficking.

Figure 63. Item 4 polished aggregate and cracking at failure (42,881 passes).

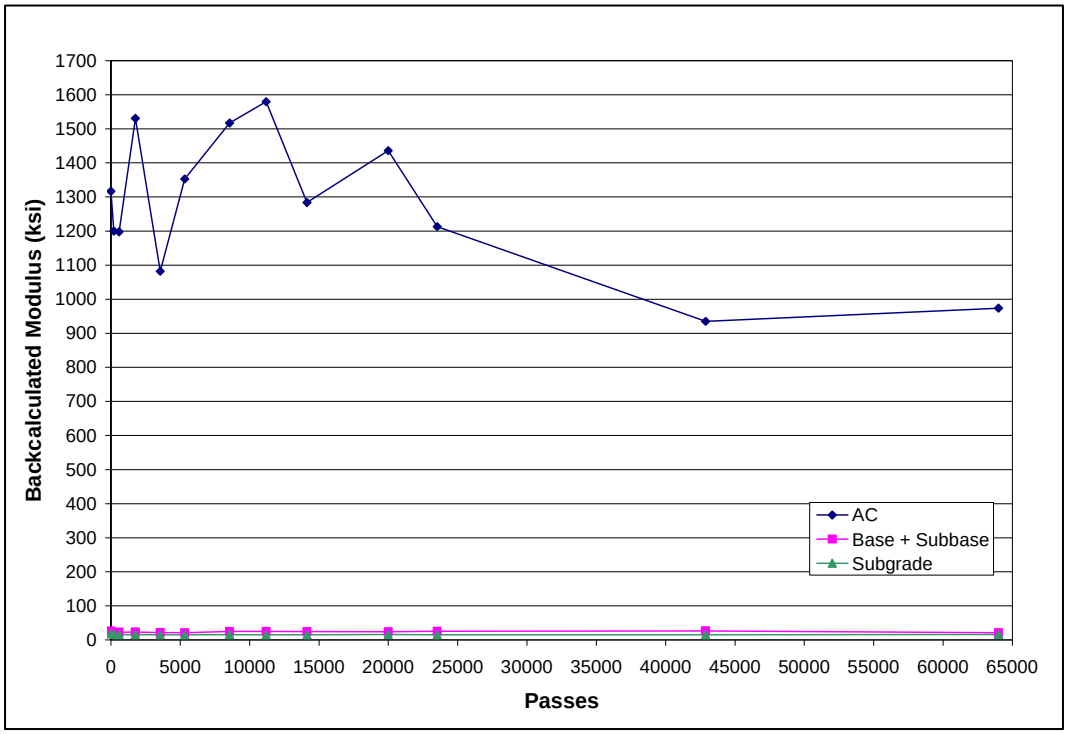

Figure 64. Item 4 backcalculated moduli results.

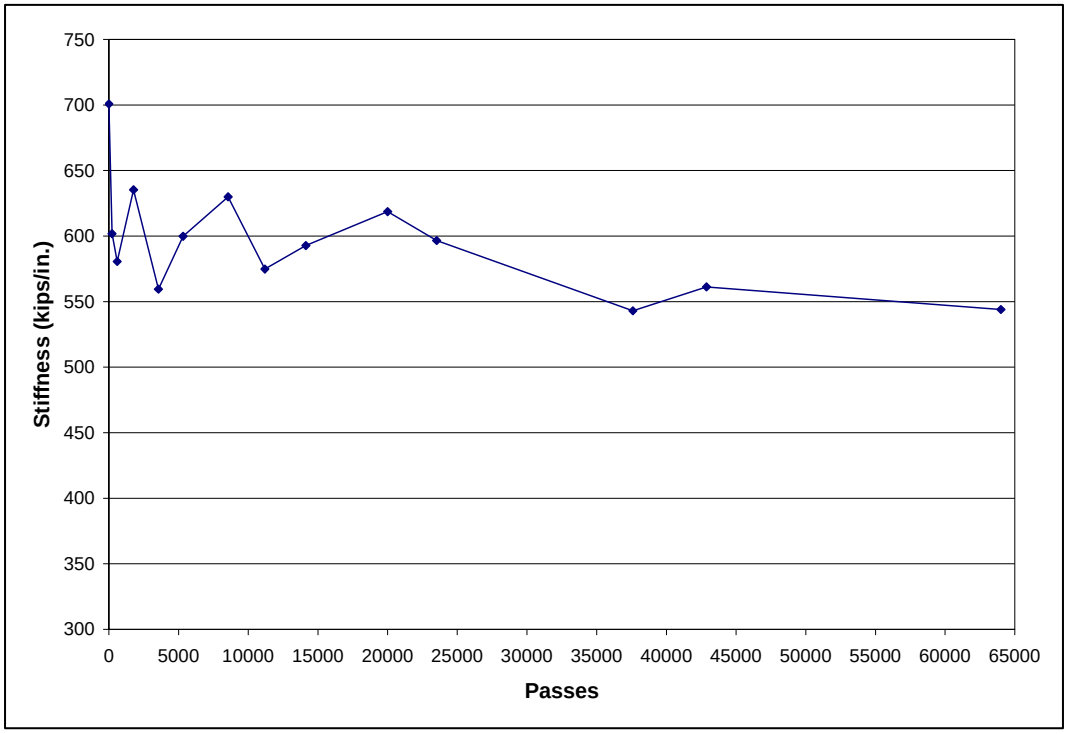

Figure 65. Item 4 stiffness results.

Centerline and cross section profiles

Figures 66 and 67 show the centerline and cross section profiles of Item 4. The plots show upheaval on the sides and ends of the traffic lane. Item 4 received a maximum of about 0.35 in. of upheaval on the sides of the traffic lane at failure (42,881 passes) and after 98,897 passes. The upheaval did not increase once failure occurred.

Rut depths

Figure 68 shows the rut depth measurements versus increasing pass level for Item 4. Item 4 failed around 42,881 passes. Figure 68 also shows that the pavement structure at Station 12.5 was slightly weaker than at the other stations. Again, this is most likely due to an inconsistent compaction effort across the item or from the HVS-A "pushing off" at Station 5 after each pass. A higher rate of rutting began around 40,000 passes.

Instrumented pavement response

Earth pressure cells

Figure 69 shows a plot of Item 4's maximum pressure measurements recorded throughout the pavement structure. There was a stress increase

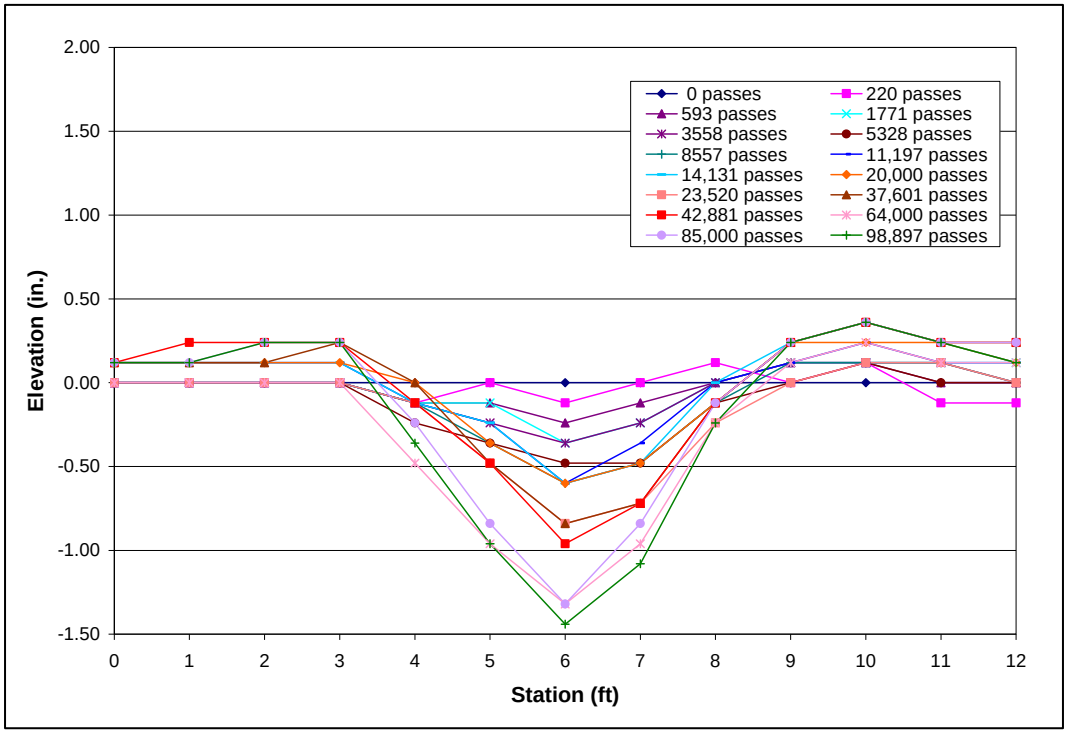

Figure 66. Item 4 cross section profiles at Station 25.

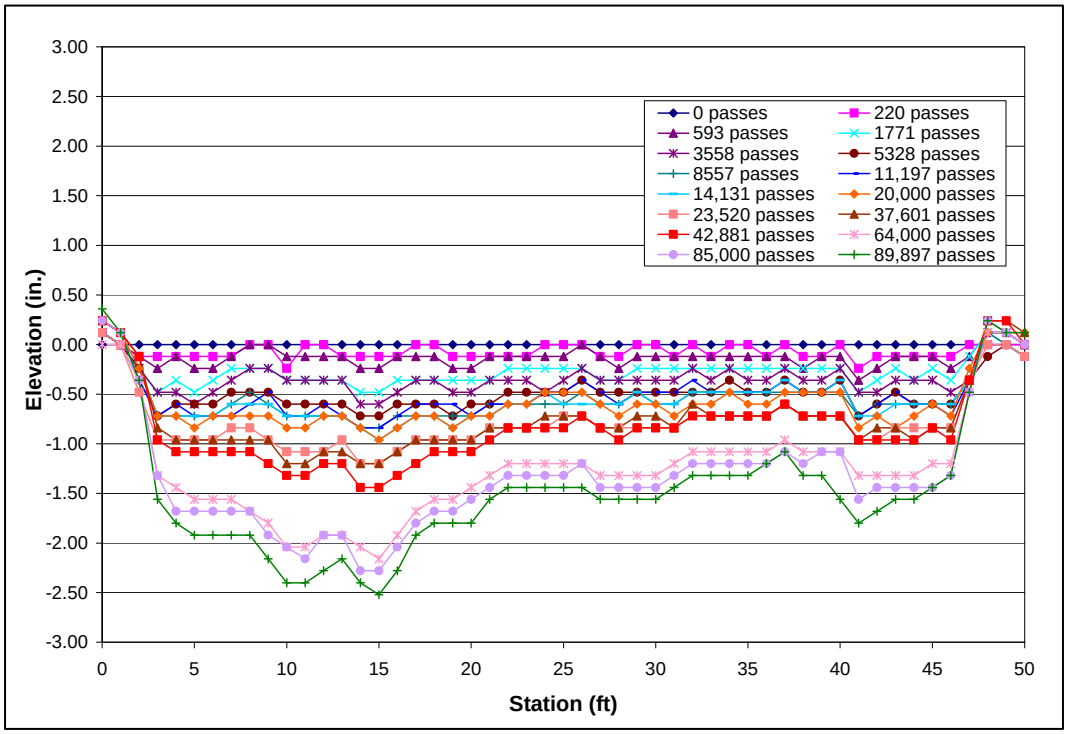

Figure 67. Item 4 centerline profiles.

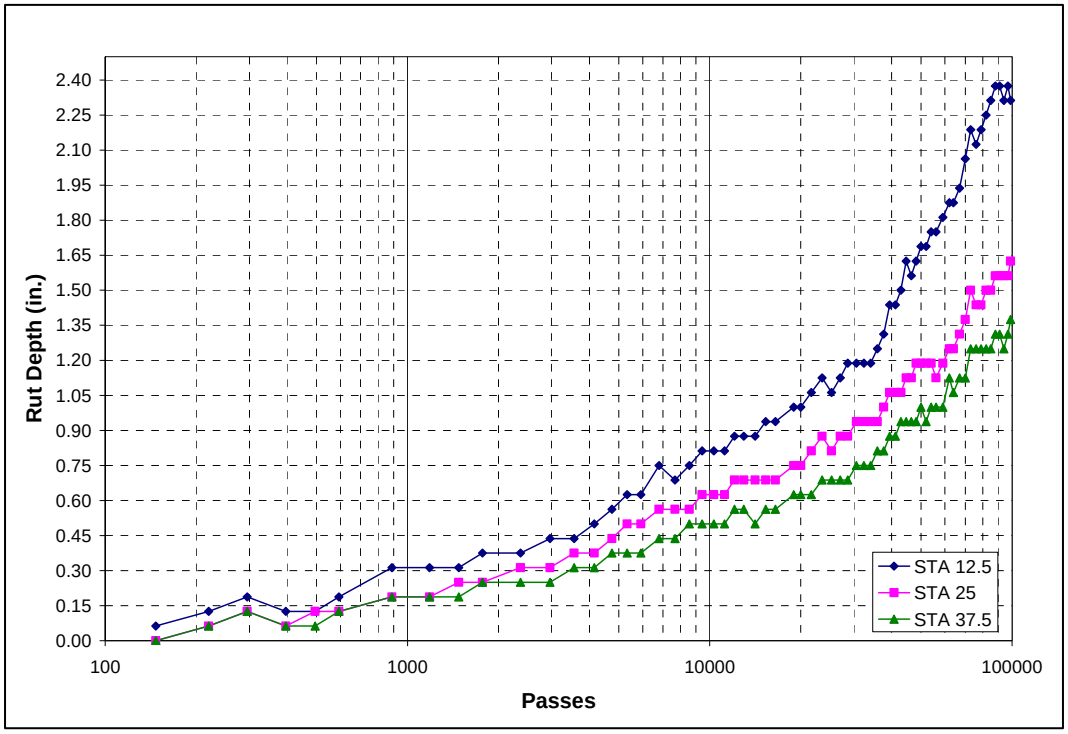

Figure 68. Item 4 centerline rut depth measurements.

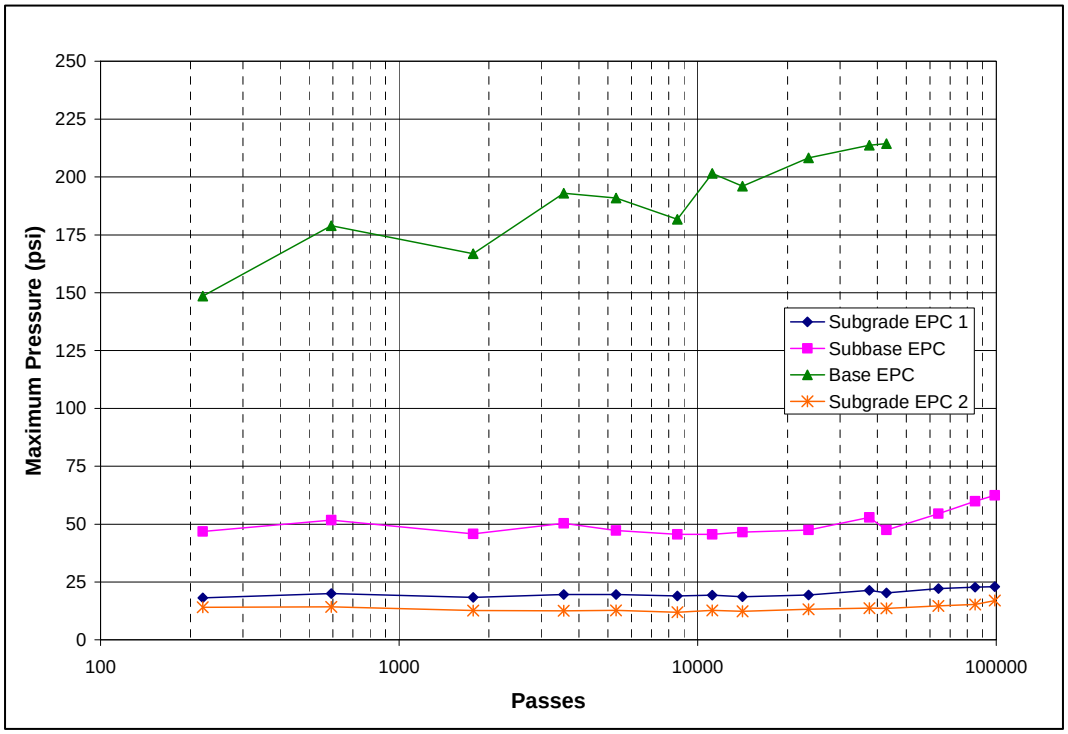

Figure 69. Item 4 maximum pressure measurements.

in the base course with increasing pass level. This was expected because as the traffic level of the F-15E wheel increased, the pavement structure became weaker causing the stresses to the base course to be higher. Once the traffic level was over 42,880 passes, the EPC in the base course started to over range because the measurements were outside of the EPC gauge's limits. No accurate base course pressure measurements were recorded from this point forward. Linear elastic analysis predicted the stress measurements in the base course to be approximately 120 psi, which is slightly lower than what was measured at the beginning of trafficking (145 psi). The predicted stresses in the subbase and subgrade were 65 and 25 psi, respectively. These predictions were slightly higher than the measured results (approximately 48 and 18 psi, respectively).

Asphalt concrete strain gauges

The maximum horizontal strains for Item 4 were much higher than expected. Figure 70 presents the maximum dynamic tensile strain measurements recorded under the asphalt concrete of Item 4. Linear elastic analysis using the backcalculated modulus values from the FWD data predicted the strain measurements for Item 4 to be between 550 and 800 microstrain. The gauges under the asphalt concrete pavement parallel to traffic (strain gauges 1 and 3) measured average maximum strains of 900 to 1,300 microstrain. The gauges perpendicular to traffic (strain gauges 2 and 4) measured average maximum strains of 2,200 to 2,800 microstrain. There was no trend associated with the tensile strain and increasing pass for any strain gauge.

Single depth deflectometers

Figure 71 shows the deformations recorded in the subgrade of Item 4. The deformations are an order of magnitude lower than those recorded from the other items. This was not unusual because of the difference in how the vertical stresses are distributed with the cargo and fighter aircraft. One would not expect as much movement in the subgrade of Item 4 trafficking with the F-15E wheel.

Forensics

Item 4 was trenched across Station 25 for forensic investigation. The post-analysis DCP and CBR test results showed that the pavement structure maintained or improved its strength with time. At the center of the rut and

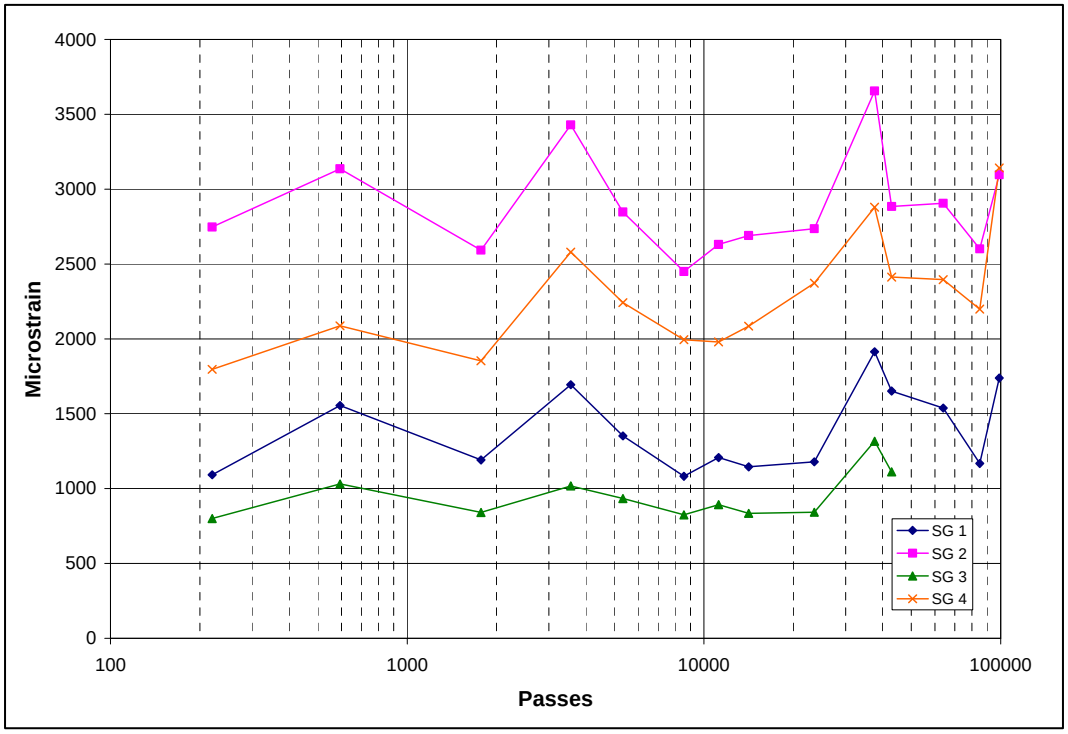

Figure 70. Item 4 maximum strain gauge measurements at the bottom of the asphalt concrete.

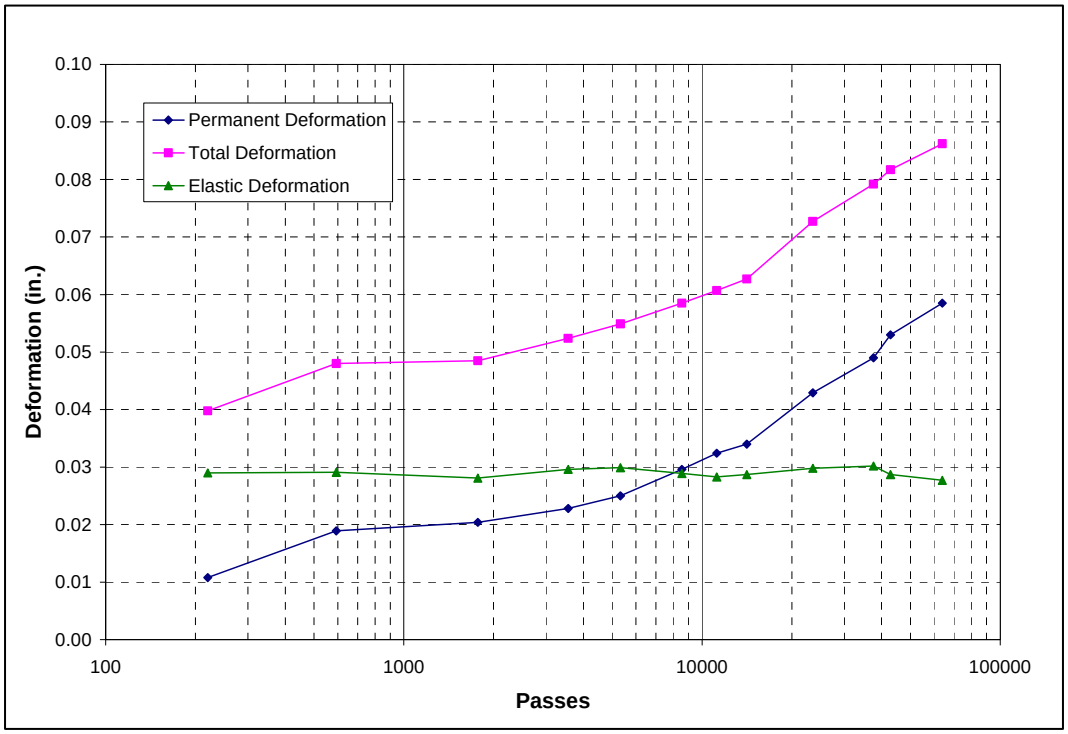

Figure 71. Item 4 subgrade SDD measurements.

outside of the traffic lane, the base course for Item 4 was still 100 CBR, and, similar to Item 3, the subbase improved to approximately 100 CBR. The subgrade strength remained around 10 CBR both inside and outside of the rut.

Post-test moisture measurements showed essentially no loss in moisture in the base, subbase, or subgrade. According to the pre-test and post-test density measurements, there was no densification in the subbase or subgrade layers. However, Item 4 showed a small 1.1% increase in density of the base course at the center of the rut. There was also an approximate 9 lb/ft^3 decrease in density outside the center of the rut of the base course when compared to the measured density at the center of the rut. This is an indication of possible densification and shear flow of the base course.

Visual inspection did not reveal any evidence of subgrade pumping in Item 4. Figure 72 shows a profile view of Item 4's surface, base, and subbase after trenching. The extreme right side of Figure 72 shows the transition zone into Item 6.

Figure 72. Item 4 trenched profile view.

The manual profile measurements showed that the asphalt concrete remained constant at 4 in., so the surface did not receive any failure. It appeared as though most of the movement occurred in the subbase and subgrade as a result of densification and shear flow. The base course thickness was relatively constant at about 6.5 in. across the traffic lane.

Failure of the subbase and subgrade of Item 4 were somewhat unusual because this section was trafficked with the F-15E wheel. The stresses were higher toward the top of the pavement structure because of the smaller tire leading one to believe that the majority of the movement would have occurred in the surface or base. However, although not apparent with the profile measurements, the density of the base course did increase slightly in the center of the rut. So, there was some possible densification of this layer. Item 4 profile measurements showed that the most movement occurred in the subgrade as a result of shear flow. Failure was also evident in the subbase.

Item 5

Surface distresses

Rutting and polished aggregate were the main surface distresses noted from Item 5 after trafficking. Item 5 was trafficked with the C-17 wheel until about 6,500 passes. Failure of 1 in. of permanent deformation happened around 1,278 passes. Figure 73 shows an overall view of Item 5 before trafficking began. The white line is the centerline of the traffic lane. Each horizontal blue line represents a quarter point (Stations 12.5, 25, and 37.5). The orange dots (Stations 15, 20, 25, 30, and 35) indicate that an instrumentation gauge is directly under that location within the pavement structure. The orange dot locations are also where the FWD tests were conducted. Figure 74 shows a rut depth measurement after 262 passes.

Falling weight deflectometer

Figure 75 shows the backcalculated moduli of the pavement structure from the FWD testing. The results show that the subbase and subgrade moduli remained consistent throughout trafficking. The base course moduli showed no trend with increasing passes. The backcalculated asphalt concrete moduli were inconsistent. Figure 76 also shows no trend with the stiffness of the pavement structure as the pass level increased.

Figure 73. Overall view of Item 5 at the start of trafficking.

Figure 74. Item 5 rutting at Station 37.5 after 262 passes.

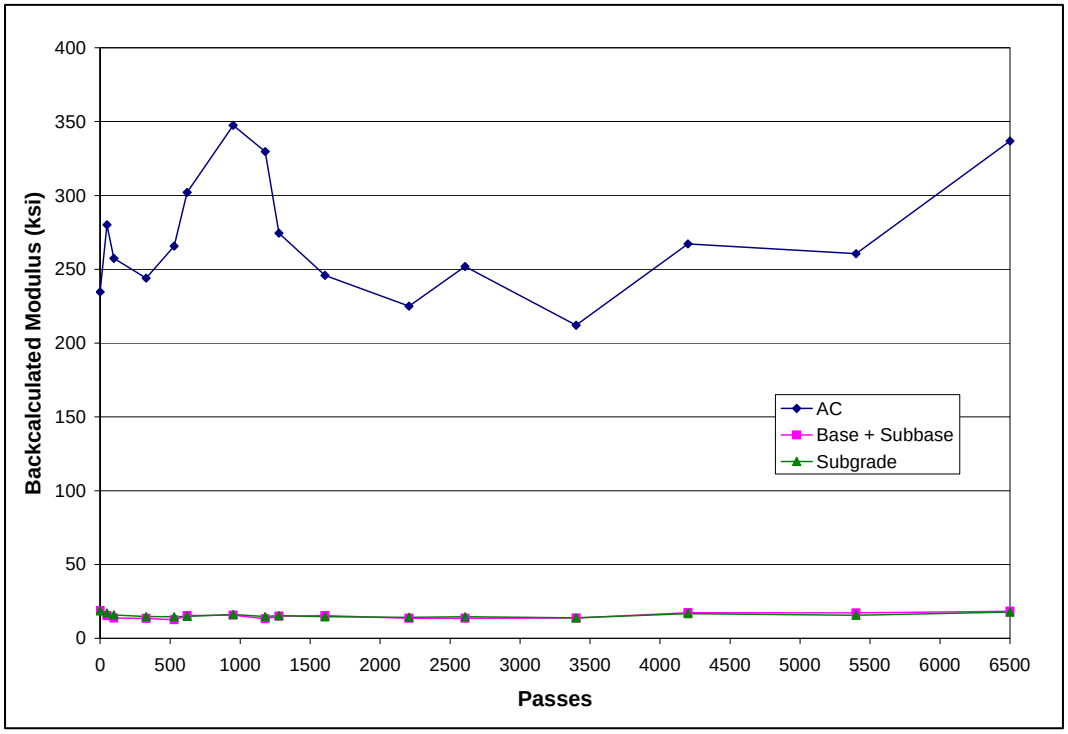

Figure 75. Item 5 backcalculated moduli results.

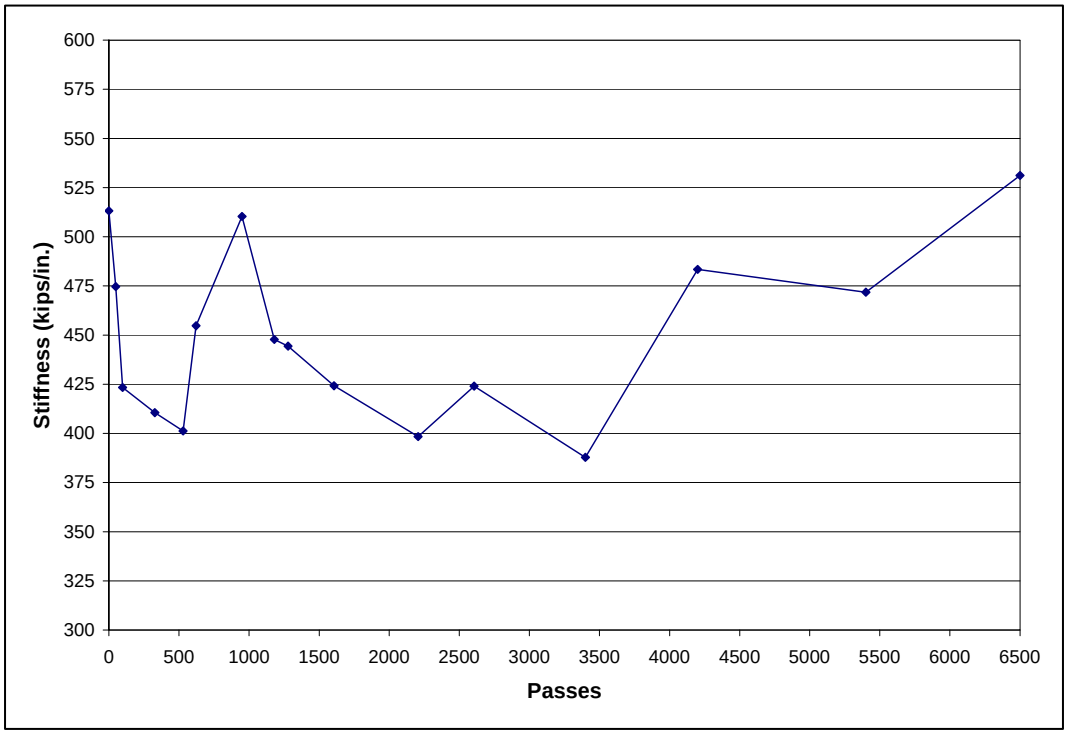

Figure 76. Item 5 stiffness results.

Centerline and cross section profiles

As with the other items, Figures 77 and 78 show upheaval on the sides and ends of the traffic lane of Item 5. Item 5 received a maximum of about 0.24 and 0.70 in. of upheaval on the sides of the traffic lane at failure (1,278 passes) and after 6,500 passes, respectively. There was slightly more upheaval on the east side of the traffic lane for all quarter points.

Rut depths

Figure 79 shows an overall steady increase in rut depth with each pass for Item 5. Item 5 failed around 1,278 passes. An average of 2 in. of rutting occurred around 6,500 passes.

Instrumented pavement response

Earth pressure cells

Dynamic pressure measurements were recorded at selected traffic intervals. The EPC installed in the base course layer of Item 5 malfunctioned, so no pressure measurements were recorded. Linear elastic analysis results predicted the pressure measurement in the base course to be approximately 75 psi. Figure 80 shows that the stresses measured in the subbase and subgrade increased slightly after failure of 1 in. of rutting occurred (approximately 1,300 passes). Linear elastic analysis predicted the measurements in the subbase and subgrade to be approximately 55 and 25 psi, respectively. The predictions are comparable with the in situ measurements.

Asphalt concrete strain gauges

Figure 81 presents the maximum strain gauge measurements recorded at the bottom of the asphalt concrete. There was no response with strain gauges 3 and 4 for a few of the passes. The maximum horizontal strains for Item 5 were higher than expected. Linear elastic analysis using the backcalculated modulus values from the FWD data predicted the strain measurements for Item 5 to be between 900 and 950 microstrain. The gauges under the asphalt concrete pavement parallel to traffic (strain gauges 1 and 3) measured average maximum strains of 1800 microstrain. The gauges perpendicular to traffic (strain gauges 2 and 4) measured average maximum strains of 2,500 to 3,000 microstrain. There was no trend associated with the tensile strain and increasing pass for any strain gauge.

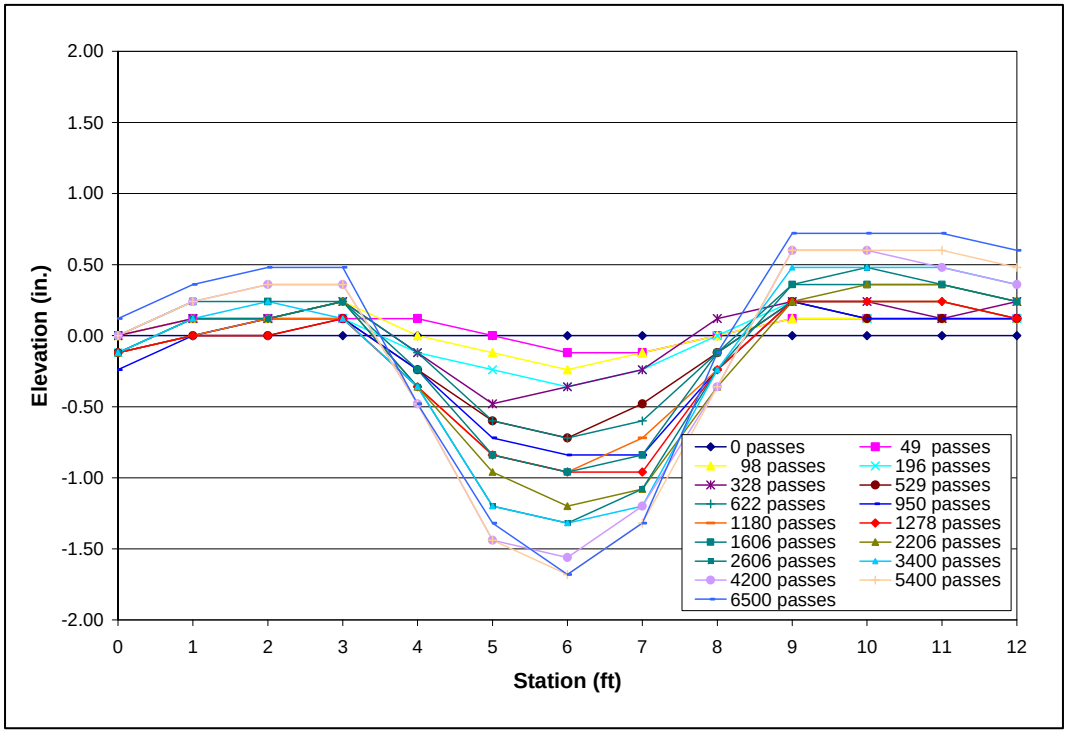

Figure 77. Item 5 cross section profiles at Station 12.5.

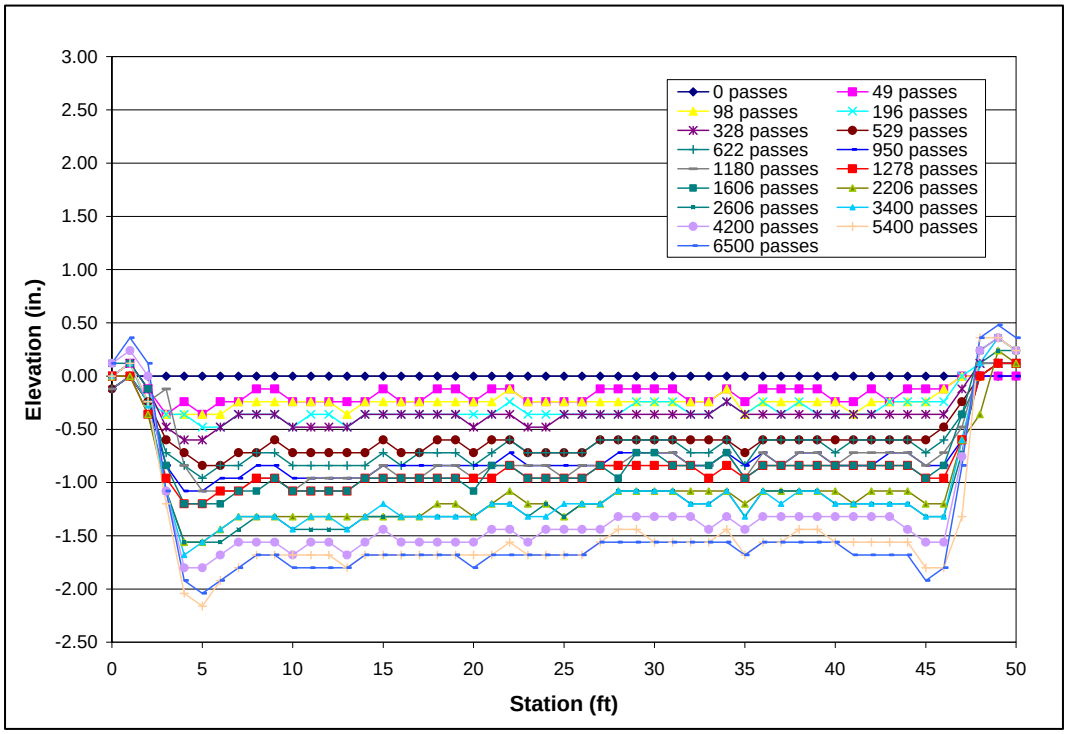

Figure 78. Item 5 centerline profiles.

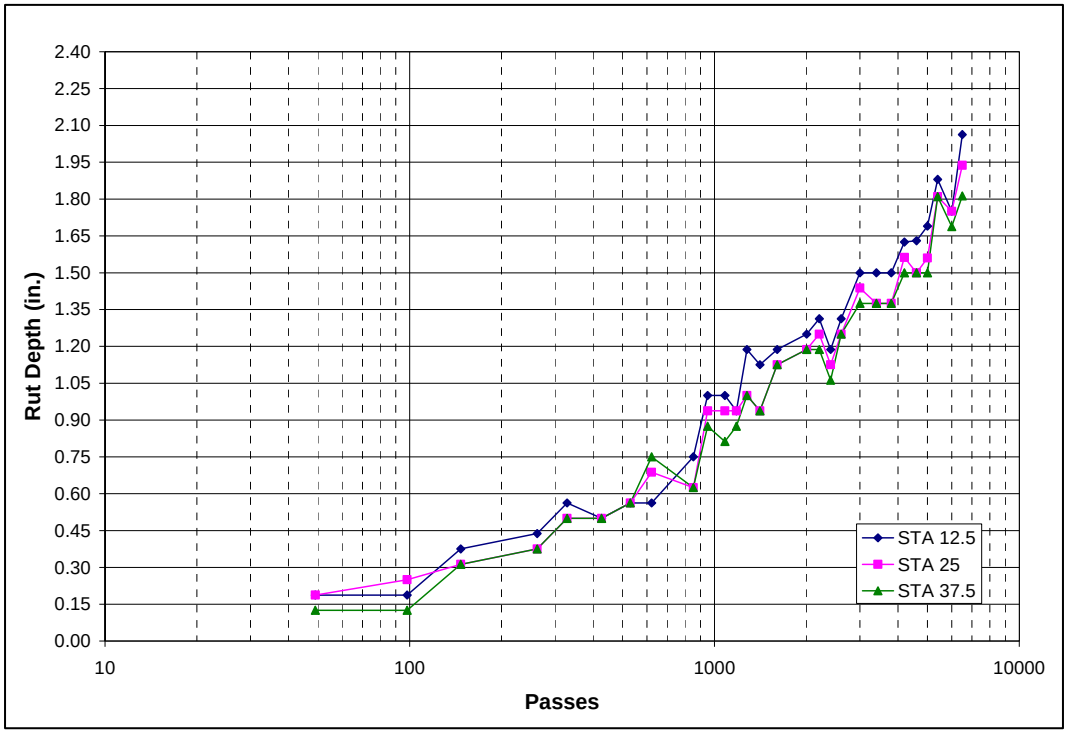

Figure 79. Item 5 centerline rut depth measurements.

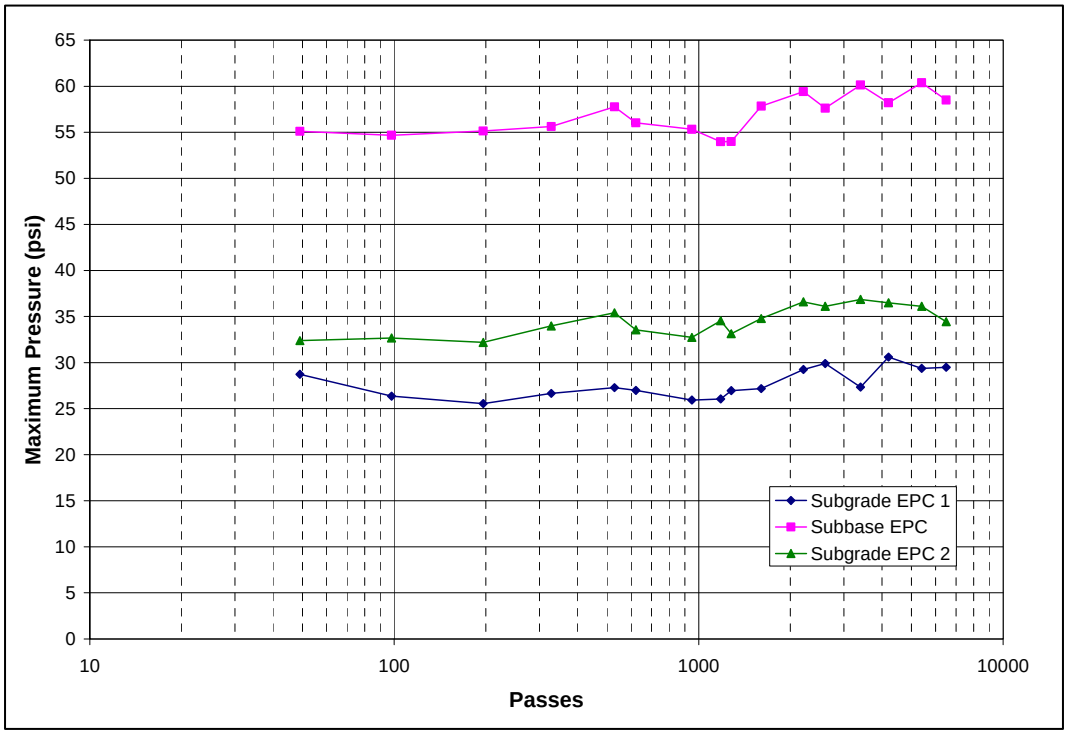

Figure 80. Item 5 maximum pressure measurements.

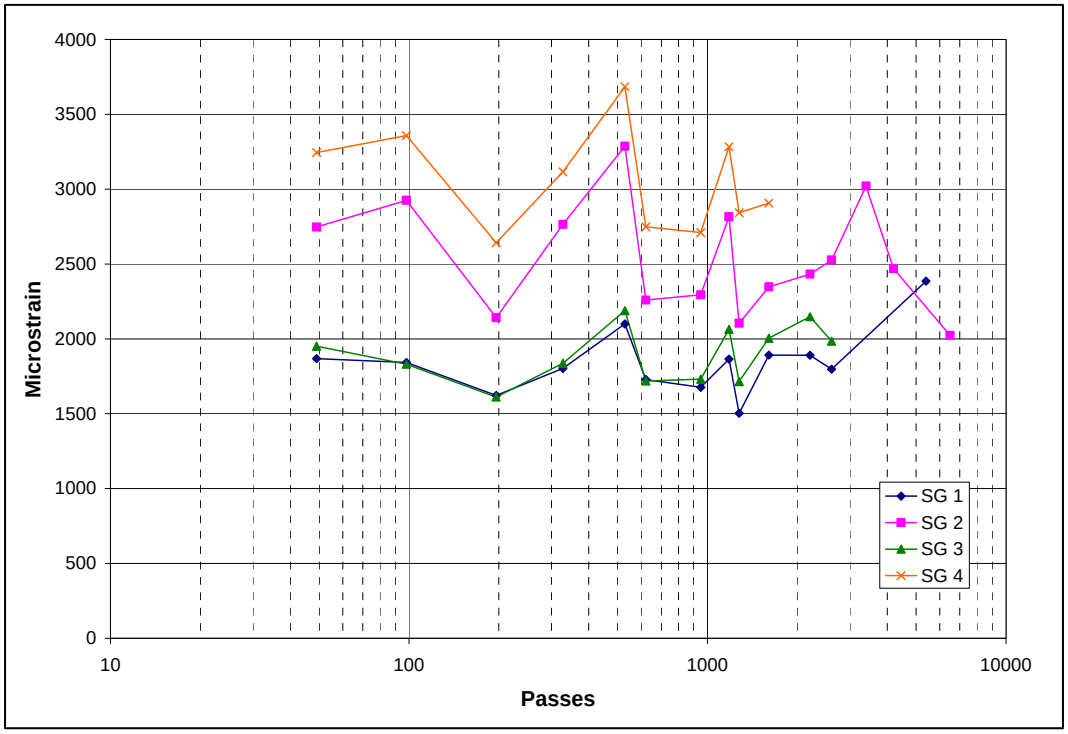

Figure 81. Item 5 maximum strain gauge measurements at the bottom of the asphalt concrete.

Single depth deflectometers

Figure 82 shows the dynamic SDD measurements recorded in the subgrade of Item 5. Figure 82 shows a slow, steady increase until failure of 1 in. of rutting happened. The permanent deformation in the subgrade increased at a greater rate after about 1,200 passes. Failure was around 1,278 passes.

Forensics

Item 5 was trenched across Station 25 for forensic investigation. The post-analysis DCP tests results showed that there was an increase in strength over time in the base and subbase. The base course CBR increased approximately 6%. Similar to Items 1 through 4, the subbase had a large increase in strength (approximately 20%). There was essentially no measurable difference in strength in the middle of the rut and outside of the traffic lane for any of the underlying layers.

Post-test moisture measurements showed essentially no change in moisture for the base, subbase, and subgrade. Comparing pre-test and

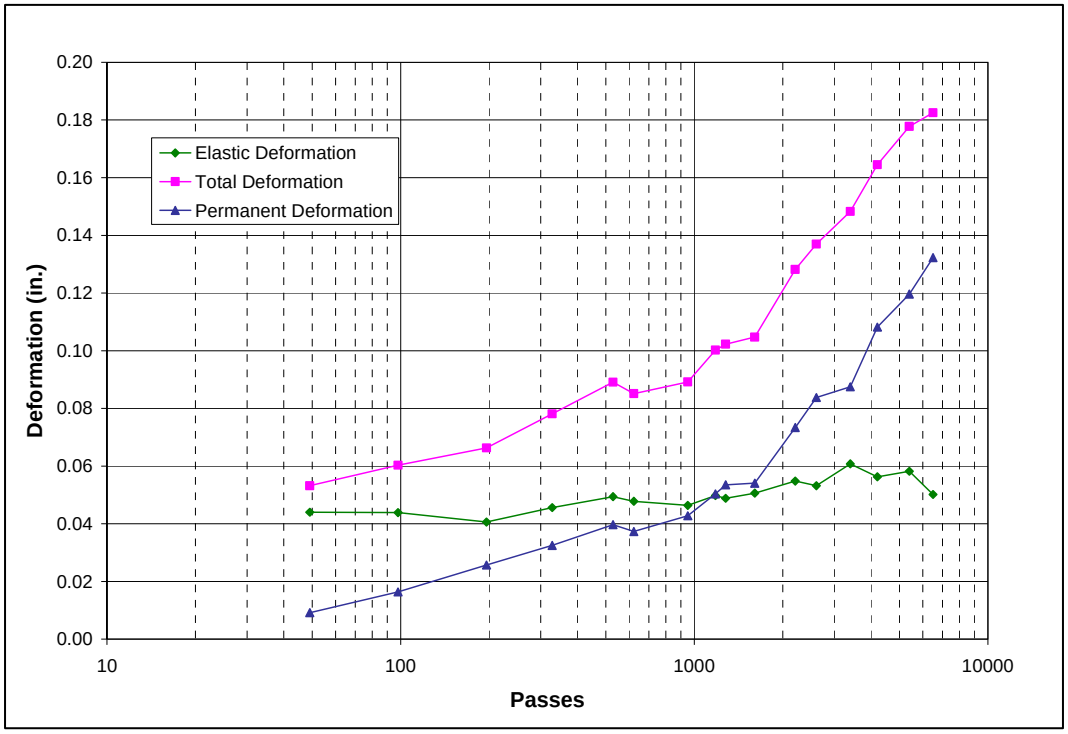

Figure 82. Item 5 subgrade SDD measurements.

post-test nuclear density gauge measurements indicated that the base, subbase, and subgrade densities did not increase.

Figure 83 shows a profile view of Item 5 after trenching. The red line depicts the interface between the base and subbase. Visual inspection did not reveal any evidence of subgrade pumping in Item 5.

The manual profile results showed that the asphalt concrete thickness remained constant at 5 in., so the surface was not the cause of the failure. As expected, the underlying layers were more difficult to assess. The base course thickness for Item 5 was relatively constant at 6 in. Based on the profile measurements, movement appeared to be in the subbase and subgrade. It was difficult to determine which layer received the most movement.

Item 6

Surface distresses

As with Item 4, rutting, polished aggregate, and cracking were the surface distresses noted from Item 6 after trafficking (Figures 84 and 85). Cracking occurred on Item 6 because the pavement temperature was about 21°F

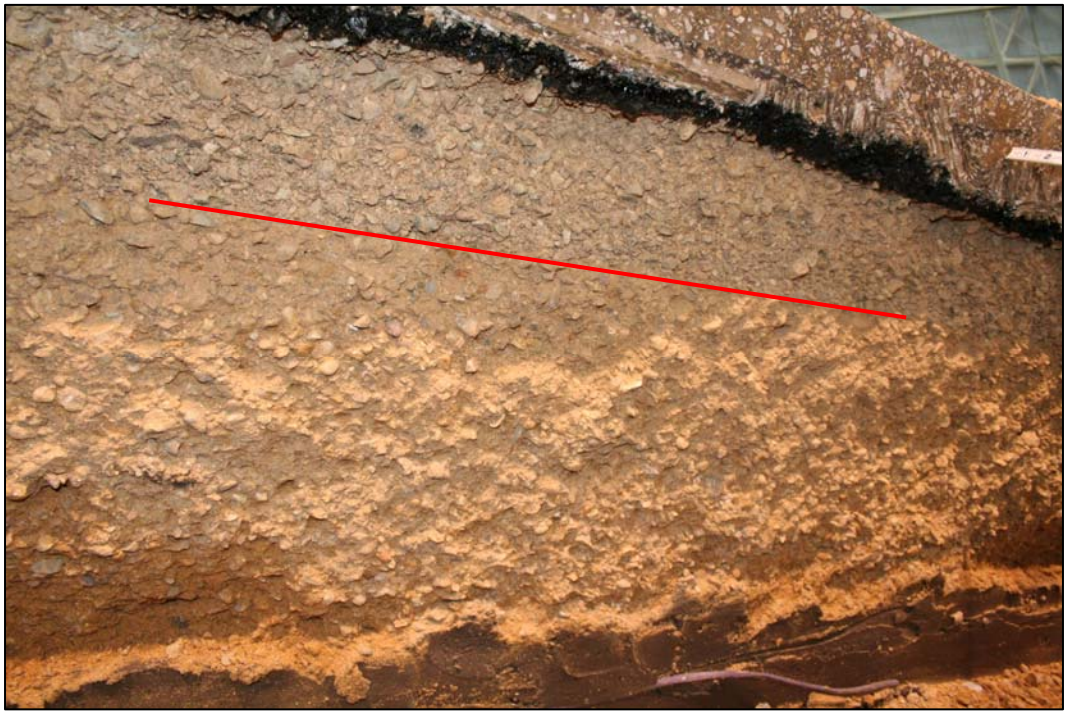

Figure 83. Item 5 trenched profile view.

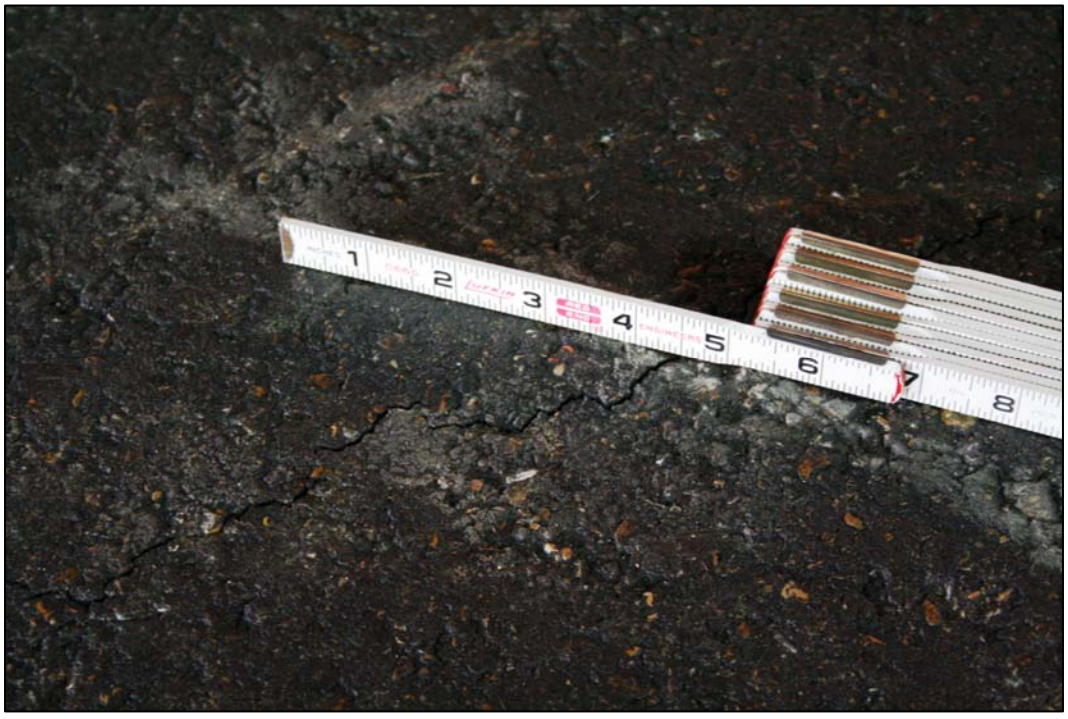

Figure 84. Item 6 cracking after 16,500 passes.

Figure 85. Item 6 cracking inside and outside of the traffic lane after 43,000 passes.

cooler than the surface temperatures of Items 1, 2, 3, and 5. Also, cracking may have occurred because the item was trafficked with the F-15E wheel. Item 6 was trafficked until about 58,500 passes. Failure of 1 in. of permanent deformation happened around 32,500 passes. Figure 86 shows an overall view of Item 6 after traffic completion.

Falling weight deflectometer

Figures 87 and 88 present the results of Item 6's FWD testing. The backcalculated asphalt concrete modulus values were higher than those measured in all the items. The stiffness values of the pavement structure were also higher. This was expected because the item was trafficked in cooler weather, and the surface was 1 in. thicker than the surface of Item 4.

Centerline and cross section profiles

Overall, the centerline and cross section profiles of Item 6 showed slight upheaval on the sides and at the beginning and end of the traffic lane (Figures 89 and 90). Item 6 received a maximum upheaval of 0.36 in. on the sides of the traffic lane after trafficking. At failure (32,500 passes), the maximum upheaval measured on the sides of the traffic lane was about 0.24 in.

Figure 86. Overall view of Item 6 after traffic completion.

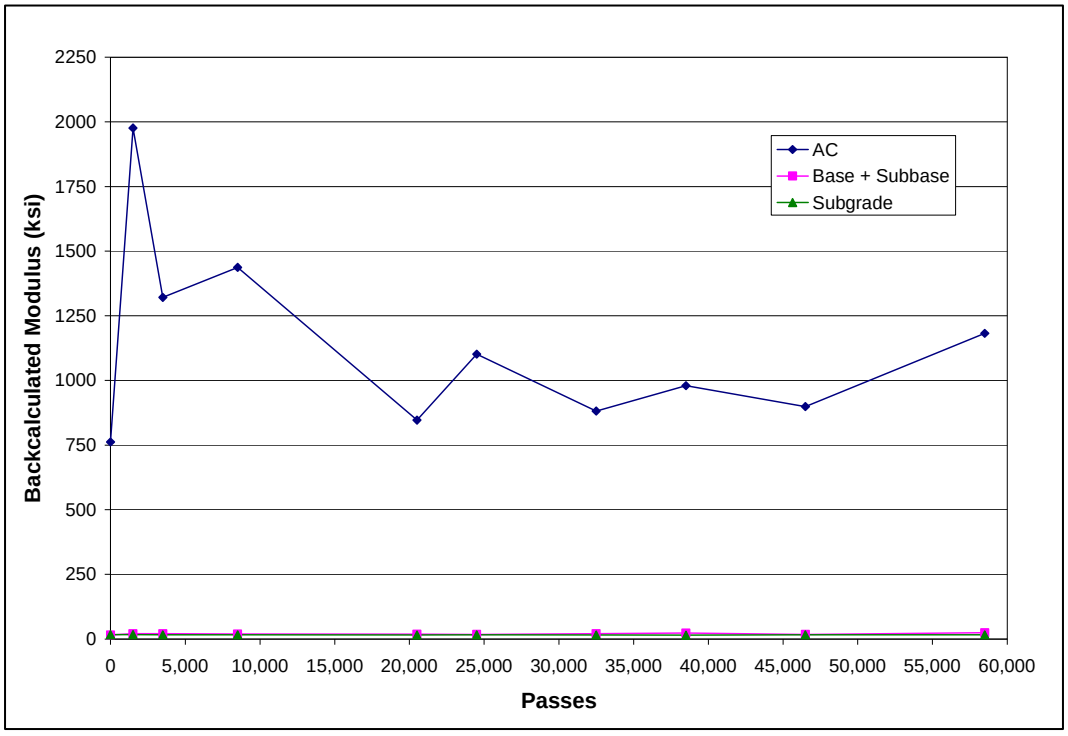

Figure 87. Item 6 backcalculated moduli results.

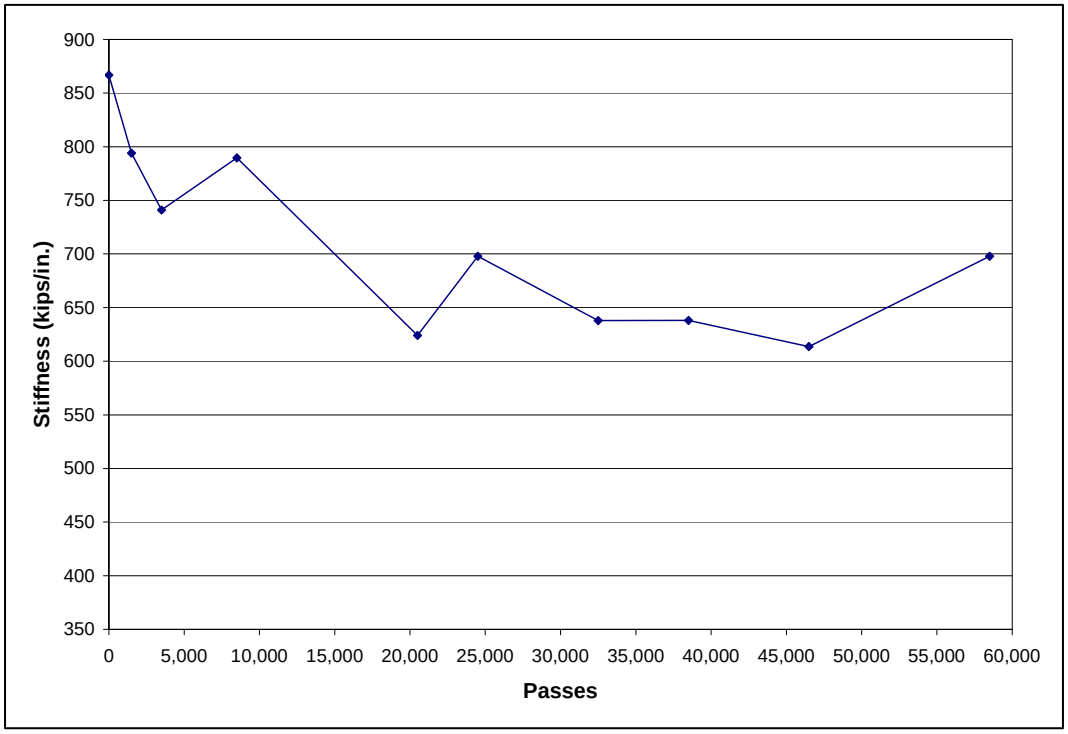

Figure 88. Item 6 stiffness results.

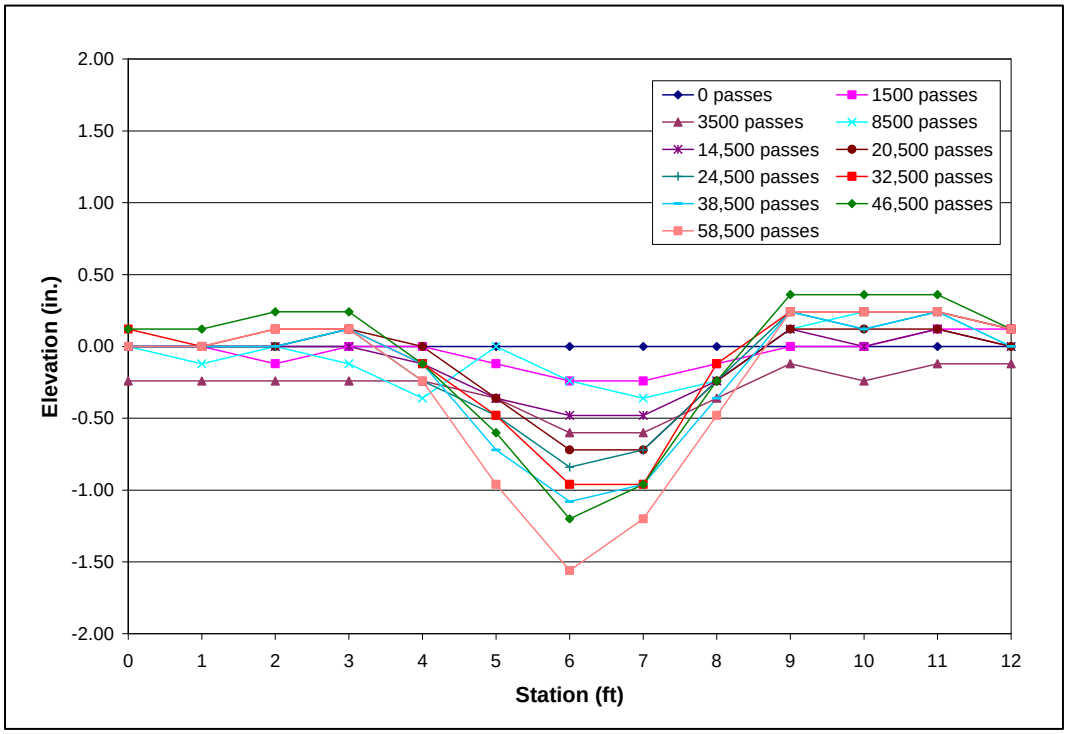

Figure 89. Item 6 cross section profiles at Station 37.5.

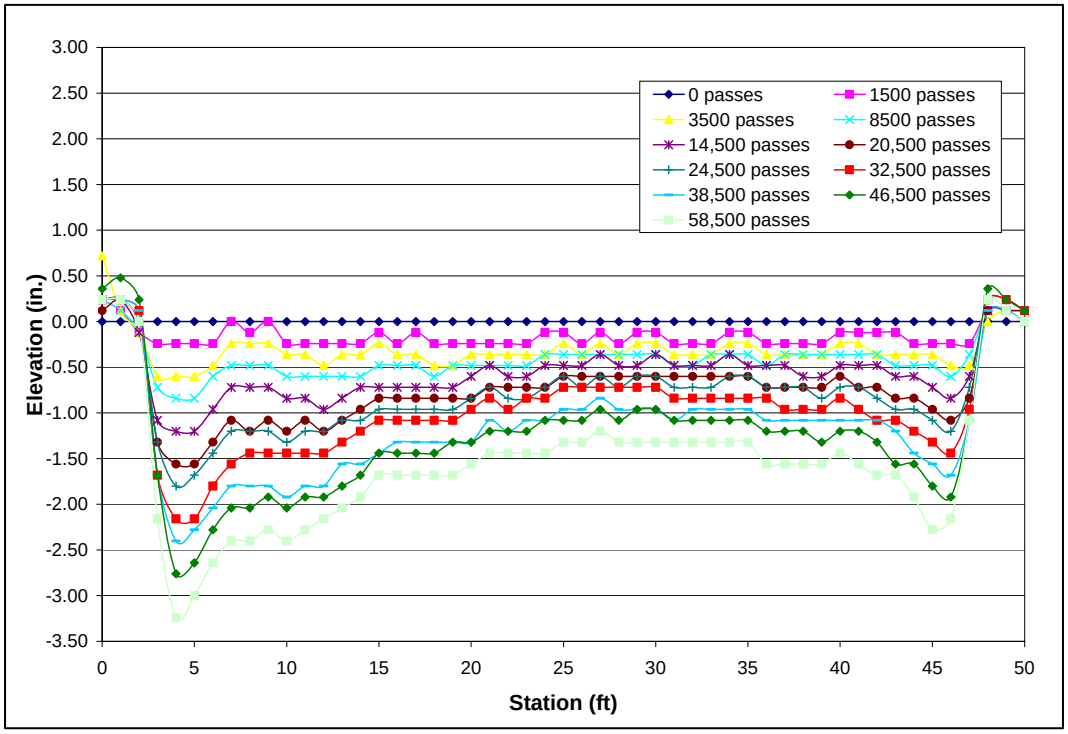

Figure 90. Item 6 centerline profiles.

Rut depths

Figure 91 shows the rut depth measurements of Item 6. Item 6 failed around 32,500 passes. The rut depths at Station 12.5 did increase at a faster rate than those measured at Stations 25 and 37.5. Again, this is most likely due to an inconsistent compaction effort across the item or from the HVS-A wheel "pushing off" at Station 5 after each pass. Figure 91 shows a steady increase in rut depths until about 10,000 passes. The rut depth then begins to increase at a greater rate with each pass.

Instrumented pavement response

Earth pressure cells

Figure 92 shows the dynamic pressure measurements within Item 6's pavement structure. The results show inconsistent pressure measurements in the base course and consistent pressure measurements in the subbase and subgrade. Overall, the stresses increased in the base course after about 10,000 passes. The stresses slightly increased in the subbase and subgrade after about 10,000 passes. Linear elastic analysis predicted the vertical stresses in the base, subbase, and subgrade to be approximately 85, 50, and 25 psi, respectively.

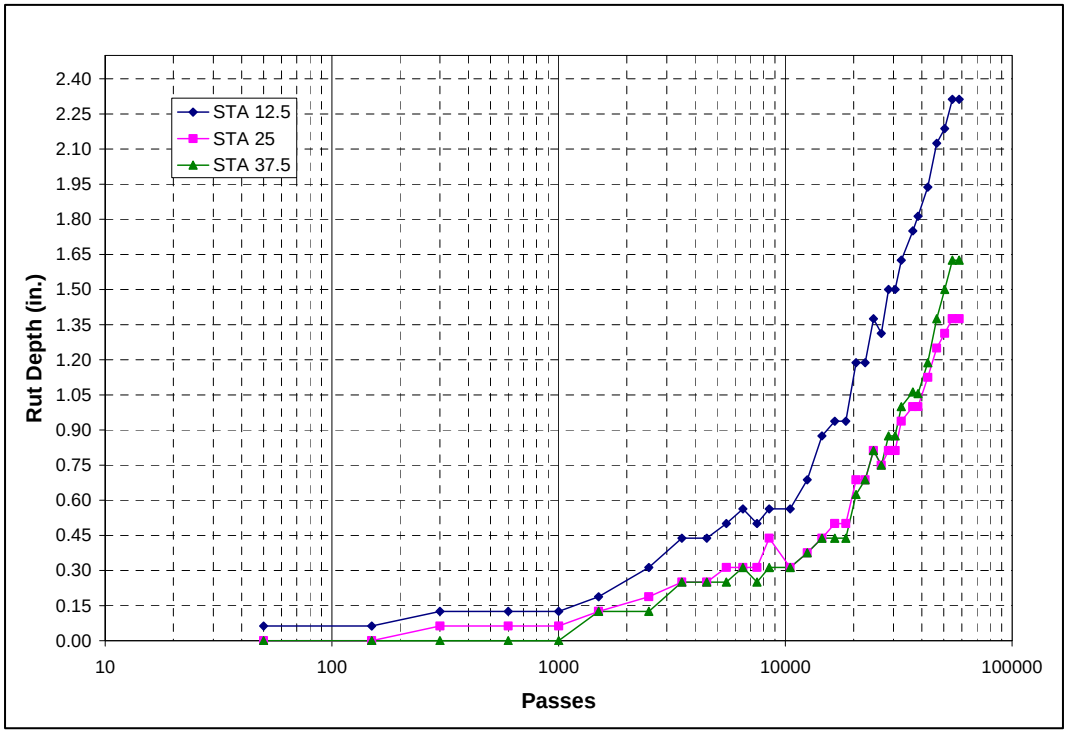

Figure 91. Item 6 centerline rut depth measurements.

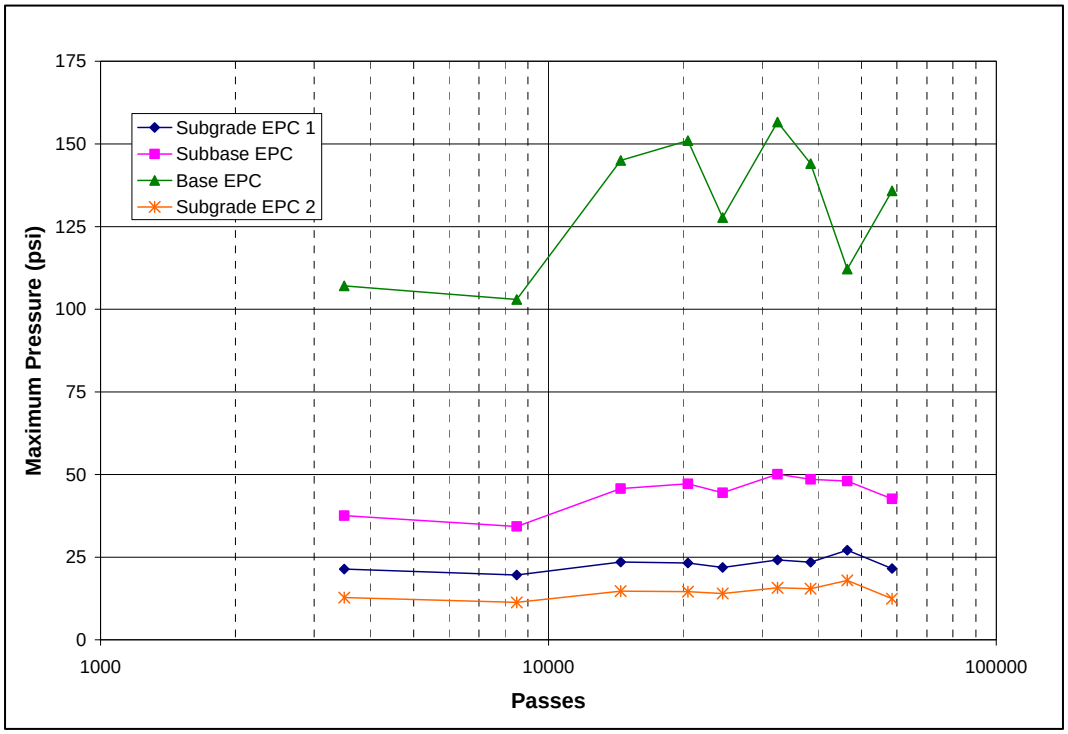

Figure 92. Item 6 maximum pressure measurements.

Asphalt concrete strain gauges

The maximum horizontal strains for Item 6 were much higher than expected. Figure 93 shows the in situ maximum dynamic strain gauge measurements under the asphalt concrete. Linear elastic analysis using the backcalculated modulus values from the FWD data predicted the strain measurements for Item 6 to be between 500 and 800 microstrain. The gauges under the asphalt concrete pavement parallel to traffic (strain gauges 1 and 3) measured average maximum strains of 1,000 to 1,200 microstrain. The gauges perpendicular to traffic (strain gauges 2 and 4) measured average maximum strains of 1,800 to 2,300 microstrain. Overall, there was a slight increasing trend associated with the tensile strain and increasing passes for the strain gauges. Figure 93 shows a noticeable increase in maximum strain measurements after about 10,000 passes. This was not surprising because there was also an increase in the rut depth and EPC measurements after about 10,000 passes.

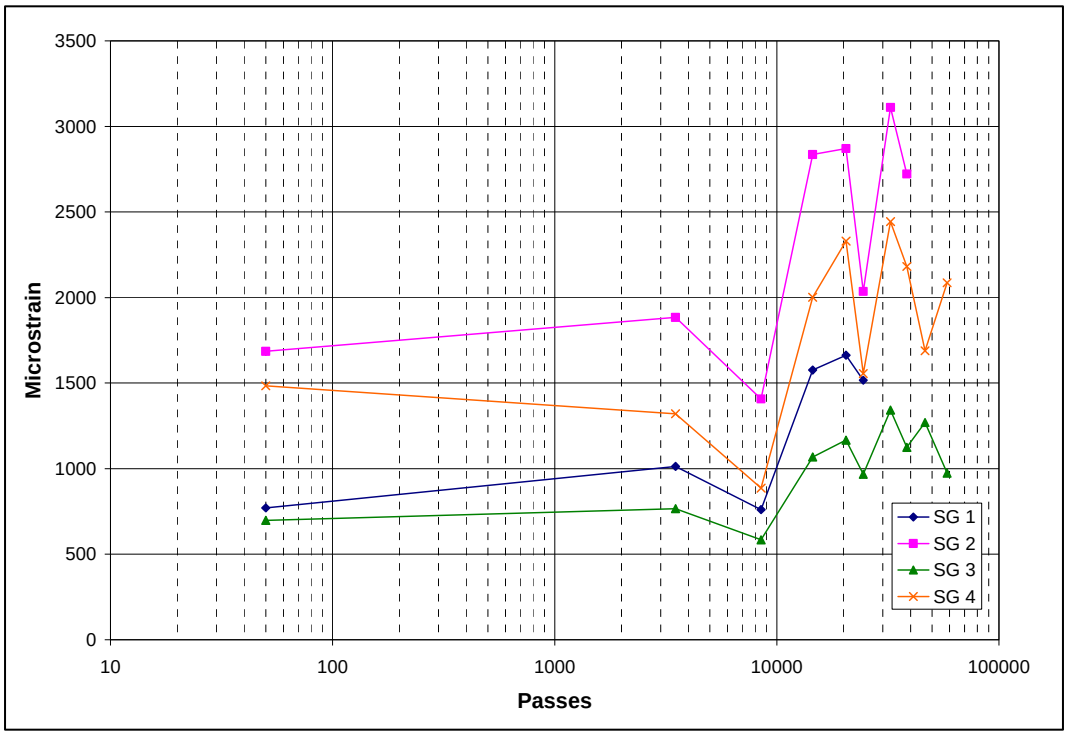

Figure 93. Item 6 maximum strain gauge measurements at the bottom of the asphalt concrete.

Single depth deflectometers

The SDD installed in the subgrade of Item 6 malfunctioned, so no deformation measurements were recorded.

Forensics

Item 6 was trenched across Station 25 for forensic investigation. According to the DCP tests, the base and subbase gained strength during and/or after trafficking. The base course for Item 6 increased from 40 CBR to approximately 55 CBR at the center of the rut and outside of the traffic lane. The subbase improved from 42 CBR to approximately 90 CBR. The subgrade strength remained around 10 CBR both inside and outside of the rut.

Post-test moisture measurements showed that there was no change in moisture within the pavement structure. According to the pre-test and post-test density measurements, there was no densification in the base, subbase, or subgrade layers.

Visual inspection did not reveal any evidence of subgrade pumping in Item 6. Figure 94 shows a profile view of Item 6's surface, base, and subbase after trenching. The red line depicts the interface between the base course and subbase materials.

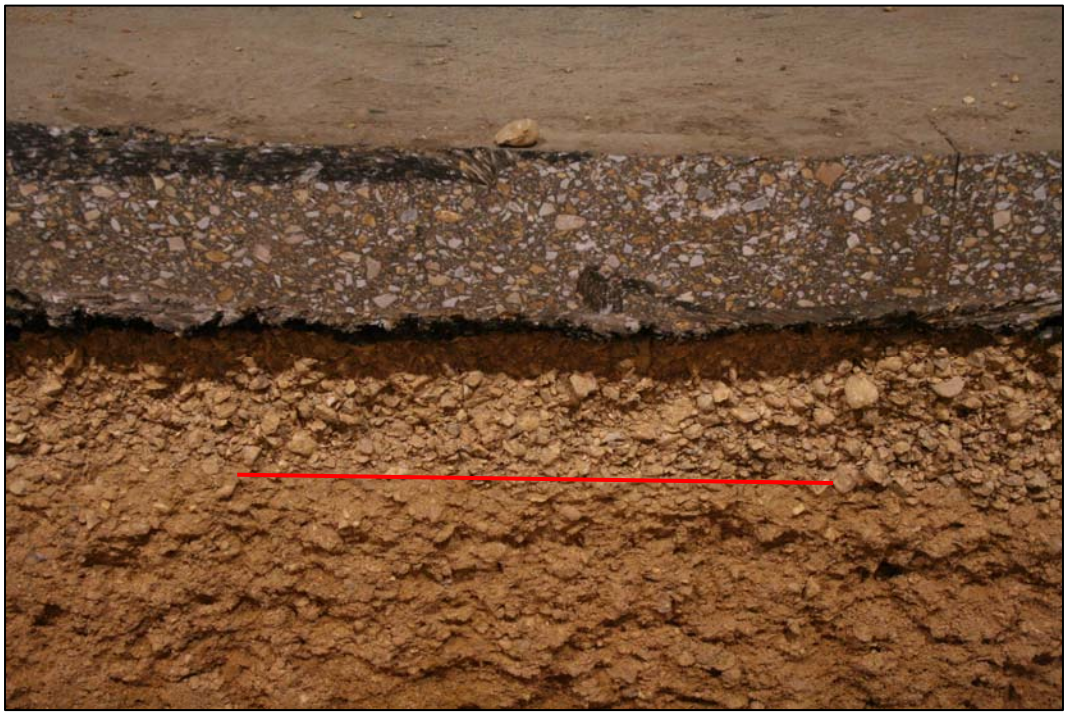

Figure 94. Item 6 trenched profile view.

The manual profile measurements showed that the asphalt concrete remained constant at 5 in., so the pavement structure did not fail as a result of the asphalt concrete. The base course thickness was relatively constant at about 6 in. across the traffic lane. It appeared as though movement occurred in the subbase and subgrade as a result of densification and shear flow.

As with Item 4, movement in the subbase and subgrade of Item 6 was rather unusual because this section was trafficked with the F-15E wheel. Item 6 profile measurements showed that movement was evident in the subbase; however, the most movement seemed to have occurred in the subgrade as a result of shear flow.

7 Discussion of Results

Test section failure

Failure location in the pavement structure of any item was not clear based on visual inspection alone. The items were not trafficked to catastrophic failure, so it was difficult to visually identify what layer or layers may have failed or had movement. The surface was easy to assess whether damage had occurred. The further down into a pavement structure, the more difficult it is to identify what may have occurred as a result of the aircraft traffic.

Overall, what was seen with the test section was more of a failure of the pavement structure, not necessarily the subbase and subgrade. There was gradual movement with each increasing pass. The load from each increasing pass forced the underlying materials repeatedly to be pressed down (densification or consolidation) and/or out (shear flow or lateral movement). This resulted in the gradual failure of the pavement structure over time.

The possible failure locations were not clearly evident based on the forensic analysis, and the majority of movement for each item appeared to be in either the subbase or subgrade. There was minimal movement in the base courses. This supports the fact that, overall, there was failure of the pavement structure over time rather than in a certain underlying layer or layers.

Predicted passes to failure

Passes to failure were predicted for each item before trafficking began. The predictions were based on the pavement structure depths, CBR, FWD backcalculated data (pre-test), pass to coverage ratios, aircraft loads, and/or aircraft tire pressures. Table 10 presents the predicted passes to failure of each item using three different methods.

The CBR method was conducted in the PCASE software. This prediction method, based on the depth and CBR of each layer in the pavement structure and the aircraft characteristics, is currently being used for pavement design. The layered elastic evaluation program (LEEP) predicted passes to

Table 10. Predicted and measured passes to failure.

Item	Predicted Passes to Failure					Measured Passes to Failure
	CBR Method (PCASE)	LEEP	Stress-Based CBR Design Procedure			
			Base	Subbase	Subgrade	
1	29	1	650	200	10,000+	234
2	1,862	11	675	200	10,000+	623
3	2,801	125	10,000	175	10,000+	2,850
4	7,562	2,600	2,000	100	10,000+	42,881
5	1,665	289	900	300	10,000+	1,278
6	600	1,907	50	200	10,000+	32,500

failure based on the pre-test FWD backcalculated data at each depth within the pavement structure and the aircraft characteristics. The Stress-Based CBR Design Procedure for flexible pavements is currently being evaluated for replacing the classical CBR equation (Barker and Gonzalez 2008). This method predicted passes to failure based on the depth of the pavement structure, pass to coverage ratio, and aircraft characteristics. The base, subbase, and subgrade values shown under the Stress-Based CBR Design Procedure in Table 10 are the number of predicted passes to failure for each of the pavement layers. Other than Item 6, the critical layer is the subbase, and the predicted passes to failure are always 300 or less for each of the items.

With the exception of Items 2 and 5, the measured passes to failure surpassed the CBR Method's predicted passes to failure. The predicted passes for Item 5, however, were close to the measured passes to failure. LEEP predicted that the items would have fewer passes to failure than what was evaluated. The LEEP and CBR Method greatly underestimated the measured passes to failure of Items 4 and 6. These two items were trafficked with the F-15E wheel.

Since there was no exact "failure" location, it was difficult to determine if the Stress-Based CBR Design Procedure predicted the passes to failure most accurately. According to the Stress-Based CBR Design Procedure, Item 1 most likely had the most movement in the subbase, Item 2 most likely had the most movement in the base or subbase, and Item 3 most likely had the most movement in the base or subbase. Table 10 also shows that the Stress-Based CBR Design Procedure predicted that Item 4 most likely had the most movement in the subgrade, Item 5 most likely had the

most movement in the base or subbase, and Item 6 most likely had the most movement in the subgrade.

The Stress-Based CBR Design Procedure predictions were somewhat accurate with what was observed during the forensic investigations. The forensic analysis revealed that all items had some movement in the subbase and subgrade. The forensic analyses of Items 1, 2, 4, and 6 indicated possible movement in the base courses as well. The Stress-Based CBR Design Procedure predicted that Item 3 and 5 would have the majority of movement in the base course, which was not observed.

Pre-test versus post-test field measurements

Tables 8 and 9 (Chapters 4 and 6, respectively) present the pre-test and post-test field measurements of the test section. The measurements include dry density, moisture content, and CBR. Post-test measurements were collected at the center of the rut and outside of the rut. There was minimal change in moisture and density at each location.

The post-test field results indicated that there was a small amount of moisture lost with each foundation material (1.5% or less). Overall, the subgrade showed the lowest amount of moisture lost. This proves the affinity of high-plasticity clay to hold water over time. Also, with the exception of the subbase of Item 3 and the base of Item 4, there was no increase in density after trafficking. The small increase in density of Item 3's subbase and Item 4's base was approximately 1% or 2 lb/ft^3. The post-test density measurements indicated that there was essentially no measured densification with any of the foundation layers.

There was, however, sustained or increased strength of each foundation layer except for the base course of Item 2. The approximate 12-CBR decrease in the base course after trafficking Item 2 was likely due to movement of the material with traffic. The surface of Item 2 was only 3.5 in. thick, and the base course consisted of the weaker crushed gravel material, which was more difficult to compact. The base course CBR for the other items showed a slight increase in strength. This is most likely caused by the traffic load.

The subbase material of each item increased between 10 and 50 CBR. There are several reasons that the subbase may have a large increase in CBR after trafficking. Sometimes, traffic load will reorient the particles,

resulting in a tighter compaction, or a large amount of moisture will be lost. However, the density and moisture measurements indicated this was not the case. Most likely, the large increase in strength of the subbase was due to the aggregates' water absorption over time. Generally, an aggregate's laboratory absorption measurement of 2% or more indicates that the aggregate may absorb moisture over time. Absorption measurements were not determined from the foundation materials in the laboratory before construction. Without this data, it was not certain if this was the reason for the large increase in strength. As expected, the subgrade maintained its strength with traffic.

Instrumentation response analysis

Earth pressure cells

Table 11 shows the average maximum dynamic response measurements of the EPCs, SDDs, and strain gauges until failure of 1 in. of rutting. The maximum stress measurements in the base courses were highest for Item 1. However, the stress measurements for Item 1 were not reliable because they were unrealistic. The C-17 wheel had a tire pressure of 142 psi, and the EPC was measuring maximum pressures 4.5 in. into the base of approximately 190 psi. Linear elastic analysis predicted that the vertical stresses in the base course of Item 1 would be approximately 130 psi.

The base courses of Items 4 and 6 had the next highest average maximum pressures to failure of 187 and 124 psi, respectively. This was expected because both items were trafficked with the F-15E wheel. The F-15E wheel has a higher tire pressure (325 psi) than the C-17 wheel (142 psi), so the stresses were higher toward the top of the pavement structure. The reason for the rather large difference in pressure measurements for the base courses of Items 4 and 6 are unclear. However, the surface of Item 6 was 1 in. thicker than the surface of Item 4. Furthermore, as expected, Item 2 had the lowest recorded average maximum stress measurement (102 psi) in its base course. The EPCs installed in the base courses of Items 3 and 5 malfunctioned, likely as a result of damage during the surface paving process.

The vertical stresses measured in the subbase were highest for Items 1 and 2. Items 1 and 2 were trafficked with the C-17 wheel, and they were

Table 11. Test section data summary.

Item	Traffic Wheel	Surface Thickness (in.)	Avg. Surface Temp. (°F)	FWD Avg. Stiffness (kips/in.)	Surface Distress	Passes to Failure[a]	Avg. Vertical Stress to Failure (psi)			Avg. Total Deformation to Failure of Subgrade (in.)	Avg. Tensile Strain to Failure at Bottom of Surface (microstrain)		Possible Failure Location
							Base	Subbase	Subgrade		Long.	Trans.	
1	C-17	2.5	80	254	Rutting	234	190	80	34	0.086	2457	2809	Base, Subbase, & Subgrade
2	C-17	3.5	79	343	Rutting & Polished Aggregate	623	102	73	29	0.174	2478	2240	Base, Subbase, & Subgrade
3	C-17	4.0	82	440	Rutting & Polished Aggregate	2,850	n/a	60	25	0.137	1668	1734	Subbase & Subgrade
4	F-15E	4.0	55	596	Rutting, Polished Aggregate, & Cracking	42,881	187	48	16	0.057	1134	2501	Base, Subbase, & Subgrade
5	C-17	5.0	83	450	Rutting & Polished Aggregate	1,278	n/a	55	29	0.076	1773	2776	Subbase & Subgrade
6	F-15E	5.0	60	710	Rutting, Polished Aggregate, & Cracking	32,500	124	41	19	n/a	1079	1989	Base, Subbase, & Subgrade

[a] Failure is defined as 1 in. of surface rutting.

constructed of only 2.5 and 3.5 in. of asphalt concrete, respectively. The base courses for the items also consisted of the weaker crushed gravel material, so the modulus was not as high as the crushed limestone's modulus (Items 3 and 4). The EPCs installed in the subbases of Items 3 and 5 recorded the next highest stresses. These items were also constructed of the weaker crushed gravel material; however, the surfaces were 0.5 to 2 in. thicker than Items 1 and 2. The thicker surfaces resulted in lower vertical stresses in the subbases. The EPC installed in the subbase of Item 6 measured the lowest vertical stress (41 psi). This was not surprising because Item 6 was trafficked with the F-15E wheel on 5 in. of asphalt concrete during the cooler month of March.

The maximum stress measurements in the subgrade were highest for Items 1, 2, and 5. These items consisted of the crushed gravel base course and were trafficked with the C-17 wheel. The other items were constructed of the crushed limestone base course (Items 3 and 4) or were trafficked with the F-15E wheel (Item 6). There was a slight difference in the depth of each pavement structure. The pavement structure of Items 1, 2, and 5 were approximately 26.5, 27.5, and 25.5 in. deep, respectively, to the subgrade. In this case, Item 1 had a thicker pavement structure than Item 5, but the average vertical stress to failure of Item 1 was slightly higher (5 psi). This is most likely due to the difference in surface thickness. The asphalt concrete of Item 1 was 2.5 in. thick, while Item 5 consisted of 5 in. of asphalt concrete.

Items 4 and 6 recorded the lowest vertical stresses in the subgrades (16 and 19 psi, respectively). This is not surprising because the items were trafficked with the F-15E wheel during the cooler temperature months. Item 6 most likely had a higher stress measurement than Item 4 in its subgrade because the base course (crushed gravel) was not as strong as Item 4's base course (crushed limestone). Also, the pavement structure to the subgrade of Item 6 was 23 in. deep, while the depth of Item 4's pavement structure was 24 in.

Single depth deflectometers

SDD measurements were recorded to assess the total deformation of the subgrade. Items 1, 2, and 5 consisted of the same crushed gravel base course and were trafficked with the C-17 wheel. The surface temperatures of each of the items were also basically the same (Table 11). Surprisingly, Item 2 had a higher total deformation in its subgrade at failure when

compared to Items 1 and 5 (Table 11). The pavement structure depths of Items 1, 2, and 5 were 26.5, 27.5, and 25.5 in., respectively.

Not surprisingly, Item 4 recorded the lowest total deformation in its subgrade (0.057 in.). Item 4 was trafficked with the F-15E wheel on 4 in. of asphalt concrete with a 6.5-in. crushed limestone base. Also, the surface temperature (55°F) of Item 4 during trafficking was cooler than the other items. The vertical stresses in the subgrade of Item 4 were also the lowest of the items. The SDD installed in the subgrade of Item 6 malfunctioned.

Strain gauges

Strain gauge measurements were found to be much larger than anticipated. The average maximum strains at the bottom of the asphalt concrete were approximately two to three times higher than those predicted using linear elastic analysis. Table 11 shows the average maximum tensile strains at the bottom of the asphalt concrete to failure. Measurements were recorded in the longitudinal and transverse directions. Reasons for the large difference in predicted and measured strain are unclear. It is possible that the linear elastic analysis was not able to exhibit the viscoelastic behavior of asphalt concrete. Also, it is possible that the asphalt concrete was stressed past the elastic limit resulting in a reduction in the mixture stiffness and a corresponding increase in the measured strain. This same high strain measurement has been seen on other asphalt concrete test sections at the ERDC as well as other test sections outside of the ERDC when aircraft loadings are applied. This is an area that needs to be further investigated.

Overall, Items 1 and 2 measured the highest tensile strains at the bottom of their surfaces. This was expected because the items were constructed of the thinnest asphalt concrete. With the exception of Item 2, the strain gauges that were placed parallel to traffic (longitudinal) measured lower strains than those placed perpendicular to traffic (transverse). Overall, Items 3 and 6 measured the lowest tensile strains at the bottom of their surfaces. With the exception of Items 1 and 2 measuring the highest tensile strains because they were constructed of the thinnest asphalt concrete, there was no trend associated with tensile strain and a pavement structure characteristic.

Traffic analysis

Most traffic analyses are completed over a 20-year period. Item 1 failed at 234 passes. This is equivalent to one movement of a loaded C-17 per month for 20 years. Item 2 failed at 623 passes. This is equivalent to one movement of a loaded C-17 aircraft on an airfield every 12 days for 20 years. Items 1 and 2 did not meet the minimum asphalt concrete thickness criteria. The crushed gravel base course, intended to be 80 CBR, was only measured to be between 37.6 and 54.2 CBR. Nonetheless, with this pavement structure, increasing the flexible pavement thickness by 1 in. (from 2.5 in. to 3.5 in.) almost tripled the life of the pavement for a 20-year span.

Item 3 failed at 2,850 passes. This is equivalent to one movement of a loaded C-17 aircraft on an airfield every 2.5 days for 20 years. Item 5 failed at 1,278 passes. This is equivalent to one movement of a C-17 aircraft on an airfield almost every 6 days for 20 years. The asphalt concrete surface thickness of Item 3 was 1 in. less than the surface thickness of Item 5. However, Item 3 had a much stronger base course (crushed limestone – 100 CBR) than Item 5 (crushed gravel – 51.5 CBR). The weaker base course resulted in a much faster failure rate of the pavement structure (twice as fast).

Items 4 and 6 were trafficked with the F-15E wheel. Item 4 was constructed with the crushed limestone base course, and Item 6 was constructed with the crushed gravel base course. Item 4 failed at 42,881 passes. This is equivalent to an unrealistic six movements of a loaded F-15E aircraft on an airfield every day for 20 years. Item 6 failed at 32,500 passes. This is equivalent to an unrealistic four and a half movements of a loaded F-15E aircraft on an airfield every day for 20 years. Items 4 and 6 most likely sustained the high number of traffic passes because the asphalt concrete surface temperature was about 20 to 25°F lower than the other items and possibly because the items were trafficked with the F-15E wheel.

Criteria validated

The main purpose of this research was to validate the DoD's minimum asphalt concrete thickness criteria outlined in UFC 3-260-02 (Tables 1 and 2). The minimum asphalt concrete thickness requirements are 4 in. with a 6-in. 100-CBR base (Items 3 and 4) and 5 in. with a 6-in. 80-CBR base

(Items 5 and 6). This research also looked at the consequences of trafficking on a pavement structure that did not meet the minimum surface thickness requirements (Items 1 and 2). One can expect a pavement's life to be reduced by at least one half if the current minimum surface thickness requirements are not met. There was no failure of the surface as a result of the asphalt concrete with any of the items. Furthermore, in general, the measured passes to failure exceeded the predicted passes to failure based on the CBR Method and using LEEP. The DoD's minimum asphalt concrete thickness criteria were deemed acceptable based on the results of the traffic tests.

8 Conclusions and Recommendations

The ERDC was tasked by the AFCESA to validate the DoD's minimum asphalt concrete thickness criteria and to observe the effects of operating heavy aircraft loads and high tire pressures on representative thin asphalt concrete pavements. This report addresses the construction and evaluation processes required for the full-scale test section, the importance of materials characterization, and the impact that cargo and fighter aircraft can have on military flexible pavements. Conclusions from the assessments and recommendations for future work are provided in the following text.

Conclusions

The following conclusions resulted from the evaluation of the DoD's minimum asphalt concrete thickness criteria:

- The DoD's minimum asphalt concrete thickness criteria were deemed acceptable based on the results of the traffic tests.
- A pavement's life will be decreased by at least one half if the minimum asphalt concrete thicknesses are not met.
- The test section was not trafficked to catastrophic failure. Therefore, failure locations for each item were unclear based on visual inspection of the trenches.
- Overall, each item failed as a result of gradual failure of the pavement structure over time. There was gradual failure with each increasing pass. The load from each increasing pass forced the layer materials to be steadily pushed down and/or out.
- The principle surface failure mechanisms for the test section included rutting and polished aggregate. Surface cracking was also present on the items trafficked with the F-15E wheel (Items 4 and 6).
- Polished aggregate was noticeable on the thin flexible pavements after approximately 800 passes of the C-17 or F-15E wheel.
- An increase in 1 in. of a thin asphalt concrete surface layer (from 2.5 to 3.5 in.) resulted in an increase of about three times the number of passes to failure (based on 1 in. of rutting).
- The cool surface temperature when trafficking Items 4 and 6 resulted in stiffer pavement structures than Items 1, 2, 3, and 5. Also, Items 4 and 6 were trafficked with the F-15E wheel. One or both of these

conditions allowed Items 4 and 6 to sustain at least an order of magnitude more passes than the other items before the rutting failure of 1 in. occurred.

- There was minimal change, if any, in the pre-test and post-test density and moisture measurements of the foundation layers.
- DCP and CBR tests showed that base and subgrade of every item sustained or improved in strength over time. There was minimal change, if any, between the strength of the material in the rut and outside the traffic lane.
- The subbase strength (CBR) of each item increased between 10 and 50 CBR after trafficking. This is most likely due to a high water absorption percentage of the aggregates.
- Linear elastic analysis predicted the tensile strain measurements under the asphalt concrete (top of the base) to be two to three times lower than what the strain gauges measured for each item. It is possible that the linear elastic analysis had difficulty emulating the viscoelastic behavior of the asphalt concrete.
- Linear elastic analysis results of the vertical stresses received throughout the pavement structure were comparable with the in situ measurements.
- Trafficking the test section proved how important it is to maximize compaction efforts. The areas of the test section where compaction efforts were not adequate resulted in a faster rate of pavement permanent deformation.

Recommendations

The following recommendations are offered based upon the results of the evaluation of the full-scale asphalt concrete test section:

- The test section was not trafficked to catastrophic failure, so it was difficult to assess exactly where the majority of failure occurred. The addition of multi-depth deflectometers in each foundation layer of the pavement structure could aid in better detection of failure location.
- The effects of operating a cargo and a fighter aircraft on thin asphalt concrete pavements could not be directly compared as far as passes to failure or impact of tire pressure and weight are concerned. Further testing should be conducted on a full-scale test section under controlled environmental conditions and on asphalt concrete pavements that have been cured for the same amount of time and at the same temperatures.

- The criterion described in UFC 3-260-02 for 80-CBR base course material needs to be redefined. All requirements (gradations, fractured faces count, etc.) for an 80-CBR base course material were met for the crushed gravel chosen for the test section. However, a maximum of only 54 CBR was able to be achieved.
- Strain gauge measurements under the asphalt concrete were found to be about two to three times higher than predicted. Reasons for the large difference in predicted and measured strains are unclear. This same high strain measurement has been seen on other asphalt concrete test sections at the ERDC as well as other test sections outside of the ERDC when aircraft loadings are applied. This is an area that needs to be further investigated.

References

American Society for Testing and Materials. 2004. *Standard test method for CBR (California Bearing Ratio) of soils in place.* Designation: D 4429-04. West Conshohocken, PA.

American Society of Civil Engineers. 1950. Development of CBR flexible pavement design methods for airfields (a symposium), Paper No. 2406. In *Transactions, ASCE* 115:453.

Barker, W. R., and C. Gonzalez. 2008. Application of the new CBR equation and criteria for design of military roads. *Transportation Systems 2008 Workshop*. Phoenix, AZ.

Collop, A. C., D. Cebon, and M. S. A. Hardy. 1995. Viscoelastic approach to rutting in flexible pavements. *Journal of Transportation Engineering* 121(1):82-83.

Headquarters, Departments of the Army, the Navy, and the Air Force. 2001. Pavement design for airfields. Unified Facilities Criteria (UFC) 3-260-02, Washington, DC.

Huang, Y. H. 2004. *Pavement analysis and design*. 2d ed. Upper Saddle River, NJ: Pearson Education, Inc.

Shahin, M. Y., M. I. Darter, and S. D. Kohn. 1976-1977. Development of a pavement maintenance management system; I-V. Tyndall AFB: U.S. Air Force Engineering Services Center.

Webster, S. L., R. W. Brown, and J.R. Porter. 1994. Force projection site evaluation using the electric cone penetrometer (ECP) and the dynamic cone penetrometer (DCP). Technical Report GL-94-17. Vicksburg, MS: U.S. Army Waterways Experiment Station.

REPORT DOCUMENTATION PAGE

Form Approved
OMB No. 0704-0188

1. REPORT DATE *(DD-MM-YYYY)*	2. REPORT TYPE	3. DATES COVERED *(From - To)*
October 2008	Final report	

4. TITLE AND SUBTITLE

Evaluation of Minimum Asphalt Concrete Thickness Criteria

5a. CONTRACT NUMBER

5b. GRANT NUMBER

5c. PROGRAM ELEMENT NUMBER

6. AUTHOR(S)

Haley P. Bell and L. Webb Mason

5d. PROJECT NUMBER

5e. TASK NUMBER

5f. WORK UNIT NUMBER

7. PERFORMING ORGANIZATION NAME(S) AND ADDRESS(ES)

U.S. Army Engineer Research and Development Center
Geotechnical and Structures Laboratory
3909 Halls Ferry Road
Vicksburg, MS 39180-6199

8. PERFORMING ORGANIZATION REPORT NUMBER

ERDC/GSL TR-08-26

9. SPONSORING / MONITORING AGENCY NAME(S) AND ADDRESS(ES)

Headquarters, Air Combat Command
129 Andrews Street, Suite 102
Langley Air Force Base, VA 23666

10. SPONSOR/MONITOR'S ACRONYM(S)

11. SPONSOR/MONITOR'S REPORT NUMBER(S)

12. DISTRIBUTION / AVAILABILITY STATEMENT

Approved for public release; distribution is unlimited.

13. SUPPLEMENTARY NOTES

14. ABSTRACT

Personnel of the U.S. Army Engineer Research and Development Center (ERDC) were tasked by Headquarters, Air Combat Command, to evaluate the Department of Defense's (DoD) minimum asphalt concrete thickness criteria outlined in Unified Facilities Criteria 3-260-02. Recent improvements to the DoD's flexible pavement design procedure and a renewed emphasis on the design and construction of contingency pavements has prompted concerns regarding the design and evaluation of thin asphalt concrete pavements. An evaluation of the DoD's minimum asphalt concrete thickness criteria was conducted during February 2007 to April 2008 under the ERDC's Hangar 4 test facility. The project consisted of constructing a full-scale test section with six varying test items that represented three airfield types encountered in both peacetime and contingency scenarios. Four of the items met the DoD's minimum asphalt concrete thickness criteria, and two items did not meet the criteria. Each item was instrumented and trafficked with either a C-17 wheel or an F-15E wheel using a Heavy Vehicle Simulator. Traffic test results concluded that the DoD's current minimum asphalt concrete thickness criteria are acceptable. Further results from the evaluation are presented and include material characterization tests and data, rut depth measurements, centerline and cross section profiles, falling weight deflectometer data, instrumentation response data, and forensic investigation assessments.

15. SUBJECT TERMS

Asphalt concrete	CBR	Heavy vehicle simulator
C-17	Department of Defense	Instrumentation
	7-15E	Test section

16. SECURITY CLASSIFICATION OF:			17. LIMITATION OF ABSTRACT	18. NUMBER OF PAGES	19a. NAME OF RESPONSIBLE PERSON
a. REPORT	b. ABSTRACT	c. THIS PAGE			19b. TELEPHONE NUMBER *(include area code)*
UNCLASSIFIED	UNCLASSIFIED	UNCLASSIFIED		111	